RESEARCH & DEVELOPMENT

# SAVE Currituck Sound: Submerged Aquatic Vegetation Evaluation in Currituck Sound, NC


**D. Reide Corbett[1], PI**

**Natasha Biarrieta[1], Patrick Dickhudt[2], Mark Fonseca[3], Erin Hodel[3], Elizabeth Mason[1], Paul Paris[1], Heidi Wadman[2], and J.P. Walsh[1]**

**[1]Coastal Studies Institute**
**East Carolina University**

**[2]Field Research Facility, Coastal & Hydraulics Lab**
**Army Corps of Engineers**

**[3]CSA Ocean Sciences Inc.**



**NCDOT Project 2018-05**
**FHWA/NC/20??-???**
**June 2020**

# SAVE Currituck Sound: Submerged Aquatic Vegetation Evaluation in Currituck Sound, NC

Final Report: NCDOT Project 2018-05

D. Reide Corbett[1], PI

Natasha Biarrieta[1], Patrick Dickhudt[2], Mark Fonseca[3], Erin Hodel[3], Elizabeth Mason[1], Paul Paris[1], Heidi Wadman[2], and J.P. Walsh[1]

[1]Coastal Studies Institute
East Carolina University

[2]Field Research Facility, Coastal & Hydraulics Lab
Army Corps of Engineers

[3]CSA Ocean Sciences Inc.

**Technical Report Documentation Page**

| 1. Report No. *FHWA/NC/2018-05* | 2. Government Accession No. | 3. Recipient's Catalog No. |
|---|---|---|
| 4. Title and Subtitle<br>SAVE Currituck Sound: Submerged Aquatic Vegetation Evaluation in Currituck Sound, NC | | 5. Report Date<br>June, 2020 |
| | | 6. Performing Organization Code |
| 7. Author(s)<br>*D. Reide Corbett, Natasha Biarrieta, Patrick Dickhudt, Mark Fonseca, Erin Hodel, Elizabeth Mason, Paul Paris, Heidi Wadman, and J.P. Walsh* | | 8. Performing Organization Report No. |
| 9. Performing Organization Name and Address<br>*Coastal Studies Institute*<br>*East Carolina University*<br>*850 NC-345, Wanchese, NC 27981* | | 10. Work Unit No. (TRAIS) |
| | | 11. Contract or Grant No. |
| 12. Sponsoring Agency Name and Address<br>North Carolina Department of Transportation<br>Research and Development Unit<br>104 Fayetteville Street<br>Raleigh, North Carolina 27601 | | 13. Type of Report and Period Covered<br>Final Report<br>*July 1, 2017 – June 30, 2020* |
| | | 14. Sponsoring Agency Code<br>*NCDOT Project # 2018-05* |

Supplementary Notes:

16. Abstract

Submerged aquatic vegetation (SAV) provide numerous ecosystem services including enhanced biodiversity, erosion control and sediment stabilization, nutrient cycling, improved water quality, and organic carbon sequestration. Rapid environmental changes and increased coastal development have resulted in significant SAV losses globally. Currituck Sound, the northernmost estuary in North Carolina, was once known for extensive SAV beds serving as a refuge and food source to an abundance of fish and waterfowl that attracted anglers and hunters from all over the country. However, declines in water quality as a result of rapid population growth and development have led to massive declines in SAV habitats that have been devastating to the local ecology. This study investigated changes in historical and current SAV distribution and evaluated how these changes have been influenced by water depth, light availability, and bed-sediment composition.

The past and present relationship between water depth and SAV cover was examined in several ways: (1) historical SAV cover maps, (2) hydroacoustic surveys, (3) quadrat transect surveys, (4) modeling using light attenuation data, and (5) comparisons with historical ground surveys. In Currituck Sound, SAV is not present beyond a water depth of 1.8 m and are preferentially located at depths shallower than 1.0 m. The median light attenuation for the combined 2016 and 2017 growing seasons was 1.99 $m^{-1}$. The calculated minimum water-column light requirement was 2.8% and water-column light requirement for peak growth was ≥13.7%. Sediments were dominated by sand (average weight percent >90%) and had very low organic content (average percent loss on ignition ~1.0%). While some spatial and temporal variations in sediment composition were identified, no statistical relationships between SAV cover and sediment characteristics were observed. Light availability with water depth proved to be the dominant factor limiting SAV growth and distribution in Currituck Sound. Therefore, the light and depth thresholds identified in this study are key to developing a sound management and mitigation plan.

| 17. Key Words<br>*Submerged Aquatic Vegetation; sedimentation; habitat; water quality* | 18. Distribution Statement | | |
|---|---|---|---|
| 19. Security Classif. (of this report)<br>Unclassified | 20. Security Classif. (of this page)<br>Unclassified | 21. No. of Pages<br>*147* | 22. Price |

**Form DOT F 1700.7** (8-72) **Reproduction of completed page authorized**

# DISCLAIMER

## ACKNOWLEDGMENTS

Many people within the ECU Department of Geological Sciences and Coastal Studies Institute have helped with data collection and processing. A special thanks to Corey Adams, Julia Bachman, Noah Corbett, Kira Foster, Madison Sawyer, Dave Sybert, and Trip Patterson for help their contributions.  Financial support was provided by the North Carolina Department of Transportation.

## EXECUTIVE SUMMARY

The Mid-Currituck Bridge is a pending NCDOT project decades in the making. The 11-km-long two-lane toll bridge will span across Currituck Sound, connecting US 158 on the Currituck County mainland to NC 12 on the Outer Banks (NCDOT, 2019). The bridge will yield faster hurricane evacuation times, reduce seasonal traffic congestion in the summer months, provide first responders with a more direct route to the northern communities of the Outer Banks, and could serve as a catalyst for commercial and business development in mainland Currituck County. Environmental concerns surrounding the project include the potential impacts to water quality and aquatic habitats in Currituck Sound. One important habitat being considered is the submerged aquatic vegetation (SAV) that covers large portions of the substrate in shallow waters of this system.

Submerged aquatic vegetation provide numerous ecosystem services including enhanced biodiversity, erosion control and sediment stabilization, nutrient cycling, improved water quality, and organic carbon sequestration. Rapid environmental changes and increased coastal development have resulted in significant SAV losses globally. Currituck Sound, the northernmost estuary in North Carolina, was once known for extensive SAV beds serving as a refuge and food source to an abundance of fish and waterfowl that attracted anglers and hunters from all over the country. However, declines in water quality have led to massive declines in SAV habitat that have been devastating to the local ecology. This study investigated changes in historical and current SAV distribution and evaluated how these changes have been influenced by water depth, light availability, and bed-sediment composition. The overarching goals were to characterize the distribution of SAV as it relates to the physical properties of Currituck Sound prior to the construction of the Mid-Currituck Bridge, in order to provide a better understanding of the factors driving SAV distribution and to determine if suitable habitat for SAV mitigation exists in the project area. Following are key findings from the research tasks performed and an overview of how these findings inform the development of practical mitigation strategies.

### Simulating Wave Dynamics

Wind-generated waves can profoundly impact SAV cover, particularly those associated with severe storms. An evaluation of extreme wind events for select stations along the North Carolina coast revealed that while the 95$^{th}$ percentile wind speed and duration events influence SAV bed patterns, severe changes in SAV landscapes are ultimately a result of the 99.9$^{th}$ percentile events (i.e., the ‘clock-setters’). This analysis also indicated that while most sites were similar in that the wind field extreme events tended to occur from the north, some areas, such as Oregon Inlet, may have a disproportionate impact of wind events from the south contributing to extreme events.

Wind-wave energy fields were calculated using the Wave Exposure Model (WEMo; https://coastalscience.noaa.gov/research/coastal-change/wemo/) and used to generate a map of Representative Wave Energy (RWE; j m$^{-1}$ wave crest) across Currituck Sound. The model relied on inputs of local bathymetry and exceedance wind events (here, wind speeds ≥33.84 km/h) data to simulate conditions most likely to impact SAV abundance and distribution in Currituck Sound. Wave energy was subdivided into low (<1001 J m$^{-1}$), medium (1002–2942 J m$^{-1}$), and high (>2942 J m$^{-1}$) RWE strata. These wave energy strata were then used to inform the placement of field study sites for a series of hydroacoustic and in-water quadrat surveys conducted throughout the 2-year study from October 2017 to May 2019.

**Historic Change in SAV Distribution**

Four aerial photo interpreted SAV distribution datasets from 1990 (NOAA-OCM, 2015), 2003 (ECSU, unpublished data), 2008 (APNEP, 2019), and 2012 (APNEP, unpublished data) were used to assess the historical distribution of SAV in the region and compared with local bathymetry to evaluate the associated water depth limits of SAV. For these time periods, SAV were present up to maximum depths of 2.6–2.9 m and preferentially located at depths shallower than 1.0 m.

A time series of all SAV research in Currituck Sound leading up to and including this study shows a general shallowing of both the maximum depth and peak-depth limit (i.e., 80$^{th}$ percentile depth) of SAV distribution since ~1960. This shallowing of SAV presence is likely a function of declining water clarity.

**SAV Distribution in response to sediment character, water depth, and light availability**

Sediments were dominated by sand (average weight percent >90%) and had very low organic content (average percent loss on ignition ~1.0%). On average, sediments in the southern study area contained more sand and less organic matter than sediments in the northern study area. Despite some spatial and temporal variations in sediment composition, no statistical relationships between SAV cover and sediment characteristics were observed.

Light availability with water depth proved to be the dominant factor limiting SAV growth and distribution in Currituck Sound. An evaluation of the modern-day relationship between water depth and SAV cover revealed that SAV are not present beyond a depth of 1.8 m and are preferentially located at depths shallower than 1.0 m.

Measurements of photosynthetically active radiation (PAR) were used to calculate water-column light attenuation ($K_d$). The median $K_d$ for the combined 2016 and 2017 growing seasons was 1.99 $m^{-1}$. The calculated minimum water-column light requirement was 2.8% and water-column light requirement for peak growth was ≥13.7%.

The northern study area is characterized by larger expanses of shallow water depths and, therefore, has a greater areal extent of SAV compared to the southern study area overall. However, normalizing the data to account for differences in water depth indicated that SAV coverage at any given depth interval was greater in the south versus the same depth interval in the north.

**Water quality parameters influencing light availability**

Several possible water-quality parameters (turbidity, dissolved organic matter (fDOM), and chlorophyll-a) that directly influence light attenuation were investigated. This demonstrated that fDOM levels in Currituck Sound were consistently high throughout the study period and formed what was essentially a baseline optical attenuation signal above which all other variability was manifest. Chlorophyll-a and turbidity, largely a result of aperiodic, short-duration events, such as storms, had a much smaller overall contribution to light attenuation. Once the stresses (e.g., winds and associated waves, rainfall) associated with these events pass out of the area, the system quickly re-equilibrates to one which is dominated by dissolved organics in the water column.

**Management and Mitigation Implications**

Several important criteria for the determination of suitable habitat for SAV mitigation in Currituck Sound were considered (e.g., historical and current SAV distribution, sediment characteristics, wave exposure, water depth, and water quality). Sediment character showed very little variation (spatial or temporal) in this study and does not appear to be a major factor controlling the distribution of SAV. Wave exposure was tightly linked with water depth (i.e., higher energy in deeper waters). Given our data suggest Currituck Sound is an optically shallow environment, the influence of wave energy on SAV distribution could not be adequately differentiated from that of light attenuation. Ultimately, data on light availability with water depth, historical SAV cover, and current SAV cover were used to develop a preliminary mitigation site-selection model.

Given an understanding of SAV depth distribution and light availability in this system, water depth zones were differentiated by their likelihood of sustaining planted SAV. Zones shallower than 1.0 m (i.e., receiving 13.7% or more light) were deemed very likely to sustain planted vegetation, whereas zones between 1.0 and 1.5 m (i.e., receiving between 13.7 and 5.1% light) were moderately likely, and zones between 1.5 m and 1.8 m (i.e., receiving between 5.1% and 2.8% light) were the least likely. Using this empirical summary with an understanding of SAV presence during the last decade provided an aerial extent of suitable mitigation areas throughout Currituck Sound. However, due to uncertainties of the bathymetric data and aerial SAV maps, and the lack of modern synoptic SAV data in Currituck Sound since the 2012 APNEP aerial survey, site selection based on these data alone would be imprudent without additional data collection. The mitigation site-selection model presented as part of this study should be used to identify regions where focusing additional data collection efforts would be most appropriate. Additional data collection should focus on finer scale mapping of existing SAV and bathymetry.

This study has shown that in Currituck Sound, the primary factor limiting SAV distribution is water depth, thus, prior to choosing a mitigation site, it is vital that additional bathymetry is collected in areas deemed high priority for mitigation. This is especially true near and in between the marsh islands (e.g., the Big Narrows). Both the availability of protected sections (i.e., low wave energy) and historical SAV distribution suggest this could be a favorable area for mitigation. Ideally, further studies would be conducted to support some of the other parameters that affect suitability for SAV growth and survival (e.g., TSS, chlorophyll-a, DIN, DIP, CDOM, epiphytes, bioturbation), but practically, site selection could simply focus on water depth, proximity to existing vegetation, and avoidance of peat and sediments with high organic content.

**TABLE OF CONTENTS**

## LIST OF TABLES

## LIST OF FIGURES

## 1.0 INTRODUCTION

Currituck County is the northeastern-most county in North Carolina and includes the northern communities of the Outer Banks barrier-island system, separated from the mainland by Currituck Sound. The need for a crossing connecting the east and west portions of Currituck County was first identified in 1975 and formal planning by the North Carolina Department of Transportation (NCDOT) was initiated in 1995 (https://www.ncdot.gov/news/press-releases/Pages/2019/2019-02-08-mid-currituck-bridge-record-of-decision.aspx). The approximately 7-mile-long Mid-Currituck Bridge proposed by the NCDOT in cooperation with the North Carolina Turnpike Authority (NCTA) will connect Corolla, NC on the barrier island to Aydlett, NC on the mainland (Figure 1). In March 2019, the Federal Highway Administration (FHWA) approved the project that is expected to cost $491 million dollars. The bridge will alleviate the at times severe congestion across the Wright Memorial Bridge, located nearly 20 miles south (Figure 1), and surrounding areas, particularly in the summer months when the population on the Outer Banks more than doubles due to its popularity as a vacation destination. Improving the flow of traffic is especially important when considering emergency evacuation times for severe storms including hurricanes, which primarily occur during the busy summer months (NCDOT, 2012).

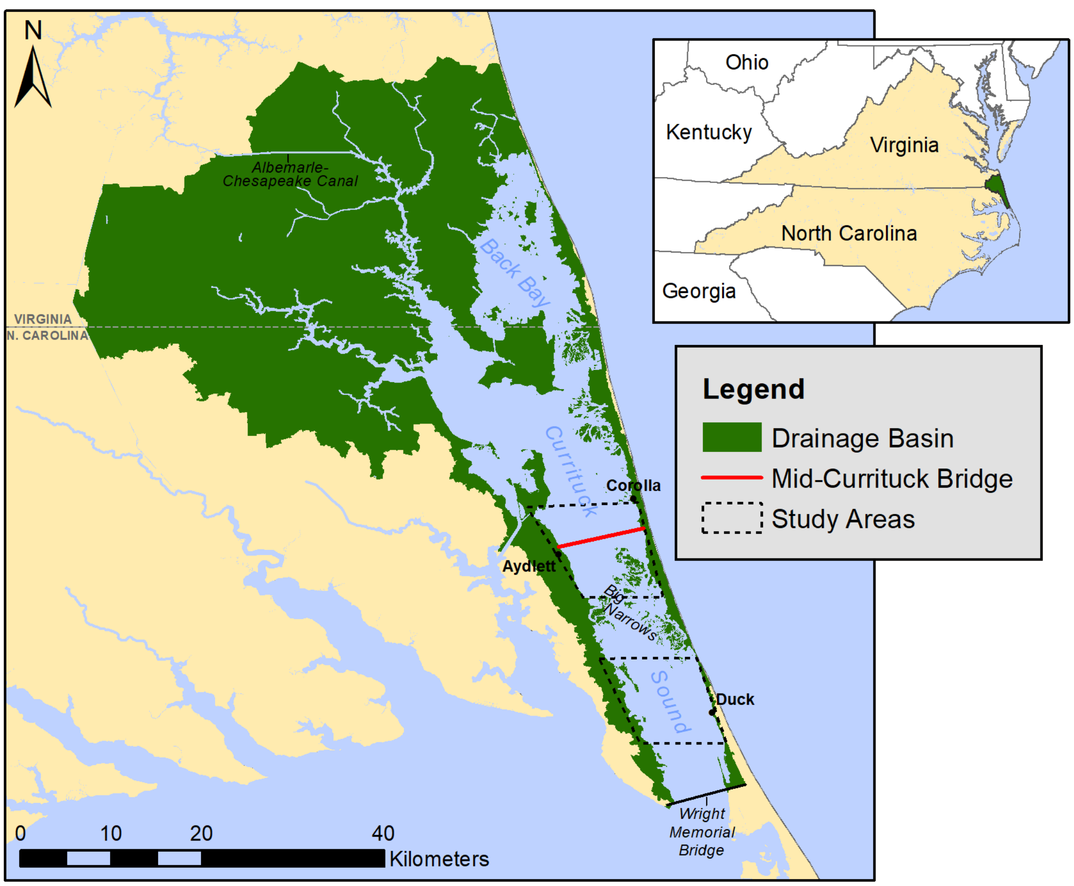


**Figure 1. Map of Currituck Sound, including the drainage basin (green shaded region), the proposed location of the Mid-Currituck Bridge (red line), and the locations of the study areas (dashed boxes). Drainage basin generated by U.S. Geological Survey, 2016, The StreamStats program, online at http://streamstats.usgs.gov.**

Concerns surrounding the construction of the Mid-Currituck Bridge include the potential impacts to water quality and aquatic habitats in Currituck Sound. One important habitat being considered is the submerged aquatic vegetation (SAV) that covers large portions of the shallow waters in this system. The immediate repercussions are direct impacts to existing SAV beds and increased turbidity from pile driving, filling, and clearing during bridge construction and maintenance (NCDOT, 2012; Wagner, 2016). The potential long-term effects include degraded water quality and loss of habitat as a result of increased stormwater discharge, primarily associated with bridge deck runoff, and decreased light availability from shading (NCDOT, 2012; Wagner, 2016). SAV beds are critical for enhancing water quality and maintaining healthy local ecosystems and are recognized as an essential fish habitat (EFH). As such, this habitat is regulated by federal and state agencies, and losses are subject to compensatory mitigation. NCDOT expects 1.4 ha of existing SAV habitat and 2.1 ha of potential SAV habitat (i.e., unvegetated areas in ≤1.8 m of water) to be permanently impacted by shading (NCDOT, 2019). Mitigation is only required for existing SAV habitat and not for potential SAV habitat. One mitigation option proposed by the NCTA is in-kind restoration at a suitable site at a 2:1 ratio (NCDOT, 2019). This study aims to characterize the distribution of SAV as it relates to the physical properties of Currituck Sound prior to the construction of the Mid-Currituck Bridge to provide a better understanding of the controls driving SAV distribution and to determine if suitable habitat for mitigation exists in the project area. Specifically, the objectives of this study are to (1) evaluate current and historic change of SAV distribution in two focus areas of Currituck Sound, and (2) relate SAV distribution to water-column and substrate parameters and physical processes (e.g., waves, salinity, turbidity, etc.). Salinity and hydrodynamics are considered both in the development of methods and as a part of the discussion, however, the primary focus of this study is on understanding the influence of light availability and sediments on SAV habitats in Currituck Sound.

## 2.0 BACKGROUND

### 2.1 Submerged Aquatic Vegetation (SAV)

Submerged aquatic vegetation (SAV) are a group of aquatic plants that are adapted to live underwater with only brief periods of exposure during extreme low tides or storms. As primary producers, SAV are integral to a variety of aquatic ecosystems. They help sustain commercial and sport fishing, hunting, and shellfish trapping by serving as a food source to various fish and waterfowl (Sincock et al., 1965; Orth et al., 2006) and providing habitat, most significantly, to juvenile fish and shellfish (Beck et al., 2001). SAV beds can attenuate wave energy and current velocities, thus reducing shore erosion, increasing rates of sedimentation, and decreasing the potential for sediment resuspension (Ward et al., 1984; Madsen et al., 2001). Additionally, SAV beds buffer nutrient inputs both directly, through assimilation, and indirectly, by enhancing nutrient sequestration (e.g., phosphorous sorption) and cycling (e.g., coupled nitrification-denitrification) in sediments, thus reducing the potential for eutrophication (McGlathery et al., 2007). These processes are critical for reducing turbidity and enhancing water clarity, which are adversely affected by excess suspended sediments and phytoplankton in the water column (Dennison et al., 1993; Moore et al., 2004; Orth et al., 2006). Perhaps one of the most important global ecosystem services that SAV habitats provide is climate regulation due to their high efficiency at storing organic carbon, also known as "blue carbon" (Fourqurean et al., 2012; Greiner et al., 2013; McLeod et al., 2011). Despite the relatively small global coverage of seagrass habitats, these "blue carbon" sinks, like other vegetated coastal ecosystems (e.g., mangroves and salt marshes), can contribute to greater long-term carbon sequestration than terrestrial habitats and, thus, are disproportionately important for reducing atmospheric carbon dioxide and mitigating climate change (Fourqurean et al., 2012; Tokoro et al., 2014; Greiner et al., 2013; McLeod et al., 2011).

The conservation of SAV has become a global issue over the past several decades as a result of significant losses worldwide at seemingly increasing rates of decline (Dennison et al., 1993; Orth et al., 2006; Waycott et al., 2009). Declines can be linked to natural disturbances such as extreme weather events (e.g., hurricanes, ice scour), disease, and over-consumption by animals, but anthropogenic impacts seem to be driving most major losses (Short and Wyllie-Echeverria, 1996; Orth et al., 2006; Waycott et al., 2009). Beyond direct physical impacts (e.g., boating, fish farming and aquaculture), the most common and significant threat to SAV is increased loading of nutrients, sediments, and contaminants associated with human activities in adjacent watersheds (e.g., agriculture, industrial and municipal waste, coastal development; Dennison et al., 1993; Kemp et al., 2005; Orth et al., 2006). Furthermore, impacts from global climate change (e.g., increased water temperature, carbon dioxide concentrations, sea level, and frequency and intensity of storms) have been recognized as another major threat with potentially catastrophic effects on SAV (Short and Neckles, 1999; Orth et al., 2006; Waycott et al., 2009). Given the vital role of SAV habitats in coastal ecosystems, both ecologically and for human interests, it is important to understand the processes that drive changes in the distribution of these plant communities to improve conservation and management strategies.

SAV abundance and distribution are entirely dependent on the complex hydrodynamic, geological, biological, and chemical parameters controlling the environments they inhabit. The primary factors promoting or limiting SAV growth are, in simple terms, light, salinity, sediments, and water motion (Batiuk et al., 2000; Koch, 2001). Compared to other plant groups, SAV require some of the highest light levels (Dennison et al, 1993; Orth et al., 2006), therefore, light is often identified as the major driver controlling SAV habitats. Light availability is mainly a function of water clarity and the parameters altering it such as total suspended sediments (TSS), dissolved inorganic nitrogen (DIN), dissolved inorganic phosphorus (DIP), chlorophyll-a, and colored dissolved organic matter (CDOM), but can also be affected by the accumulation of epiphytic materials on the surface of leaves (Batiuk et al., 2000; Kemp et al., 2004). SAV habitat requirements and growth patterns can vary substantially between salinity regimes (e.g., fresh, oligohaline, mesohaline, polyhaline; Batiuk et al., 1992; Fonseca et al., 1998) and generally have stricter requirements with increasing salinity due to the additional energy required for increased osmoregulation (Batiuk et al., 1992; Kantrud, 1991). The grain size, organic content, and nutrient concentrations in sediments and interstitial fluids can affect SAV growth (Barko and Smart, 1986; Batiuk et al., 2000; Koch, 2001), and as a result, sedimentation and spatial patterns in sediments can affect the distribution of SAV beds (Fonseca et al., 1998; Short et al., 2002; Koch et al., 2004). The effects of water movement (i.e., currents, waves, tides, and turbulence) on SAV can be seen through direct impacts such as strong currents and waves eroding sediments or tides limiting the minimum water depth of SAV growth, as well as indirect impacts like sediment resuspension and water-column mixing (Koch, 2001; Madsen et al., 2001). Developing a better understanding of the interaction between these four primary factors (i.e., light, salinity, sediments, and water motion) and their effect on SAV in a system is vital for ecosystem management (Fonseca et al., 1998).

## 2.2 SAV in Currituck Sound

Currituck Sound is the northernmost component of the Albemarle-Pamlico Estuarine System (APES) of North Carolina. The predominantly shallow (average water depth = 1.5 m; maximum water depth = 4.0 m) and oligohaline (0.5–5 ppt) estuary varies in width from 5 to 13 km and extends northward for approximately 58 km from the Albemarle Sound into southeastern Virginia where it connects with Back Bay (Figure 1). Currituck Sound has approximately 400 $km^2$ of open water bordering numerous marsh islands, particularly along the eastern shore and in the middle of the Sound. These islands make up a small portion of the nearly 1,900 $km^2$ of land that drain into the Sound, over half of which is contained in southeastern Virginia (Figure 1; Rideout, 1990; Caldwell, 2001; Wagner et al., 2016).

Historically, Currituck Sound has been associated with at least five paleo-inlets, the last of which, the New Currituck Inlet, closed between 1828 and 1830 (Figure 2; Sincock et al., 1965; Carter and Rybicki, 1994; USACE, 2012; Moran et al., 2015). After the closure of the New Currituck Inlet, the Sound became relatively isolated from the Atlantic Ocean and the once tidally influenced brackish-to-saline waters were converted into the wind-driven fresh-to-oligohaline conditions present today (Sincock et al., 1965; Carter and Rybicki, 1994; USACE, 2010; USACE, 2012; McKay et al., 2012). In 1846, the presently active Oregon Inlet was formed when a hurricane buffeting the North Carolina coast broke through the barrier spit near the site of the previously closed Gunt Inlet (Figure 2; Mallinson et al., 2008). Oregon Inlet lies nearly 40 km south of Currituck Sound (Figure 2) and remains the closest hydraulic connection to the Atlantic (Mallinson et al., 2008; Moran et al., 2015; Wagner et al., 2016). Therefore, circulation and water levels in Currituck Sound are primarily controlled by wind, with southerly winds (dominant in the summer) pushing water into the Sound (i.e., raising water levels) and northerly winds (dominant in the winter) moving water out of the Sound (i.e., lowering water levels; Sincock et al., 1965; Benner et al., 1982; Wagner et al., 2016), and minimal influence from astronomical tides.

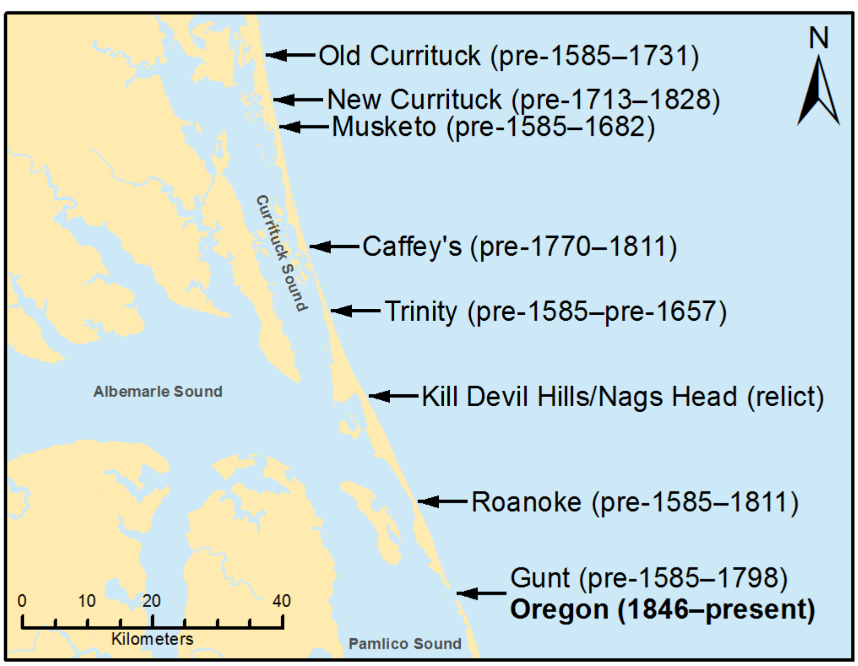


**Figure 2. Map of historic and present inlets in northeastern North Carolina and their associated opening/closing dates (Mallinson et al. 2008; Moran et al., 2015).**

Currituck Sound historically supported broad expanses of submerged and emergent aquatic vegetation with flourishing waterfowl and fish communities that led to its reputation as a “sportsman’s paradise” (Sincock et al., 1965; Wicker and Endres, 1995). However, these habitats have been increasingly subject to anthropogenic impacts, as the nearby population has surged dramatically over the past several decades (Figure 3; Rideout, 1990). From 1960 to 1970 alone, the population in the drainage basin doubled from roughly 80,000 to 160,000 (Forstall, 1996). This rapid population growth has been largely associated with increases in coastal and estuarine development, which have contributed to the degradation of water quality and ecosystem health, including loss of SAV coverage (Sincock et al., 1965; Rideout, 1990; Wicker and Endres, 1995; Fear, 2008). Although fluctuations in SAV coverage have been documented since the early 1920s and reportedly caused by both anthropogenic and natural events (Carter and Rybicki, 1994), studies have revealed a significant decline in SAV coverage coinciding with the population surge that began in the 1960s (USACE, 2011). It has been hypothesized that the greatest threats to the waters of Currituck Sound are nonpoint-source runoff from agriculture, industry, and development, septic waste contamination, and excessive turbidity from suspended sediments or increased algal productivity (NCDEHNR and EPA, 1994; USACE, 2010; USACE, 2012). Previous work in the region provides some insights into the processes driving SAV decline and has guided the focus of this study (Bourn, 1932; Dickson, 1958; Sincock et al., 1965; Davis and Carey, 1981; Davis and Brinson, 1983, 1990; Ferguson and Wood, 1994; Carter and Rybicki, 1994).

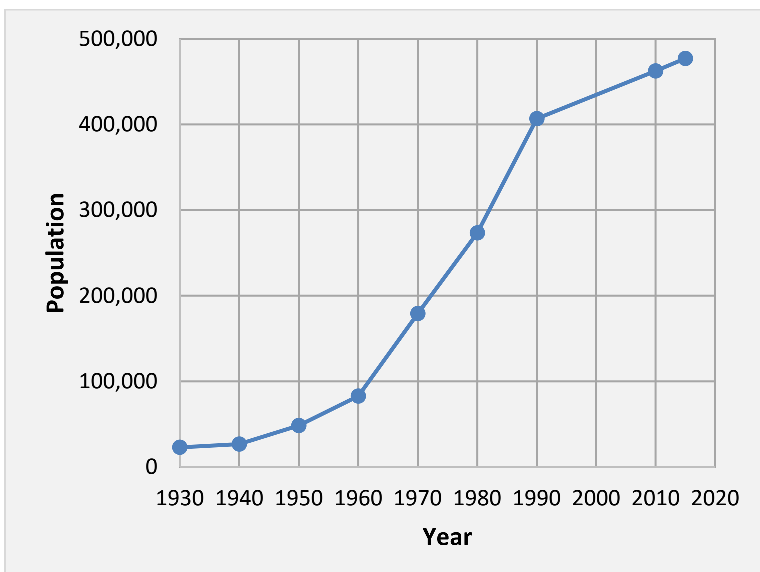


**Figure 3. Population change in the Currituck Sound drainage basin from 1930 to 2015. Based on data from the U.S. Census Bureau for Currituck County, NC and Virginia Beach City, VA.**

The importance of light in this system is undeniable as all major studies in Currituck Sound have cited turbidity as a primary factor influencing SAV abundance and distribution (e.g., Bourn, 1932; Dickson, 1958; Sincock et al., 1965; Davis and Carey, 1981; Davis and Brinson, 1983, 1990; Ferguson and Wood, 1994; Carter and Rybicki, 1994). Turbidity variations in the Sound have been attributed to several environmental changes including raw sewage and industrial waste inputs by way of the Albemarle-Chesapeake Canal (Figure 1; Bourn, 1932), dredging and filling activities in tributaries and within Back Bay (Figure 1; Bourn, 1932;

Sincock et al., 1965; Riggs et al., 1993), extreme weather events (Dickson, 1958; Sincock et al., 1965; Davis and Carey, 1981; Davis and Brinson, 1983, 1990), and changes in flocculation of suspended sediments due to unusually high or low salinity (Sincock et al., 1965; Davis and Carey, 1981; Davis and Brinson, 1983; Fear, 2008). However, these studies relied on infrequent (e.g., approximately monthly) measurements of Secchi depth as a proxy for light conditions in the water column (Sincock et al., 1965; Davis and Carey, 1981). Due in part to the fact that Secchi depth measures the full spectrum of visible light as opposed to the select light wavelengths used in photosynthesis, studies have demonstrated that it is difficult to evaluate a relationship between light penetration and SAV when using only measurements of Secchi depth, particularly when turbidity is high (Middleboe and Markager, 1997). Thus, the relationship between light attenuation in the water column and SAV distribution has not been quantitatively defined for Currituck Sound.

The spatial distribution of sediments and the relationship between SAV and sediment type were assessed by Sincock et al. (1965) in 1960 and 1962 and again by Hartis (2013) in 2010. In these studies, sediment type was estimated and classified based on perceived texture (e.g., sand, loam, silt, clay, muck, peat, or shell; Sincock et al, 1965; Hartis, 2013). While adequate for a first approximation, this method's subjectivity leads to a high margin of error as was noted by Sincock et al. (1965). Sediment grain size was analyzed three times during a 2011 to 2015 study by Wagner et al. (2016); however, samples were limited to five locations along the proposed Mid-Currituck Bridge corridor (Figure 1), leaving sediment characteristics elsewhere in the Sound largely unquantified.

Freshwater inputs in the northern portion of the Sound, mixing with the slightly more saline water from the Albemarle Sound in the south, and restricted mixing across the densely packed marsh islands in the region referred to as the "the Big Narrows" (Figure 1) has resulted in transitory salinity differences between the northern and southern reaches of the Sound (Sincock et al., 1965; Caldwell, 2001). However, these differences are likely not the norm. Under most weather conditions (i.e., no strong winds or heavy rainfall), there is little variation in salinity across the Sound (Caldwell, 2001). Because of this, salinity is likely not contributing to significant changes in SAV distribution on shorter timescales in Currituck Sound. Still, drastic salinity variations as a result of major events, such as storm-induced overwash or sea water pumping into the Sound, can engender changes to existing SAV beds (Sincock et al., 1965; Davis and Brinson, 1983; Fine, 2008; Wagner et al., 2016). Thus, it is important to consider the potential impacts of large salinity fluctuations in this system.

Currituck Sound is shallow and a predominantly wind-driven system (Sincock et al., 1965; Benner et al., 1982; Davis and Brinson, 1983; Caldwell, 2001, Fine, 2008). Therefore, SAV growth and distribution is likely influenced by wind-generated waves (Koch, 2001). Although the effect of wave exposure on SAV was not previously calculated for Currituck Sound, several studies have attributed changes in distribution to severe storms and wind events causing excessive sediment resuspension and/or breakage and uprooting of plants (Dickson, 1958; Davis and Carey, 1981; Davis and Brinson, 1983, 1990).

## 3.0 SUMMARY OF DATA COLLECTION

### 3.1 Study Design

The historical distribution of SAV for all of Currituck Sound was assessed using digitized maps derived from interpretations of aerial photographs. These maps were also used in conjunction with local bathymetry to assess the historical water depth limits of SAV at a regional scale. Modern SAV dynamics and habitat characteristics were explored using three methods: (1) hydroacoustic mapping, (2) quadrat surveys, and (3) light availability modeling. The hydroacoustic surveys were used to evaluate the modern water depth limits of SAV. Sediment and SAV species composition were characterized during quadrat surveys. Finally, the attenuation of photosynthetically active radiation (PAR) through the water column was measured and a light-depth model assessed the expected distribution of SAV based on the observed water depth limits.

Previous works have revealed that SAV are important indicators of water quality and ecosystem health, meaning that long-term changes in abundance and distribution are often symptomatic of ecosystem degradation (Dennison et al., 1993; Middleboe and Markager, 1997; Orth et al., 2006; Piepho, 2017). These changes include a shallowing of the maximum depth of distribution ($Z_{max}$),which has become an important barometer of ecosystem health useful for developing management strategies to reduce anthropogenic inputs, such as nutrients and sediments, and restore water quality (Sheldon and Boylen, 1977; Chambers and Kalff, 1985; Dennison et al., 1993; Kenworthy and Fonseca, 1996; Orth et al., 2006; Zhu et al., 2006, 2007; Piepho, 2017). However, when the goal is to successfully mitigate for SAV losses, then it is highly advised to choose mitigation sites that are shallower than $Z_{max}$ (Zimmerman et al., 1994; Fonseca et al, 1998). In addition to identifying $Z_{max}$, the "peak-depth limit" or $Z_{peak}$, defined here as the 80$^{th}$ percentile of depth for SAV presence, was also measured in this study.

**3.2 WEMo Simulation and Field Site Placement**

Wind generated waves can profoundly impact SAV cover, particularly those associated with severe storms. An evaluation of extreme wind events for select stations along the North Carolina coast revealed that while the 95$^{th}$ percentile wind speed and duration events influence SAV bed patterns, severe changes in SAV landscapes are ultimately a result of the 99.9$^{th}$ percentile events (i.e., the clock-setters; Appendix A). Identifying these events and understanding how they influence hydrodynamic conditions is critical for determining habitat susceptibility. To address this, the wave dynamics in Currituck Sound were calculated and used to develop a stratified distribution of field-survey sites.

The hydroacoustic and quadrat field-based surveys were focused on two study areas in Currituck Sound, a northern area and a southern area (Figures 1 and 4). These two areas were approximately 80 km$^2$ each and separated by the Big Narrows (Figure 1). The northern study area held a large portion of the flood tide delta created by the historic Caffey's Inlet and was, therefore, much shallower than the southern study area. Wind-wave energy fields across the Sound were calculated with the Wave Exposure Model (WEMo; https://coastalscience.noaa.gov/research/coastal-change/wemo/). WEMo is a numerical model that computes Representative Wave Energy (RWE) on user-defined grid points using local bathymetry and wind data inputs (Malhotra and Fonseca, 2007). Within these north and south boundaries, 22 field sites were distributed among wave energy strata and patchy or dense historical SAV cover.

First, bathymetry and wind data were located and evaluated. For bathymetry the NCEI Coastal Relief Model data were initially considered (https://www.ngdc.noaa.gov/mgg/coastal/grddas02/html/gna37076.htm) but upon inspection, these data were not sufficiently resolved to provide accurate wave forecasts. Instead, data from a variety of sources (shown in Figure 5) were compiled using ArcGIS to generate a comprehensive bathymetric dataset. NOAA's ADCIRC Topobathy (https://adcirc.org/) was used as the underlying bathymetry because it provided coverage for the entire region and accounted for far-field influence on wave development (i.e., out to 50 km). This dataset was then supplemented by more highly resolved, albeit less spatially extensive, data from single-beam (Forte, unpublished data; October 2017 BioSonics survey from this study) and multi-beam surveys (Forte, 2007; Wadelynn Geospatial LLC, unpublished data) conducted in the Sound for near-field (i.e., within Currituck Sound proper) bathymetry effects on wind-wave development. All these datasets were combined and interpolated to create a single raster grid of bathymetry and used to generate updated isobaths used in this study (Figure 6).

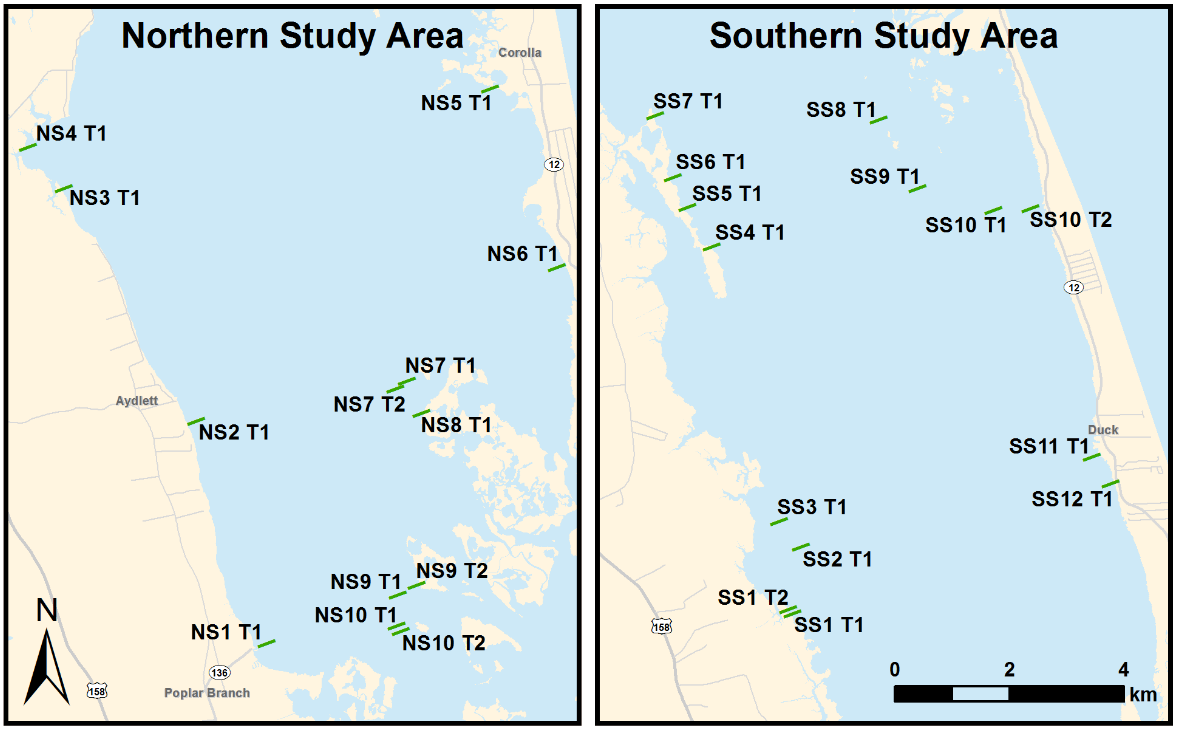


**Figure 4. Map showing the location and names of the sites and transects in the northern (left) and southern (right) study areas. See Figure 1 for location map.**

Hourly data on wind speed and direction were obtained from NOAA's National Data Buoy Center (NDBC) station DUKN7 in Duck, NC (http://www.ndbc.noaa.gov/station_history.php?station=dukn7) for all available years (i.e., 2008–2016). Only the top 5% of wind speed events (i.e., exceedance winds; after Keddy, 1982 and here, winds speeds ≥33.84 km/h) were used in the WEMo model because these represent the conditions most likely to have impact on SAV abundance and distribution (Fonseca and Bell, 1998; Malhotra and Fonseca, 2007). The frequency distribution of the wind speed events was determined using Proc Univariate in SAS (ver.9.2). The frequency at which these exceedance winds occurred from eight compass headings in 45° increments (e.g., NN, NE, EE, etc.) were calculated (Table 1). This revealed a strong northerly dominance of exceedance wind events near Duck, NC. RWE was computed by the WEMo model for a 250-m resolution grid, resulting in 2,590 points throughout Currituck Sound. Those points were then evaluated for their cumulative frequency distribution again using Proc Univariate in SAS (9.2). Wave energy was subdivided into low (<1001 J $m^{-1}$), medium (1002–2942 J $m^{-1}$), and high (>2942 J $m^{-1}$) RWE strata (Figure 7) representing 33% breakpoints in the cumulative frequency distribution (Malhotra and Fonseca, 2007).

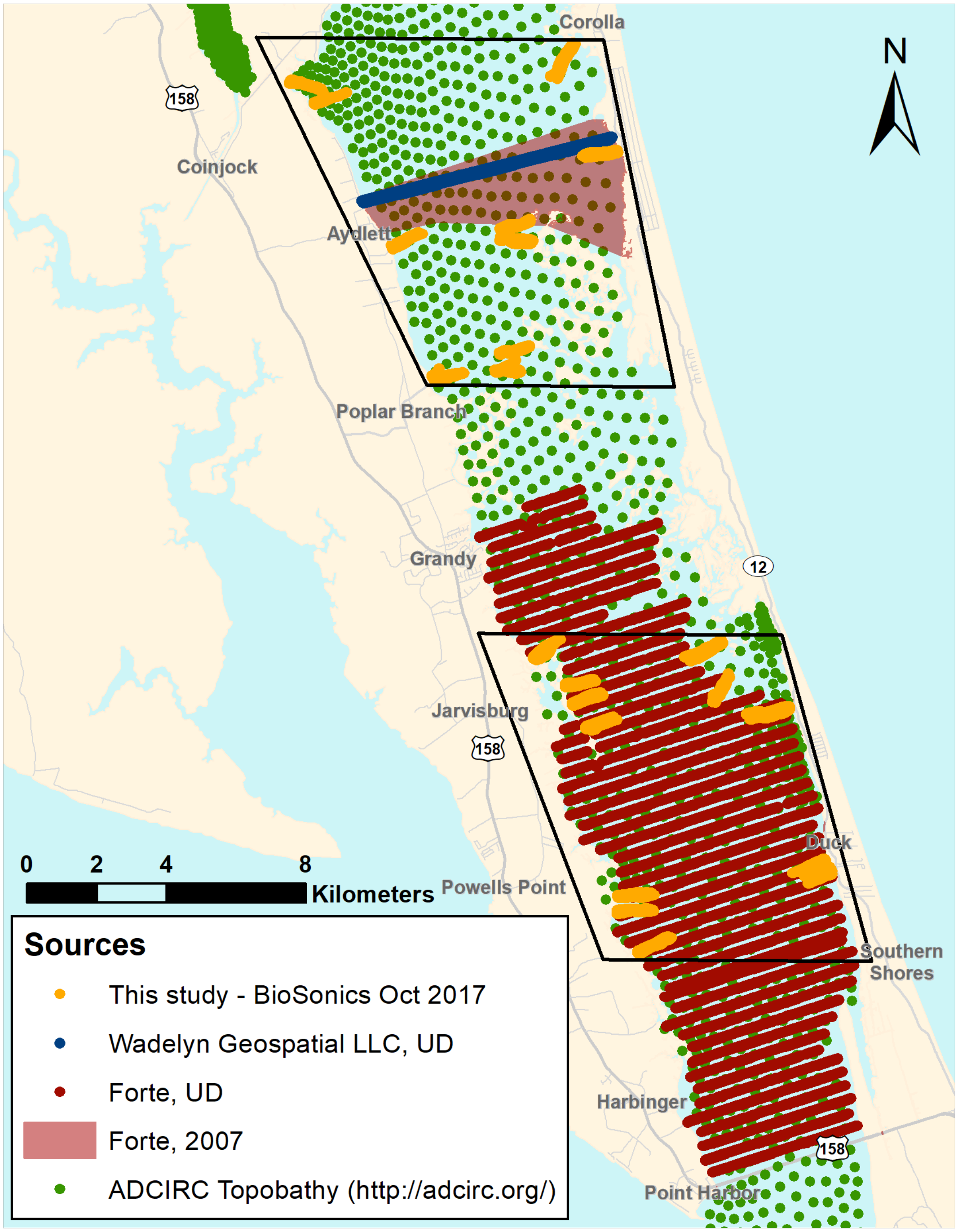


**Figure 5. Sources and spatial extent of all available bathymetry data used to create a depth raster surface and contours (Figure 6). UD = unpublished data.**

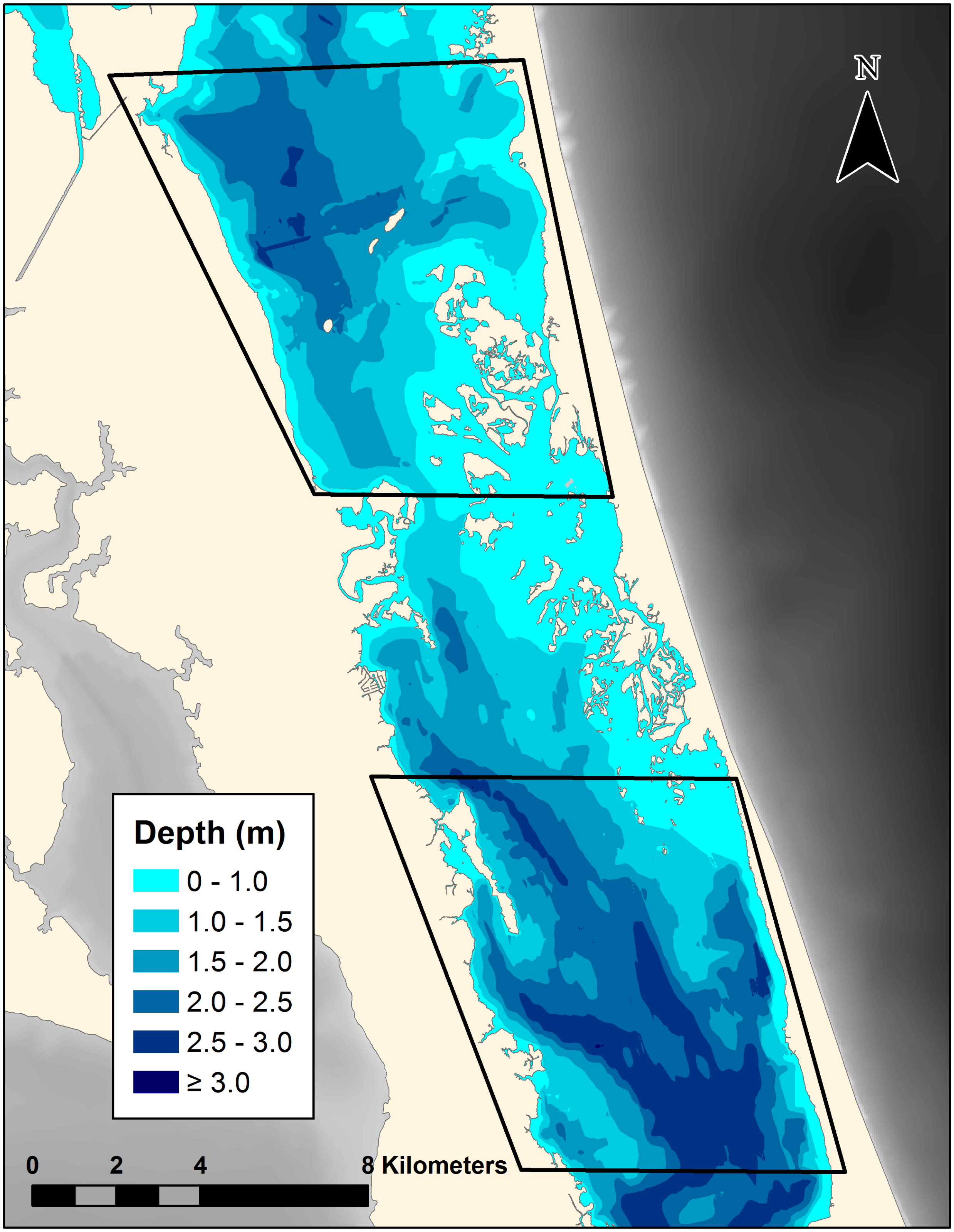


**Figure 6. Depth contours made from interpolating all available bathymetric data in Currituck Sound (data extent and sources shown in Figure 5).**

**Table 1. Percent frequency of exceedance winds (top 5% wind speeds) by compass heading.**

| Compass direction | % of events |
|---|---|
| NN | 46.72 |
| NE | 27.07 |
| EE | 2.64 |
| SE | 2.27 |
| SS | 6.58 |
| SW | 2.89 |
| WW | 3.12 |
| NW | 8.71 |

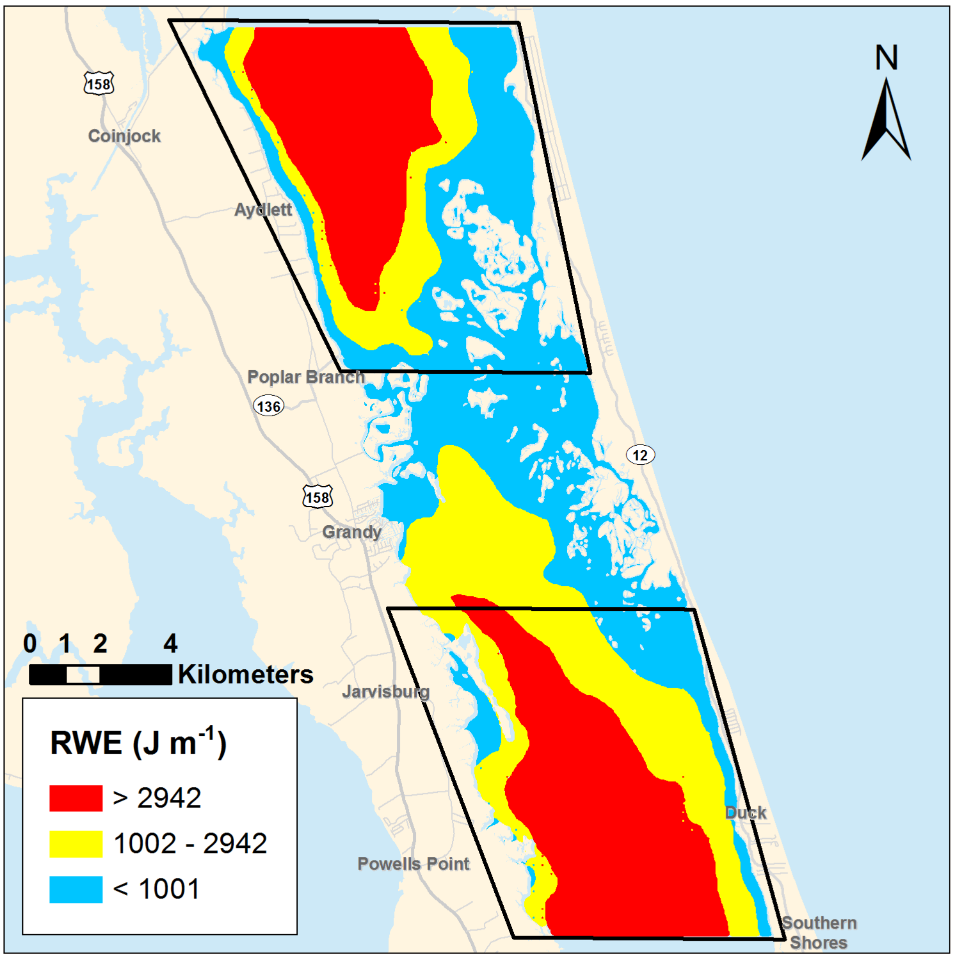


**Figure 7. WEMo computed representative wave energy (RWE) for Currituck Sound. Blue represents low wave energy (<1001 J m$^{-1}$), yellow represents medium wave energy (1002–2942 J m$^{-1}$) and red represents high wave energy (>2942 J m$^{-1}$).**

These wave energy strata were overlain by SAV distribution maps from 1990 (NOAA-OCM,2015), 2003 (ECSU, unpublished data), 2008 (APNEP, 2019), and 2012 (APNEP, unpublished data; Figure 8). Visual inspection of these data indicated that the 2008 APNEP (2019) dataset showed the greatest extent of potential SAV coverage; thus, this map was used to determine the likely present-day locations of patchy or dense SAV cover. Twenty-two field sites were then arranged within the two study areas to include variances in wind-wave energy and SAV cover (i.e., north-low energy-dense SAV, north-low energy-patchy SAV, etc.). Thus, ensuring the field assessments would capture a range of characteristics that could best represent SAV distribution for the entire Sound. Very few opportunities were observed for the combination of either patchy or dense SAV within the high or medium wave energy strata. Best professional judgement was used to select field sites within the various combinations. Final site distribution and location of monitoring transects for in-water quadrat surveys (Figure 4) was made based on modern SAV conditions observed during the first hydroacoustic survey in October 2017.

### 3.3 Historical SAV Cover

Four maps of photo-interpreted SAV beds in Currituck Sound (Figure 8) were used to assess the historical distribution of SAV at a regional scale (i.e., north of the Wright Memorial Bridge and south of the North Carolina-Virginia border; Figure 1). The aerial images were acquired and analyzed by the National Oceanic and Atmospheric Administration (NOAA) in 1990 (NOAA-OCM, 2015), Elizabeth City State University (ECSU) in 2003 (ECSU, unpublished data), and the Albemarle-Pamlico National Estuary Partnership (APNEP) in 2008 (APNEP, 2019) and 2012 (APNEP, unpublished data). Spatiotemporal variations in SAV coverage (i.e., gain, loss, and no change) were evaluated by comparing consecutive surveys (i.e., 1990–2003, 2003–2008, and 2008–2012) using the geographic information system ArcGIS (ArcGIS Desktop 10.4.1; ERSI, Inc., Redlands, CA). The areas where the datasets intersected indicated that SAV was found during both time periods (i.e., no change). SAV gain was determined by erasing an older dataset from a newer dataset and loss was determined by erasing a newer dataset from an older dataset. Based on the aerial datasets, SAV beds in Currituck Sound covered approximately 2,132 ha in 1990, 3,659 ha in 2003, 6,294 ha in 2008, and 5,730 ha in 2012. The areas that gained, lost, and had no change in SAV presence are shown in Figure 9. This analysis suggests a net gain in SAV from 1990 to 2003 and from 2003 to 2008 and a net loss from 2008 to 2012. The datasets did not provide any accuracy assessment results, therefore, the errors associated with this analysis are not quantifiable.

The SAV distribution maps (Figure 8) were compared with local bathymetry to examine the historical depth distribution of SAV and identify the associated water depth limits (i.e., $Z_{max}$ and $Z_{peak}$). The bathymetry dataset developed for the WEMo computation was combined with each of the four SAV distribution maps (i.e., 1990, 2003, 2008, and 2012) and a grid of points spaced 20-m apart was generated over the SAV polygons for each dataset (i.e., the areas where SAV was present). The histograms in Figure 10 illustrate percent frequency of SAV presence across 20-cm depth intervals for the four datasets. The maximum depth of distribution ($Z_{max}$) was determined to be 2.6 m in 1990, 2.7 m in 2003 and 2008, and 2.9 m in 2012. The peak-depth limit ($Z_{peak}$) was 1.0 m in 1990 and 2003, 0.9 m in 2008, and 0.8 m in 2012. The existing bathymetry for the region was improved by incorporating single-beam and multi-beam data; however, due to some prevailing issues (i.e., limited data in the shallowest regions and strong reliance on the low-resolution NOAA ADCIRC dataset in some areas) along with the challenges of mapping SAV in poor water-clarity environments, it is likely that the largest errors occur at the depth extremes (i.e., shallowest and deepest) and in the regions relying primarily on the ADCIRC dataset (e.g., northwards and in between the marsh islands; Figure 5).

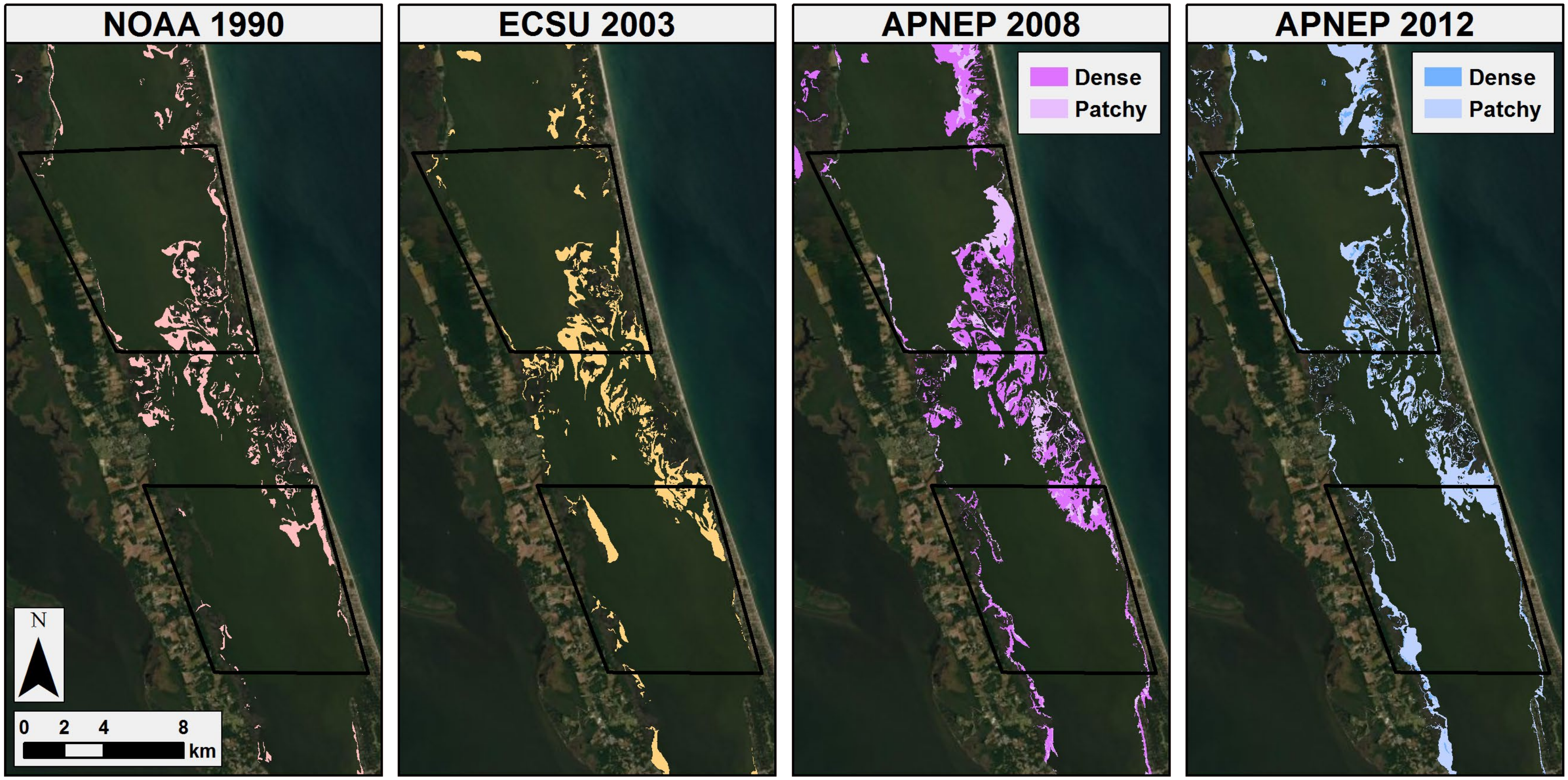


**Figure 8. SAV distribution maps for 1990 (NOAA-OCM, 2015), 2003 (ECSU, unpublished data), 2008 (APNEP, 2019), and 2012 (APNEP, unpublished data) created from digitized aerial photography.**

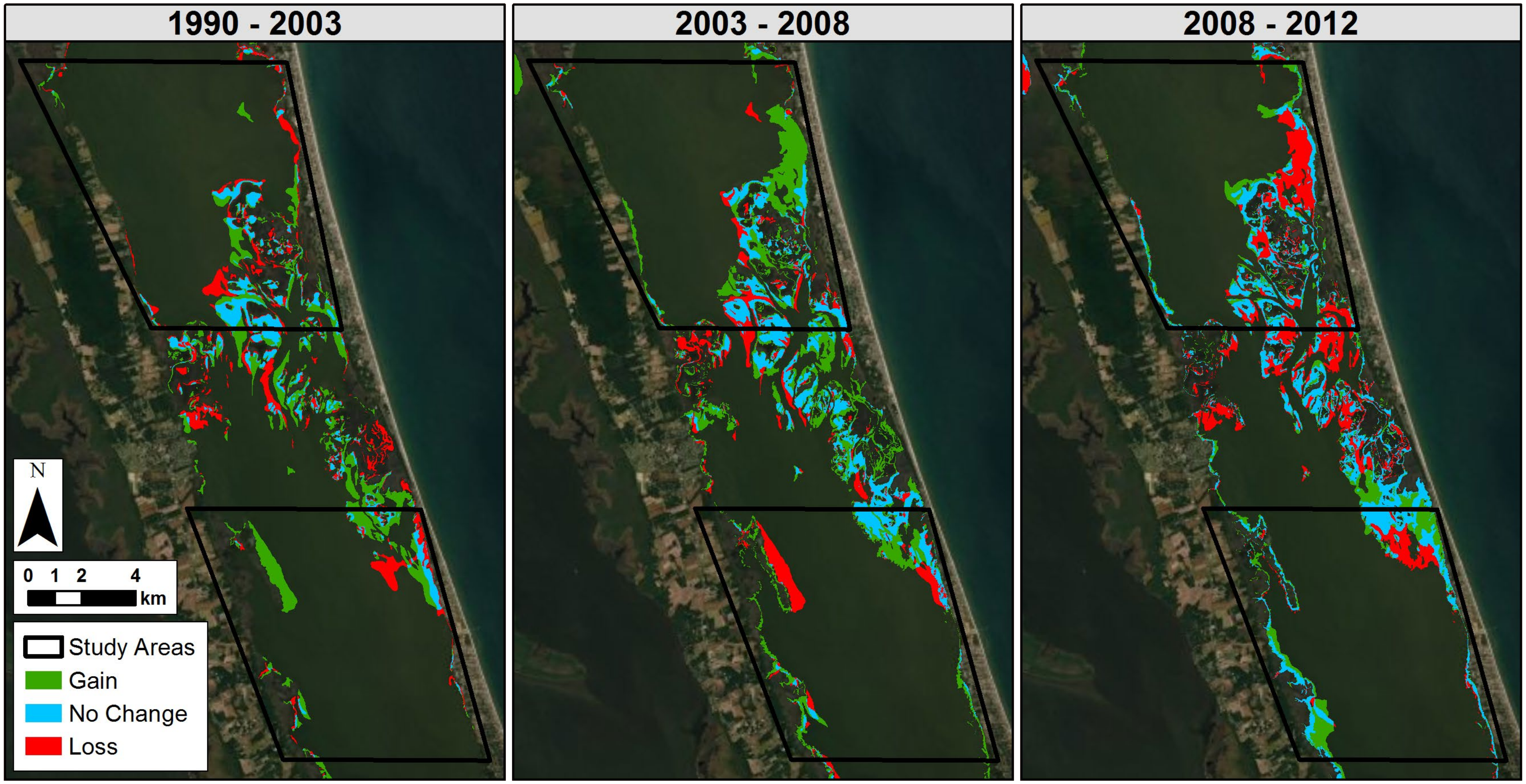


**Figure 9. Maps illustrating the areas that experienced SAV gain (green), loss (red), and no change (blue) from 1990 to 2003 (left), 2003 to 2008 (middle), and 2008 to 2012 (right). Created using the SAV distribution datasets shown in Figure 8.**

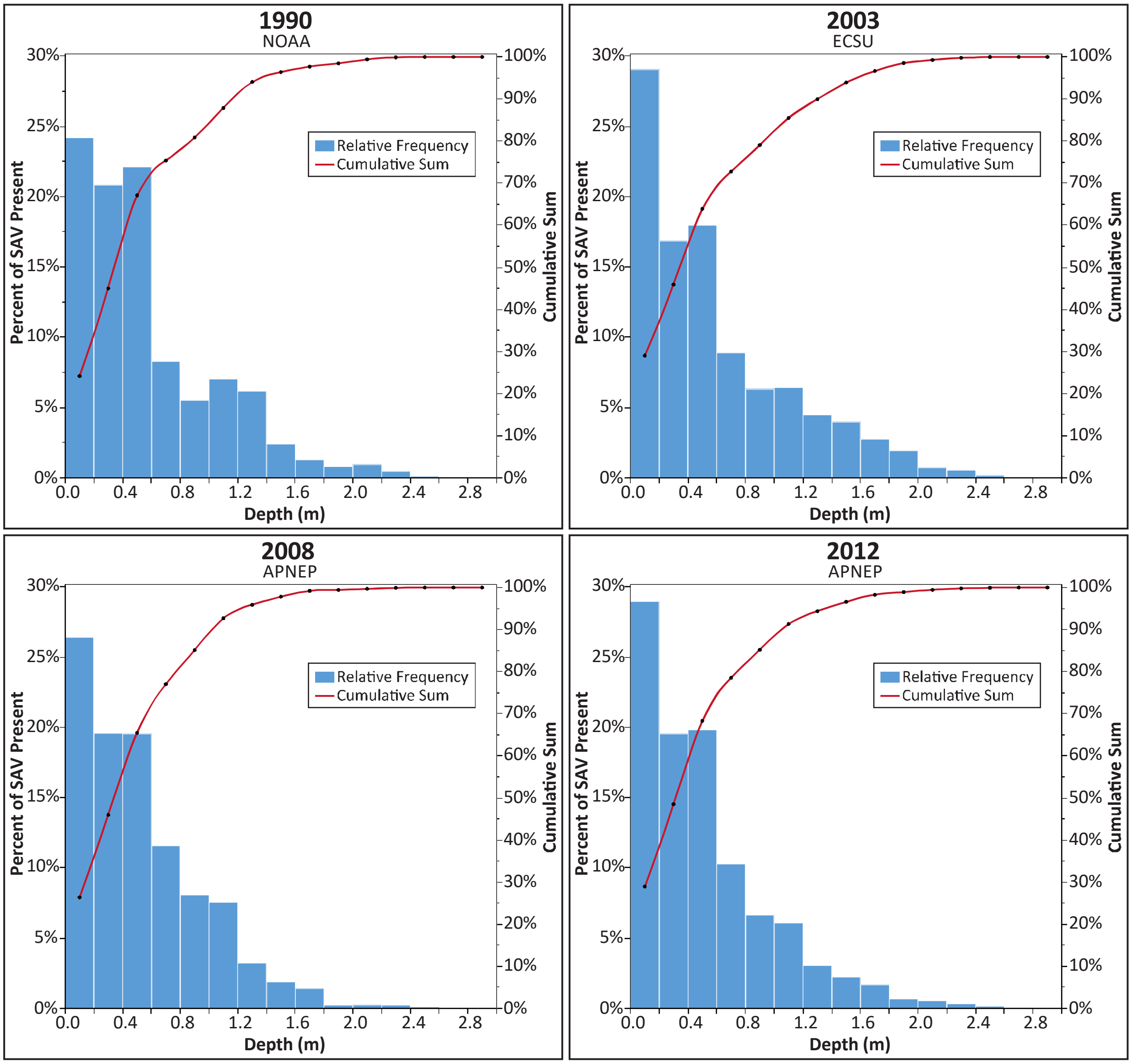

**Figure 10. Histograms showing the distribution of SAV presence with depth as mapped with aerial surveys in 1990, 2003, 2008, and 2012 (shown in Figure 8).**

### 3.4 Hydroacoustic Surveys

Three hydroacoustic surveys were conducted throughout the 2-year study period to evaluate the modern relationship between SAV and water depth: in October 2017, June 2018, and May 2019. Data were collected with a BioSonics 204.8 kHz single-beam echosounder (i.e., BioSonics MX Aquatic Habitat Echosounder, transducer beam angle 8.4°, pulse length 0.4 ms, ping rate 5 Hz) and recorded by the proprietary Visual Acquisition software (BioSonics, Inc., Seattle, WA). The transom-mounted transducer was attached to the side of the vessel and transducer depth (i.e., the distance from the transducer face to the water surface) was measured to the nearest 0.01 m and recorded for future bottom depth correction. At all 22 field sites, data were collected along two approximately 1-km-long shore-normal transects that were connected by a shorter (~120-m-long) near-shore transect (Figure 11).

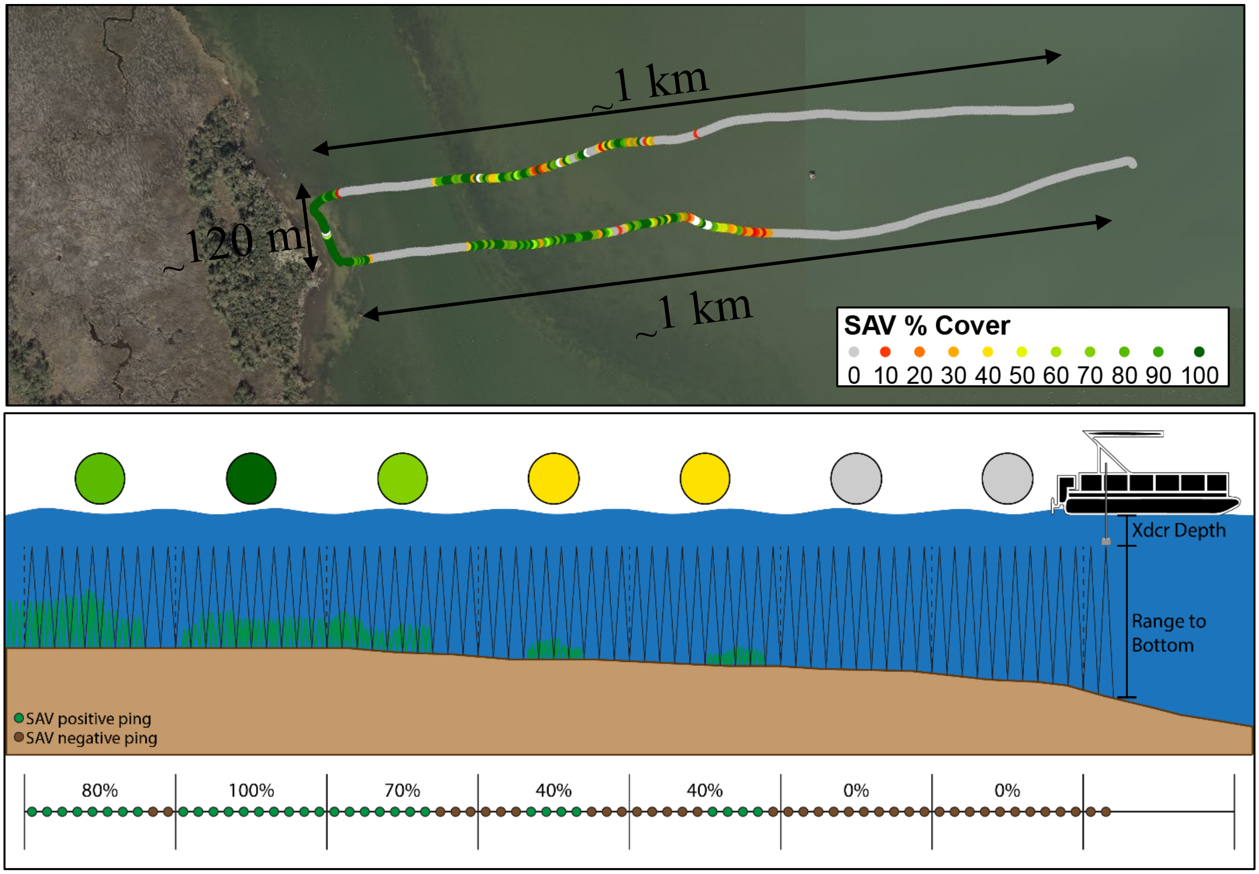


**Figure 11. Example of hydroacoustic data collected at each site along three transects. The diagram depicts how water depth and SAV percent cover are calculated. Water depth in meters is equal to the transducer depth plus the range to the bottom from the transducer face. Each ping is classified as either SAV-positive (green dots) or SAV-negative (brown dots). The resulting data points (large circles with SAV %cover symbology) are a summary of 10 pings where SAV cover is calculated as the number of SAV-positive pings out of the possible 10.**

The echosounder is equipped with an integrated DGPS (horizontal accuracy <3 m) to position the survey-obtained information including water depth, plant height, and plant cover data. The data were analyzed and edited with the BioSonics Visual Habitat post-processing software (BioSonics, Inc., 2016). Water depth was calculated as the distance from the transducer face to the seabed plus the transducer depth measured before data collection (Figure 11). All data collected at distances <0.4 m from the transducer are in the transmit pulse range and, therefore, excluded by the Visual Habitat algorithm (BioSonics, Inc., 2013). Thus, for this study, only water depths >0.65 m were considered. Water-level data were collected by the U.S. Army Corps of Engineers Field Research Facility (USACE-FRF) in Duck, NC using instruments (Xylem Waterlog water-level sensors for survey 1 and Nortek Aquadopp Profilers for surveys 2 and 3) placed at known elevations. These data were then used to correct the hydroacoustic depth measurements to the vertical datum NAVD88. The plant detection settings were constrained to plant heights ≥5 cm above the bottom. Plant percent cover was calculated as the number of pings with a positive plant signal divided by the total number of pings in a survey point (10 pings) and was extracted at 10% cover intervals. Although percent cover was considered, most of the analyses using the hydroacoustic data focused on a simple presence/absence protocol (i.e., presence = ≥10% cover, absence = <10% cover).

In October 2017, SAV was present at 23% of survey points (n = 10,770). The maximum depth surveyed was 2.9 m, and the maximum depth of SAV presence ($Z_{max}$) was 1.8 m (Table 2; Figure 12). Considering only the points with SAV presence, the peak-depth limit ($Z_{peak}$) was determined to be 1.1 m (Table 2). In June 2018, SAV was present at 18% of survey points (n = 11,392). The maximum depth surveyed was 3.1 m, and $Z_{max}$ was 1.6 m (Table 2; Figure 12). Like the October 2017 survey, $Z_{peak}$ was determined to be 1.1 m (Table 2). In May 2019, SAV was present at 16% of survey points (n = 12,041). The maximum depth surveyed was 3.8 m, $Z_{max}$ was 1.8 m, and $Z_{peak}$ was 1.2 m (Table 2; Figure 12).

**Table 2. BioSonics surveys depth and relationship with SAV.**

| | Oct 2017 | Jun 2018 | May 2019 |
|---|---|---|---|
| n | 10,770 | 11,392 | 12,041 |
| Max depth surveyed (m) | 2.9 | 3.1 | 3.8 |
| $Z_{max}$ (m) | 1.8 | 1.6 | 1.8 |
| $Z_{peak}$ (m) | 1.1 | 1.1 | 1.2 |

### 3.5 Quadrat Surveys

Assessments on sediment characteristics, *in situ* measurements of SAV cover, and SAV species distribution were completed using an in-water quadrat survey method. At each of the 22 field sites, one to two 100-m sections of the 1-km BioSonics transects were selected for *in situ* monitoring, resulting in 27 monitoring transects (13 in the northern study area and 14 in the southern study area; Figure 4). Efforts were made to choose transect locations with a wide range of characteristics (e.g., SAV cover, wind-wave energy, etc.), however, water depth was ultimately a limiting factor due to personnel safety. Thus, data were not collected beyond a depth of 1.3 m. Monitoring transects were delineated by placing physical markers (metal stakes or PVC pipes) at each end and stretching a measuring tape between markers. These markers remained in place for the duration of the 2½ year study.

The monitoring transects were surveyed a total of four times: October 2017, May 2018, October 2018, and May 2019. Each transect had six sampling (i.e., quadrat) locations (at 0-m and 100-m on the measuring tape and every 20-m in between) where latitude/longitude, water depth, and SAV percent cover were measured and sediment samples collected. Coordinate location and water depth (NAVD88) were recorded with a Trimble TSC3 (controller) and RTK-GPS SPS882 (receiver). Measurements of SAV percent cover were made using a 1-$m^2$ quadrat sectioned into 100 10-cm x 10-cm (0.01-$m^2$) squares, where percent cover was defined as the number of squares containing SAV. Due to poor water clarity, species composition assessment within quadrats was not feasible; instead, species presence and dominance were recorded along the 100-m transects. Surface sediment samples were collected by hand grabs, placed in whirl-pack bags, and refrigerated until processed. Sediments were collected at all quadrat locations during the first survey to obtain a broad understanding of spatial variations in sediment characteristics within the two study areas. For subsequent surveys, a subset of sediment samples was collected. For the second survey, sediments were collected at two randomly selected quadrat locations per transect. For the third survey, in addition to resampling locations from the second survey, sediments were collected at one additional quadrat location. The final survey resampled the same locations of the third survey.

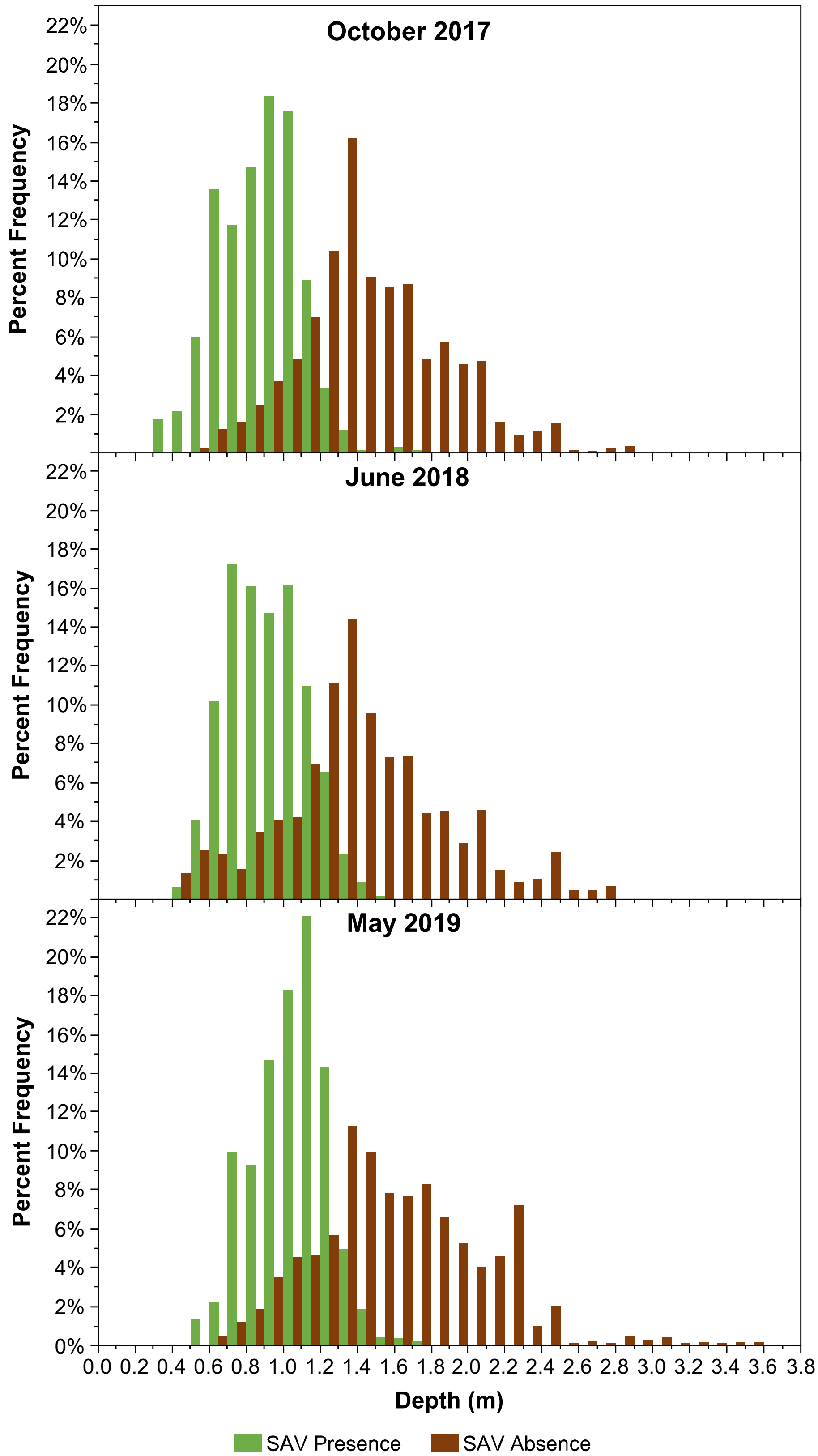


**Figure 12. Histograms of SAV presence (green) and absence (brown) with depth for the October 2017, June 2018, and May 2019 hydroacoustic surveys.**

### 3.5.1 Sediments

The sediment samples were analyzed for grain-size distribution and organic-matter content. Grain-size was determined by using a combination of wet sieving (yielding the sand-mud boundary) and pipette analysis (yielding the silt-clay boundary) to calculate percent sand, silt, and clay (Poppe et al., 2000). The samples were homogenized and approximately 15 to 40 g (less if muddy and more if sandy) subsamples were disaggregated in 0.5% sodium hexametaphosphate solution before being wet sieved through a 63-μm sieve to separate sediments into coarse (>63 μm) and fine (<63 μm) fractions. The remaining fine fraction was stirred into suspension in a uniform volume of 0.5% sodium hexametaphosphate solution and 20-mL aliquots were withdrawn by pipette at a depth of 5-cm, 20 seconds and 1 hour after stirring to delineate silt and clay fractions. The three resulting fractions were dried at 80°C for at least 24 hours before weighing.

Loss-on-ignition (LOI) was used as a proxy measurement of sediment organic content. Homogenized sediments were dried at 80°C for at least 24 hours and a 1- to 1.5-g subsample was weighed to get the pre-combustion weight ($DW_{80}$). This subsample was heated to 550°C for 4 hours to allow all organic matter to be combusted to carbon dioxide (Heiri et al., 2001). The post-combustion weight ($DW_{550}$) was measured and compared to the pre-combustion weight to calculate percent organic content (% LOI) using the following equation (Heiri et al., 2001):

$$\%\ \mathrm{LOI} = \frac{\mathrm{DW}_{80} - \mathrm{DW}_{550}}{\mathrm{DW}_{80}} \times 100 \qquad (1)$$

The data from the surface sediments collected during the quadrat surveys indicated that the region is dominated by sandy sediments that are low in organic matter. Statistical analyses of grain-size and LOI data were completed with the statistical software JMP Pro 14 (SAS Institute, Inc., Cary, NC). Since grain-size is a clastic-sediment descriptor, samples that had abundant plant matter and were extremely organic-rich (e.g., peaty; here defined as percent LOI > 5%; Table 3) were excluded from the sediment data summary.

In October 2017, sediment samples were collected at every quadrat location for a total of 166 samples, 6 of which were peaty. For this first survey, the mean (± SE) weight percent of sand, silt, and clay was 94.5 ± 0.7%, 2.6 ± 0.4%, and 2.9 ± 0.3%, respectively and average percent LOI was 1.0 ± 0.1% (Table 3). In May 2018, sediments were collected at two randomly selected quadrats per transect for a total of 54 samples, 6 of which were peaty. While still primarily sandy, there appeared to be an increase in fines from the first to the second survey with the average weight percent of sand, silt, and clay being 91.5 ± 1.9%, 3.7 ± 1.3%, and 4.8 ± 0.6%, respectively (Table 3), although this change could have been a function of the 70% decrease in the number of samples collected. Despite the apparent increase in fine sediments, average percent LOI remained unchanged at 1.0 ± 0.1% (Table 3). For the third survey in October 2018, sediment was collected at a third quadrat location per transect in addition to the two sites sampled in May 2018 for a total of 81 samples including 3 that were peaty. The average weight percent of sand, silt, and clay was 93.0 ± 0.8%, 3.1 ± 0.5%, and 3.9 ± 0.4%, respectively (Table 3). The average percent LOI was 1.1 ± 0.1% (Table 3). For the final May 2019 survey, 81 sediment samples, including 2 peaty, were collected from the same quadrat sites sampled in the third survey. Once again, there appears to be an increase in fines but little change in organic-matter content with the average weight percent of sand, silt, and clay being 90.5 ± 1.2%, 5.1 ± 0.8%, and 4.5 ± 0.4%, respectively, and average percent LOI was 0.9 ± 0.1% (Table 3). A two-tailed *t*-test ($\alpha = 0.05$) of the resampled quadrats from October 2017 and May 2018 (n = 46) indicates that there is a statistical difference in average weight percent sand ($p = 0.0365$) and average weight percent clay ($p$ = 0.0004). No statistical difference for any of the variables was found when comparing May 2018 and October 2018 (n = 47). From October 2018 to May 2019 (n = 76), the differences between average percent sand ($p$ = 0.0239), average percent silt ($p$ = 0.0117), and average percent LOI ($p$ = 0.0476) were statistically significant.

**Table 3. Summary statistics of SAV percent cover (% Cover), weight percent (wt. %) of sand, silt, and clay, and percent loss on ignition (% LOI) as measured from the quadrat surveys.**

| | Minimum | Median | Maximum | Mean ± SE | n |
|---|---|---|---|---|---|
| **Oct 2017** | | | | | |
| % Cover | 0 | 52 | 100 | 47 ± 3 | 166 |
| wt. % Sand[a] | 47.5 | 97.6 | 100.0 | 94.5 ± 0.7 | 160 |
| wt. % Silt[a] | 0.0 | 0.5 | 33.2 | 2.6 ± 0.4 | |
| wt. % Clay[a] | 0.0 | 1.5 | 21.5 | 2.9 ± 0.3 | |
| % LOI[a] | 0.2 | 0.8 | 3.8 | 1.0 ± 0.1 | |
| **May 2018** | | | | | |
| % Cover | 0 | 30 | 100 | 41 ± 3 | 162 |
| wt. % Sand[b] | 29.6 | 96.5 | 99.2 | 91.5 ± 1.9 | 48 |
| wt. % Silt[b] | 0.0 | 0.3 | 53.5 | 3.7 ± 1.3 | |
| wt. % Clay[b] | 0.7 | 3.2 | 20.1 | 4.8 ± 0.6 | |
| % LOI[b] | 0.3 | 0.7 | 4.2 | 1.0 ± 0.1 | |
| **Oct 2018** | | | | | |
| % Cover | 0 | 19 | 100 | 36 ± 3 | 162 |
| wt. % Sand[c] | 67.9 | 95.4 | 99.3 | 93.0 ± 0.8 | 79 |
| wt. % Silt[c] | 0.0 | 0.9 | 18.5 | 3.1 ± 0.5 | |
| wt. % Clay[c] | 0.6 | 3.1 | 20.6 | 3.9 ± 0.4 | |
| % LOI[c] | 0.2 | 0.8 | 4.8 | 1.1 ± 0.1 | |
| **May 2019** | | | | | |
| % Cover | 0 | 15 | 100 | 36 ± 3 | 162 |
| wt. % Sand[d] | 56.8 | 96.1 | 98.4 | 90.5 ± 1.2 | 79 |
| wt. % Silt[d] | 0.0 | 1.1 | 36.8 | 5.1 ± 0.8 | |
| wt. % Clay[d] | 1.3 | 3.0 | 19.1 | 4.5 ± 0.4 | |
| % LOI[d] | 0.2 | 0.6 | 3.9 | 0.9 ± 0.1 | |

[a] Excluding peaty samples (LOI > 5% = NS3 T1 Q6, NS9 T1 Q5, SS4 T1 Q2, SS4 T1 Q3, SS4 T1 Q4, SS7 T1 Q6)
[b] Excluding peaty samples (LOI > 5% = NS3 T1 Q5, NS3 T1 Q6, NS8 T1 Q6, SS4 T1 Q2, SS4 T1 Q4, SS7 T1 Q5)
[c] Excluding peaty samples (LOI > 5% = NS3 T1 Q5, NS5 T1 Q3, NS8 T1 Q6)
[d] Excluding peaty samples (LOI > 5% = NS8 T1 Q6, SS4 T1 Q3)

On average, for all four survey periods, the sediments from the southern study area had more sand and less silt, clay, and organic matter than those collected in the northern study area (Table 4). Because the data were not normally distributed and were primarily heteroscedastic, both parametric (Student's $t$-test) and non-parametric (Wilcoxon signed-rank test) analyses were used to test whether the differences between the two study areas were statistically different ($\alpha$ = 0.05; Appendix B). The mean weight percent of sand was significantly greater in the southern study area than in the northern study area (Table 4). Conversely, the mean weight percent of silt and clay was statistically greater in the northern study area (Table 4). The difference in percent LOI is not always significant (Table 4), which suggests that sediment organic matter is homogenous from north to south. In general, grain-size differences between the two study areas tended to be greater for the May surveys than the October surveys, although always <10%.

**Table 4. Mean weight percent (wt. %) of sand, silt, and clay and percent loss on ignition (% LOI) as measured from the quadrat surveys for northern and southern study areas and the absolute difference between the means of the two study areas.**

| | North | South | Difference ± SE |
|---|---|---|---|
| **Oct 2017** | | | |
| n | 76 | 84 | |
| Mean wt. % Sand[a] ± SE | 92.1 ± 1.2 | 96.7 ± 0.6 | 4.7 ± 1.3 P, NP |
| Mean wt. % Silt[a] ± SE | 4.0 ± 0.8 | 1.3 ± 0.3 | 2.7 ± 0.8 P, NP |
| Mean wt. % Clay[a] ± SE | 3.9 ± 0.6 | 1.9 ± 0.3 | 2.0 ± 0.6 P |
| Mean % LOI[a] ± SE | 1.1 ± 0.1 | 1.0 ± 0.1 | 0.0 ± 0.1 |
| **May 2018** | | | |
| n | 23 | 25 | |
| Mean wt. % Sand[b] ± SE | 86.2 ± 3.6 | 96.4 ± 0.4 | 10.2 ± 3.5 P, NP |
| Mean wt. % Silt[b] ± SE | 7.0 ± 2.7 | 0.6 ± 0.2 | 6.4 ± 2.6 P, NP |
| Mean wt. % Clay[b] ± SE | 6.7 ± 1.1 | 2.9 ± 0.3 | 3.8 ± 1.1 P, NP |
| Mean % LOI[b] ± SE | 1.2 ± 0.2 | 0.7 ± 0.1 | 0.5 ± 0.2 P |
| **Oct 2018** | | | |
| n | 36 | 43 | |
| Mean wt. % Sand[c] ± SE | 91.1 ± 1.3 | 94.5 ± 0.8 | 3.4 ± 1.5 P, NP |
| Mean wt. % Silt[c] ± SE | 4.0 ± 0.8 | 2.3 ± 0.5 | 1.7 ± 0.9 NP |
| Mean wt. % Clay[c] ± SE | 4.9 ± 0.7 | 3.2 ± 0.3 | 1.7 ± 0.7 P, NP |
| Mean % LOI[c] ± SE | 1.3 ± 0.2 | 0.8 ± 0.1 | 0.5 ± 0.2 P |
| **May 2019** | | | |
| n | 38 | 41 | |
| Mean wt. % Sand[d] ± SE | 86.2 ± 2.0 | 94.4 ± 1.0 | 8.3 ± 2.2 P, NP |
| Mean wt. % Silt[d] ± SE | 8.3 ± 1.5 | 2.0 ± 0.5 | 6.3 ± 1.5 P, NP |
| Mean wt. % Clay[d] ± SE | 5.5 ± 0.5 | 3.5 ± 0.5 | 2.0 ± 0.7 P, NP |
| Mean % LOI[d] ± SE | 1.1 ± 0.1 | 0.7 ± 0.1 | 0.4 ± 0.1 P, NP |

[a] Excluding peaty samples (LOI > 5% = NS3 T1 Q6, NS9 T1 Q5, SS4 T1 Q2, SS4 T1 Q3, SS4 T1 Q4, SS7 T1 Q6)
[b] Excluding peaty samples (LOI > 5% = NS3 T1 Q5, NS3 T1 Q6, NS8 T1 Q6, SS4 T1 Q2, SS4 T1 Q4, SS7 T1 Q5)
[c] Excluding peaty samples (LOI > 5% = NS3 T1 Q5, NS5 T1 Q3, NS8 T1 Q6)
[d] Excluding peaty samples (LOI > 5% = NS8 T1 Q6, SS4 T1 Q3)
[P] Significantly different according to parametric test
[NP] Significantly different according to non-parametric test
$p < 0.01$ $p < 0.05$

### 3.5.2 SAV Cover

The average percent cover of SAV for the entire surveyed area (i.e., northern and southern study areas combined) was greatest in October 2017 at 47 ± 3% and lowest in May 2019 at 36 ± 3% (Table 3), but two-tailed *t*-tests (α = 0.05) comparing consecutive surveys (i.e., October 2017 vs May 2018, May 2018 vs October 2018, and October 2018 vs May 2019) showed that the changes in percent cover were not significant. As with sediments, the parametric Student's *t*-test ($\alpha = 0.05$) and non-parametric Wilcoxon signed-rank test ($\alpha = 0.05$) were performed to determine if the means of SAV percent cover for the northern and southern study areas were significantly different within each study period (Table 5; Appendix B). The south had significantly greater mean percent SAV cover in May 2018 (+32 ± 5%), October 2018 (+21 ± 6%), and May 2019 (+24 ± 6%), but the difference was not significant in October 2017 (+8.23 ± 6%; Table 5). Additional spatial comparisons of the data were made by grouping the transects based on their location within Currituck Sound: west, east, and mid(dle). The west group, those near the western shore, include 12 transects (NS1 T1, NS2 T1, NS3 T1, NS4 T1, SS1 T1, SS1 T2, SS2 T1, SS3 T1, SS4 T1, SS5 T1, SS6 T1, SS7 T1). The east group, those near the eastern shore, include 6 transects (NS5 T1, NS6 T1, SS10 T1, SS10 T2, SS11 T1, SS12 T1). The middle (or mid) group of transects, those that are in the middle of the Sound near the Big Narrows, include 9 transects (NS7 T1, NS7 T2, NS8 T1, NS9 T1, NS9 T2, NS10 T1, NS10 T2, SS8 T1, SS9 T1). The parametric Student's *t*-test ($\alpha = 0.05$) and non-parametric Wilcoxon signed-rank test ($\alpha = 0.05$) were performed to determine if the means of SAV percent cover for each group differed from one another (Table 6; Appendix B). Mean percent cover of SAV was greater in the east than the west for all study periods and the differences were always significant (Table 6). In general, the mid transects showed more variation in SAV percent cover over time compared to the west or east. While percent cover in the middle of the Sound was always greater than that in the west and less than that in the east, these differences were not always significant (Table 6).

**Table 5. Mean SAV percent cover as measured from the quadrat surveys and results of the Student's t-test comparing the northern and southern study areas.**

| | North | | South | | | |
|---|---|---|---|---|---|---|
| Survey | n | % Cover | n | % Cover | Difference | p |
| Oct 2017 | 78 | 42 ± 4 | 88 | 51 ± 4 | 8 ± 6 | 0.15 |
| May 2018 | 78 | 24 ± 3 | 84 | 56 ± 4 | 32 ± 5 | <0.01 $^{P, NP}$ |
| Oct 2018 | 78 | 25 ± 4 | 84 | 46 ± 4 | 21 ± 6 | <0.01 $^{P, NP}$ |
| May 2019 | 78 | 23 ± 4 | 84 | 47 ± 5 | 24 ± 6 | <0.01 $^{P, NP}$ |

$^{P}$ Significantly different according to parametric test
$^{NP}$ Significantly different according to non-parametric test
$p < 0.01$ $p < 0.05$

**Table 6. Mean SAV percent cover as measured from the quadrat surveys and results of the Student's t-test comparing the grouped transects found along the western shore, eastern shore, and middle marsh areas (i.e., west, east, mid).**

| | Mean % Cover ± SE | | | Difference ± SE | | |
|---|---|---|---|---|---|---|
| Survey | West n = 72 | Mid n = 54 | East n = 36 | West & East | West & Mid | Mid & East |
| Oct 2017 | 29 ± 4 | 59 ± 5 | 65 ± 5 | 35 ± 7 $^{P, NP}$ | 30 ± 6 $^{P, NP}$ | 6 ± 7 |
| May 2018 | 35 ± 4 | 36 ± 4 | 60 ± 6 | 26 ± 7 $^{P, NP}$ | 1 ± 6 | 25 ± 8 $^{P, NP}$ |
| Oct 2018 | 22 ± 3 | 41 ± 5 | 58 ± 7 | 36 ± 7 $^{P, NP}$ | 19 ± 6 $^{P, NP}$ | 17 ± 8 $^{NP}$ |
| May 2019 | 28 ± 4 | 36 ± 5 | 49 ± 6 | 21 ± 8 $^{P, NP}$ | 8 ± 7 | 13 ± 8 |

$^{P}$ Significantly different according to parametric test
$^{NP}$ Significantly different according to non-parametric test
$p < 0.01$ $p < 0.05$

### 3.5.3 SAV Species

A total of seven SAV species were identified during the quadrat surveys. They include the native widgeon grass (*Ruppia maritima*), wild celery (*Vallisneria americana*), redhead grass (*Potamogeton perfoliatus*), and bushy pondweed (or southern naiad; *Najas guadalupensis*); the invasive Eurasian watermilfoil (*Myriophyllum spicatum*); and two unidentified species of the branched macro-alga muskgrass (*Chara* spp.). Widgeon grass was the species most frequently observed throughout the entire study with 61–77% of all quadrat sites containing widgeon grass (Table 7). Wild celery was the second most prevalent at 33–54% (Table 7). The once dominant Eurasian watermilfoil had the third highest frequency of occurrence but was observed in only 5–12% of quadrats (Table 7). During all four surveys, widgeon grass was more prevalent in the southern versus the northern study area (Figure 13) as well as preferential to either the western or eastern shores rather than near the marsh islands in the middle (Figure 14). The opposite was true of wild celery, which was dominant in the northern study area and in the middle regions.

**Table 7. Frequency of occurrence of each species observed during the quadrat surveys.**

| | Widgeon grass | | Wild celery | | Eurasian water-milfoil | | Redhead grass | | Bushy pond-weed | | Musk-grass A | | Musk-grass B | |
|---|---|---|---|---|---|---|---|---|---|---|---|---|---|---|
| Survey | n | % | n | % | n | % | n | % | n | % | n | % | n | % |
| Oct 2017 n = 166 | 114 | 69 | 89 | 54 | 9 | 5 | 6 | 4 | 7 | 4 | 6 | 4 | 7 | 4 |
| May 2018 n = 162 | 124 | 77 | 74 | 46 | 19 | 12 | 5 | 3 | 10 | 6 | 12 | 7 | 4 | 2 |
| Oct 2018 n = 162 | 99 | 61 | 62 | 38 | 11 | 7 | 2 | 1 | 4 | 2 | 0 | 0 | 7 | 4 |
| May 2019 n = 162 | 101 | 62 | 53 | 33 | 19 | 12 | 7 | 4 | 1 | 1 | 0 | 0 | 18 | 11 |

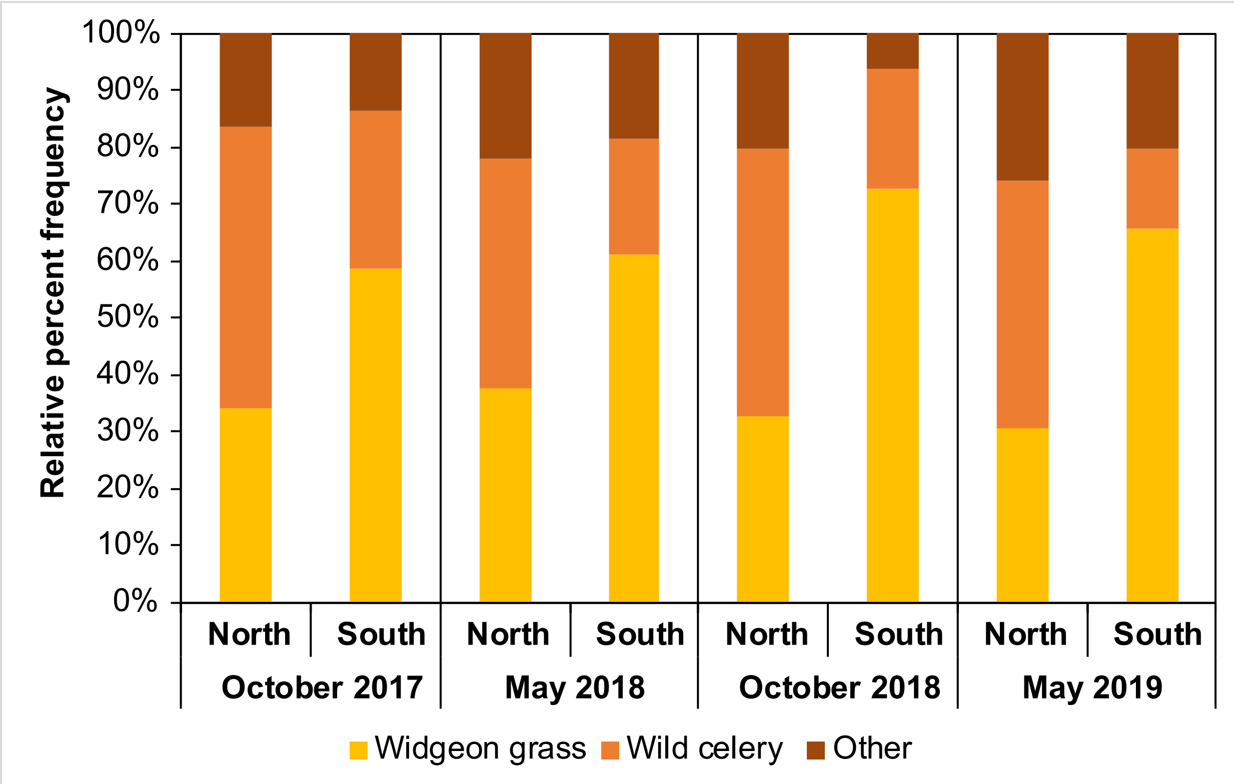


**Figure 13. Variation in species distribution for the northern and southern study areas.**

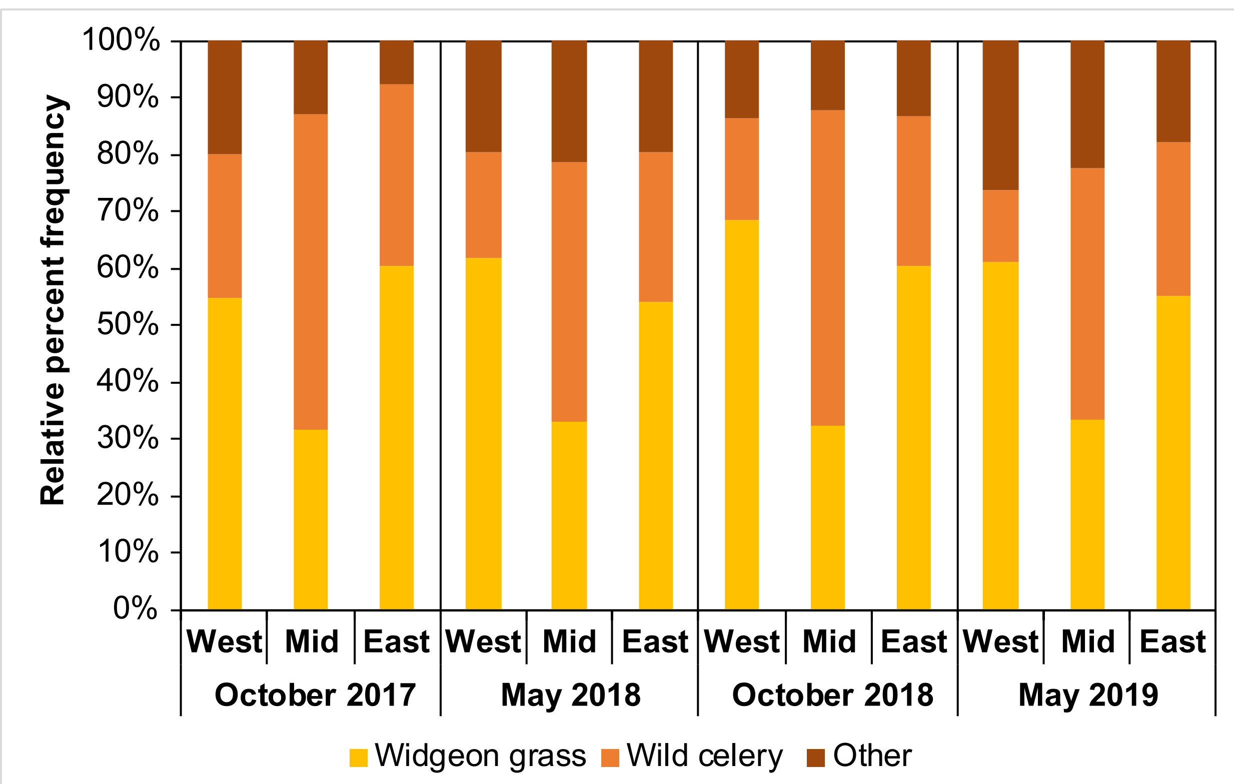


**Figure 14. Variation in species distribution for the west, mid, and east portions of the Sound.**

## 3.6 *In Situ* Monitoring

In 2016, the USACE-FRF installed an estuarine monitoring array in Currituck Sound. The array consisted of five monitoring platforms (Figure 15) equipped with instruments providing real-time meteorological, hydrodynamic, and water-quality measurements. These measurements included winds, waves, currents, water level, water temperature, salinity, pH, turbidity, chlorophyll-a, blue-green algae, fluorescent dissolved organic matter (fDOM), dissolved oxygen (DO), and photosynthetically active radiation (PAR). These data are available on the USACE-FRF Data Portal (https://frfdataportal.erdc.dren.mil/). Figure C1 (Appendix C) shows the parameters that were measured at the five platform stations and summarizes the data continuity of each parameter by depicting daily time-intervals on a color gradient scale ranging from black, representing a complete record, to white, denoting no available data. In general, data collection began in late January 2016 and continued through early January 2018. Gaps in the data records resulted from either instrument failures causing interruptions in the measurements or removed values following quality control checks. Due in part to the unprecedented amounts of ice that formed in the Sound in the winter of 2018, and in particular impacts associated with the January 2018 North American blizzard, all five platforms sustained irreparable damage (four were completed destroyed) forcing the suspension of data collection in the Currituck Sound for several months. Daily-averaged time series of the data collected at each platform station are available in Appendix D.

In an effort to continue *in situ* monitoring following the loss of the platforms, USACE-FRF and CSI deployed instrumented landers at two sites in Currituck Sound: one approximately in the center of the northern study area (Curri-N-Obs) and one in the southern study area (Curri-S-Obs) in the immediate vicinity of former monitoring station CS04 (Figure 15). The two lightweight landers were designed to collect hydrodynamic and water-quality measurements. Each was fitted with a YSI EXO2 sensor measuring water temperature, salinity, turbidity, chlorophyll-a, blue-green algae, and fDOM, and a Nortek Aquadopp acoustic Doppler current profiler (ADCP) measuring waves, currents, and water level. These data are available on the USACE-FRF Data Portal (https://frfdataportal.erdc.dren.mil/). The sensors were configured to record data 4 times per hour. Battery life and memory for all the deployed instruments was expected to last about 2.5 months. At that time, instrument turnarounds were scheduled and included data download, battery replacement, and cleaning. The landers were deployed a total of five times starting in May 2018 through September 2019. Figure C2 (Appendix C) shows the parameters that were measured at the two lander sites and, just as with the platforms, summarizes the data continuity of each parameter by depicting daily time-intervals on a color gradient scale ranging from black, representing a complete record, to white, denoting no available data. Both EXO2 sensors malfunctioned within the first two deployments and had to be sent in to YSI for repairs resulting in large gaps in the water-quality measurements (Figure C2). For the third deployment (Nov 2018–Dec 2018), turbidity was instead measured with a WETLabs BB3 turbidity sensor deployed at site Curri-N-Obs. Daily-averaged time series of the data collected at each lander station are available in Appendix D.

These data were primarily used to evaluate light conditions in Currituck Sound. Light attenuation through the water column was calculated and coupled with the regional bathymetry to assess the expected spatial distribution of SAV. In addition, several physical and biogeochemical parameters were explored in hopes of gaining some understanding of the relative influence of these mechanisms on light attenuation.

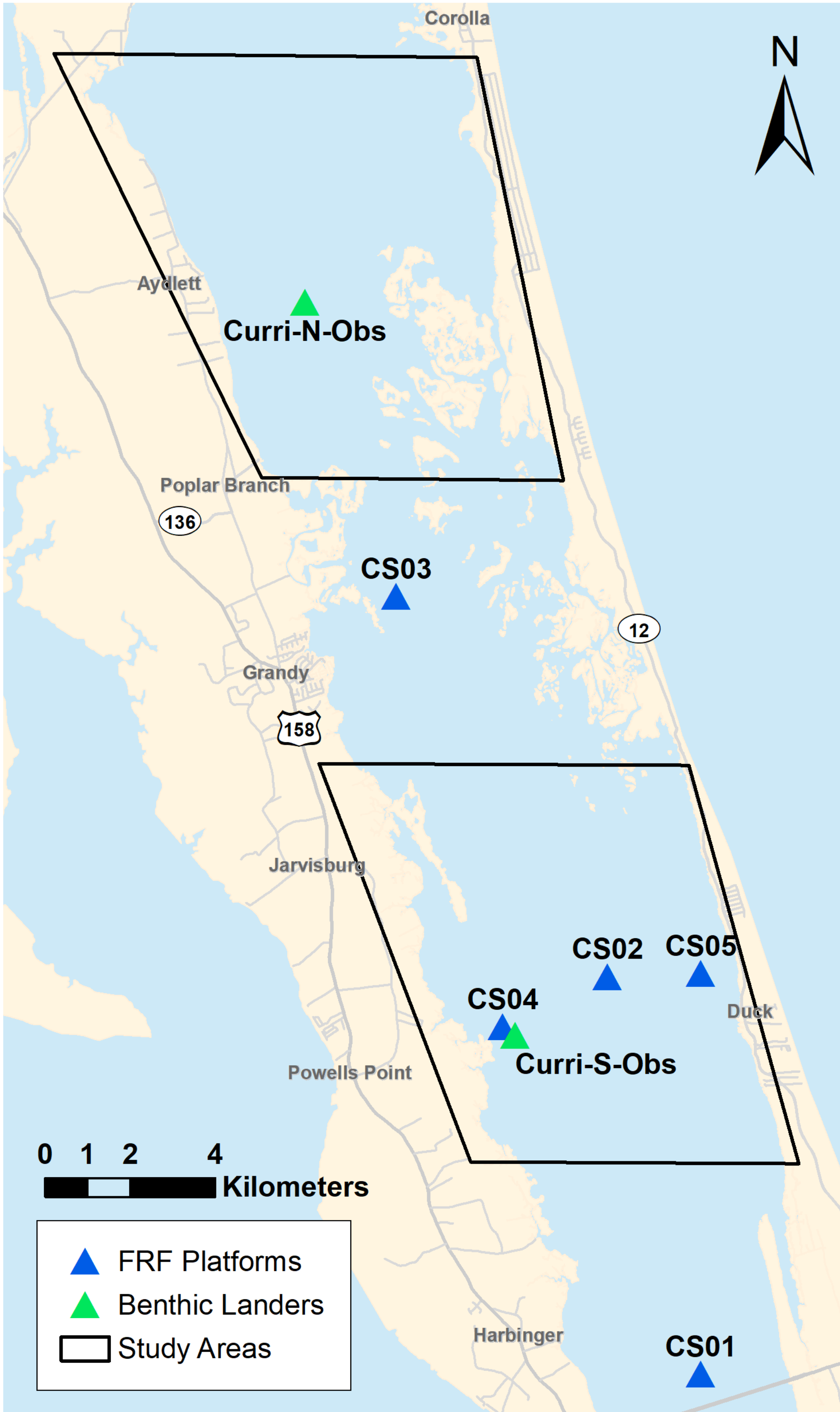


Figure 15. Locations of *in situ* monitoring stations. Blue triangles represent the USACE-FRF platforms where data were collected from Jan 2016 to Jan 2018. Green triangles represent the instrumented benthic landers where data were collected from May 2018 to Sep 2019.

### 3.6.1 Light Attenuation Model

Three of the five USACE-FRF monitoring platforms were fitted with pairs of WetLabs ECO-PARS sensors to measure photosynthetically active radiation (PAR, 400–700 nm) across Currituck Sound (CS01, CS02, and CS03; locations shown in Figure 15). At each platform, the top sensors were placed at a nominal depth (NAVD88) of 1.0 m and the bottom sensors were placed exactly 0.5 m below at a nominal depth of 1.5 m. The sensors sampled at 5-minute intervals. Data collection began in late April/early May 2016 and continued through January 2018 with a few periods when no data were collected due to instrument failures (Appendix C, Figure C1). To prevent biofouling, the sensors had copper faceplates and a mechanical copper wiper. Data were collected in real-time and telemetered to the USACE Field Research Facility. The water-column attenuation of light was determined by the light attenuation coefficient ($K_d$) and calculated from simultaneous PAR measurements of corresponding top and bottom sensors using the Lambert-Beer equation:

$$K_d = -\frac{1}{dz}\ln\left(\frac{PAR_{bot}}{PAR_{top}}\right) \tag{2}$$

where dz is the distance between the two PAR sensors (0.5 m in this case; Ganju et al., 2014; Pedersen et al., 2012; Batiuk et al., 2000). $K_d$ was only calculated for peak daylight hours (between 15:00 and 20:00 UTC; Ganju et al., 2014) and any values $\leq 0$ $m^{-1}$ were discarded. Mean and median growing-season light attenuation for Currituck Sound were calculated using all $K_d$ values from the 2016 and 2017 growing seasons (April 1 to October 31; Batiuk et al., 2000). The median $K_d$ was used to calculate the percent light through the water column (PLW) for various threshold water depths (Z) using the equation (Batiuk et al., 2000):

$$PLW = e^{(-K_d)(Z)} \times 100 \tag{3}$$

This approach provides an estimate of the amount of light that can be transmitted to the bottom through the water column at the various threshold depths that can be useful for both understanding present SAV distribution and developing restoration goals (Batiuk et al., 2000). The relationship between Z and PLW was coupled with the bathymetry dataset and used to model the predicted areal coverage of SAV beds in the Sound based on light availability.

Collectively considering the three platform stations with PAR data (CS01, CS02, CS03; Figure 15), the median $K_d$ for the combined 2016 and 2017 growing seasons was determined to be 1.99 $m^{-1}$. The median was chosen over the mean for further calculations following the convention established by Batiuk et al. (1992) because it provides a better estimate of the typical light attenuation given the skewed distribution of the measured $K_d$. Percent light through the water column (PLW) was calculated for threshold depths of 0.50, 1.00, 1.50, 1.80, and 2.00 m (Table 8). From this calculation, PLW was found to be greater than 13.7% in areas shallower than 1.00 m and areas deeper than 2.00 m receive less than 1.9% light (Table 8). A contour map of PLW was created in ArcMap to help visualize anticipated areas for SAV and possible mitigation sites (Figure 16).

**Table 8. PLW at threshold depths (Z) given the median growing-season $K_d$ is equal to 1.99 $m^{-1}$.**

| Depth (Z) | PLW |
|---|---|
| 0.50 m | 37.0% |
| 1.00 m | 13.7% |
| 1.50 m | 5.1% |
| 1.80 m | 2.8% |
| 2.00 m | 1.9% |

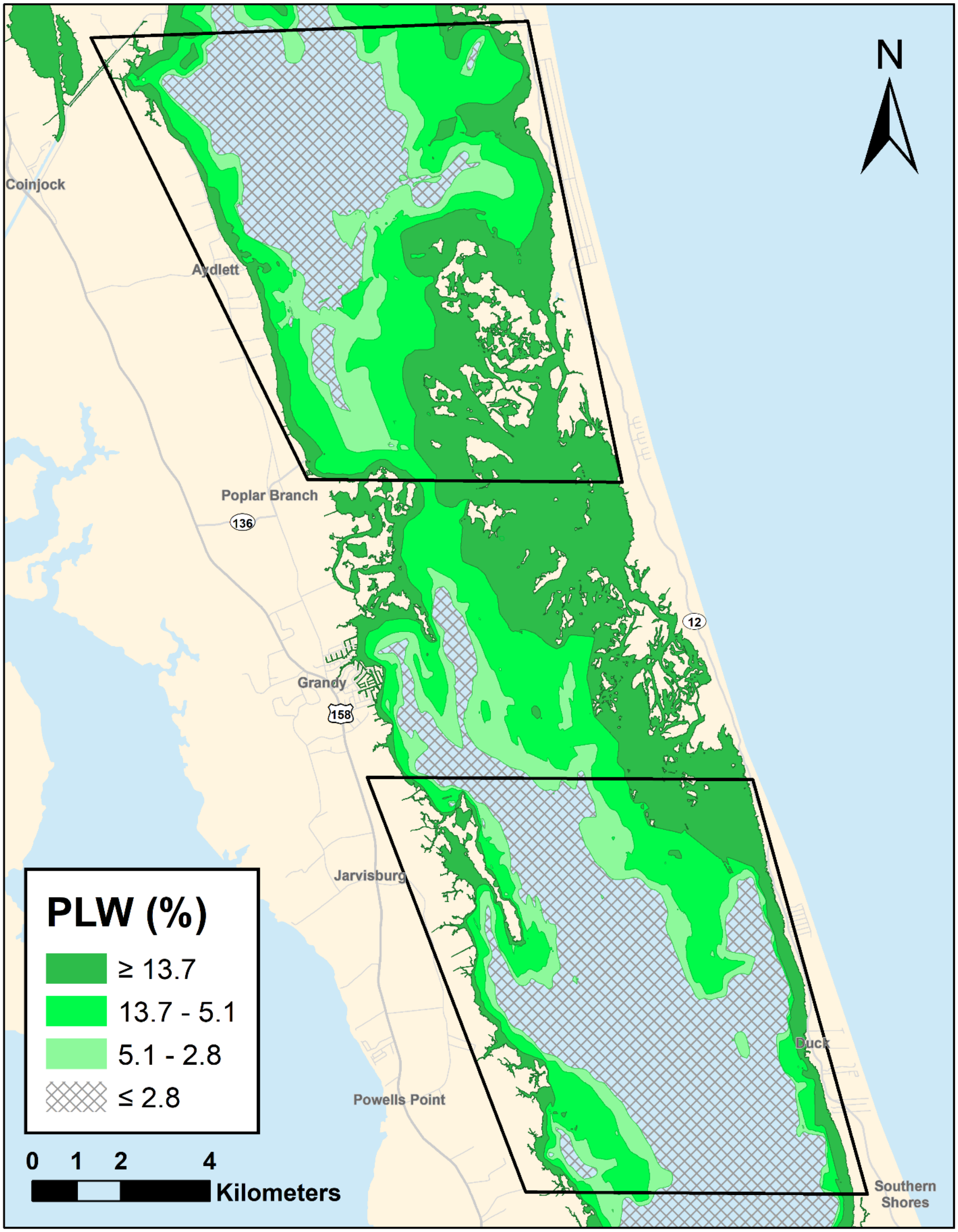


**Figure 16. Model predicted ranges of the percent of light able to reach the bottom after traveling through the water column (PLW) calculated from median growing-season light attenuation ($K_d$) and depth. Hashed areas are not at all likely to support SAV due to insufficient light.**

### 3.6.2 Light Attenuation Contributors

Waters in Currituck Sound, as this study points out, are optically shallow. That is, sunlight attenuation with water depth is high, and this is likely the single most important factor limiting SAV growth. Only the shallowest areas (roughly <1–1.5 m water depths) show sufficient photometric density to support more than sporadic colonization of SAV. This study focused on only few of several possible water quality attributes (e.g., turbidity, colored dissolved organics (fDOM), and chlorophyll-a) that directly influence light attenuation. A direct influence attribute, as referenced here, is one that directly absorbs or scatters incident sunlight. Indirect attributes (e.g., temperature, salinity, surface waves and winds) do not themselves alter incident energy but rather may in some way alter the behavior of one or more of the direct attributes.

Figure 17, plots a, b, and c show a relationship between light attenuation as the radiative light attenuation coefficient $K_d$, and turbidity, chlorophyll-a, and fDOM, respectively. At first glance these plots suggest a strong coherence between turbidity and $K_d$. Chlorophyll-a is also coupled to $K_d$, but to a lesser degree. Dissolved organics, as measured via the fDOM proxy, initially appear to have little relationship with light attenuation.

Rescaling the three time series, however, provided a novel and contrasting perspective into the relationship between turbidity, chlorophyll, and dissolved organics (fDOM), and water column light attenuation. Rescaling in this instance refers to the transformation of each of the three attributes from their native minimum and maximum extents to span a new dimensionless range between 0 and 1, using the general formula

$$x' = \frac{x - x_{min}}{x_{max} - x_{min}} \tag{4}$$

where $x$ is the original attribute value and $x'$ is the rescaled value.

This transformation allows for direct, relative (qualitative), comparisons between the three otherwise disparate measures. A combined time series of these rescaled data for observations from Army Corps of Engineers Currituck Sound Observation Platform 2 (CS02, Figure 15) is shown in Figure 18. Aside from the irregular, semi-oscillatory, behavior seen particularly with the fDOM (gold) and chlorophyll-a (green) signals in the time series, of note here are the relative magnitudes of the medians (dashed horizontal lines on the plot) for each of the three attributes. The fDOM signal (scaled median = 0.46), while exhibiting considerable variation, was, with few exceptions, the more prevalent factor relative to chlorophyll-a (scaled median = 0.29) which also displayed a varying signal, and turbidity (scaled median = 0.027). The scaled median was selected as representing central tendency over the scaled mean due to the strong right skewness (6.53) observed in the turbidity data. This finding suggests that fDOM was generally the more persistent and overall more dominant of the three light attenuation attributes measured during the study period.

Although the time series of data spanned from March 2016 to November 2017, a period of only 20 months, with a significant 7 month break midway during the period, analysis of this series at times when both turbidity and chlorophyll levels were very low also supports the suggestion that dissolved organics (via the fDOM proxy) play an enduring role in controlling light attenuation in the Currituck Sound. For example, when both turbidity and chlorophyll levels were below values equal to their respective 5$^{th}$ percentiles (interpreted as the subset of observations that represent the smallest 5%, in magnitude, of all observations in the dataset, which in this instance only 5% of all observations in the dataset were measured at less than or equal to 3.9 FNU for turbidity and 1.48 µg/L for chlorophyll) the median value of $K_d$(PAR) remained > 1 (1.27 m$^{-1}$). Further, dropping the threshold down to the attributes' respective 1$^{st}$

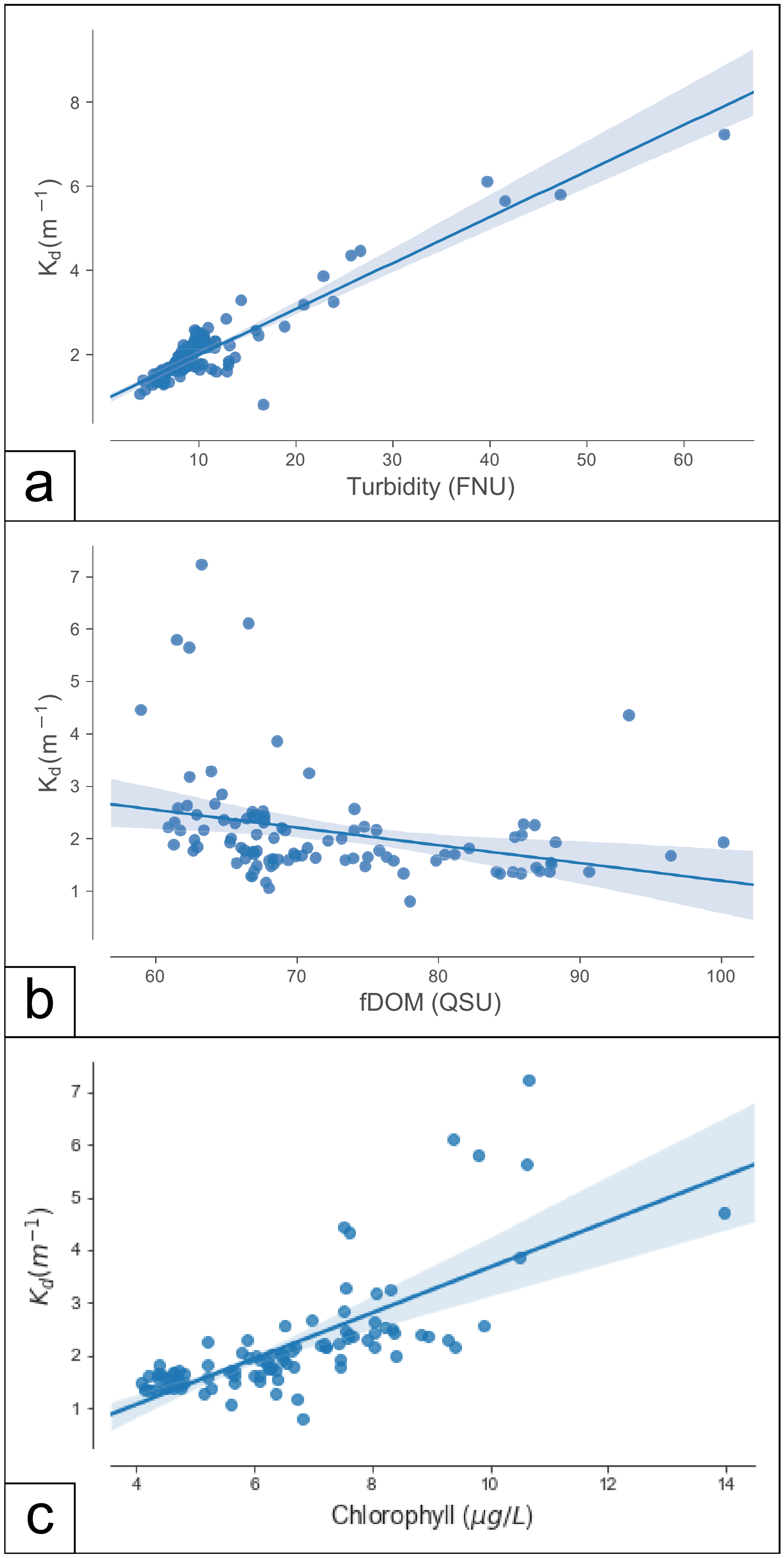


**Figure 17. Linear regressions for $K_d$ as a function of (a) turbidity, (b) fDOM, and (c) chlorophyll for platform CS01.**

percentiles (only 1% of all observations in the data were less than or equal to 3.03 FNU turbidity and 0.37 µg/L chlorophyll) still revealed a $K_d$(PAR) median > 1 (1.09 $m^{-1}$). The values of $K_d$(PAR) > 1 $m^{-1}$ observed point to relatively high levels of light attenuation through the water column (i.e., poor water clarity) persisting in the Sound even during periods when suspended solids are at very low levels.

Moreover, when both turbidity and chlorophyll were at their respective lowest levels measured (at or below the 1st percentile threshold), the light attenuation ($K_d$) was such that, applying the Beer-Lambert relationship, the percent of incident light reaching the bottom (PLW) at the maximum depth of SAV colonization ($Z_{max}$), 1.8 m in this study, was approximately 14% of incident (Equation 3). At the 5th percentile threshold the PLW dropped to 10% of surface incidence at 1.8 m water depth. Thus, light attenuation appears to have remained consistently high in Sound waters in large measure independent of the presence or absence of suspended solids. Such would provide yet additional evidence for dissolved organic matter's role as a consistent, albeit varying, baseline factor controlling light-attenuation in the Currituck Sound.

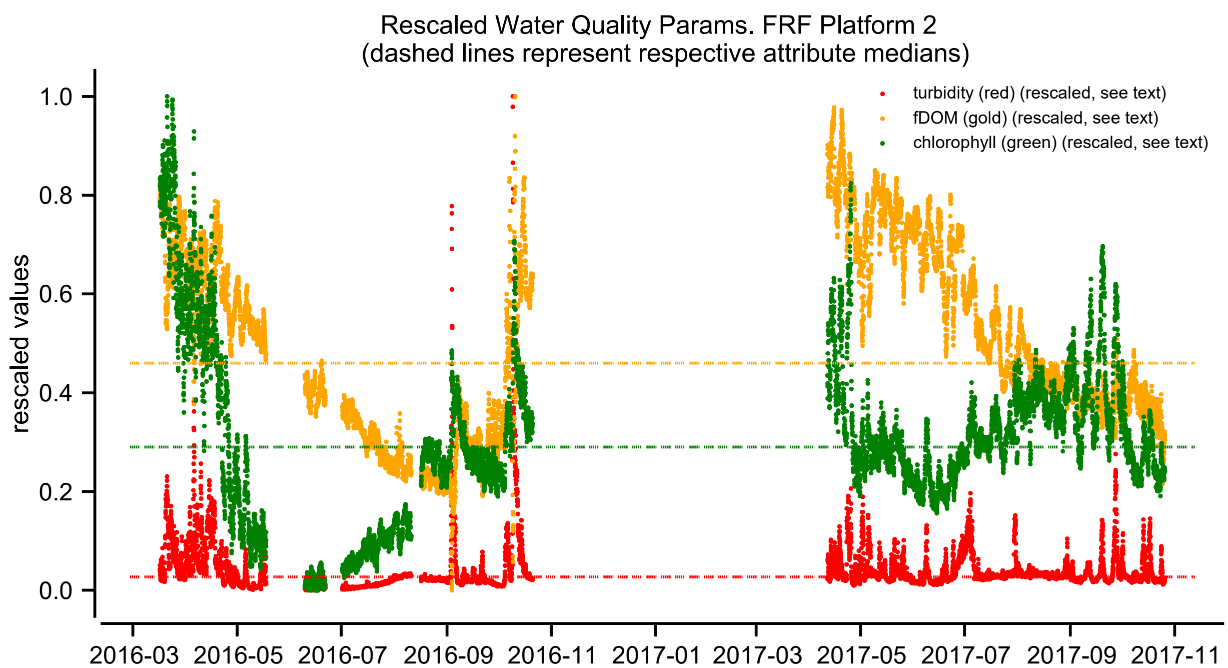


**Figure 18. Time series of normalized turbidity (red), fDOM (gold), and chlorophyll (green) signals for platform CS02.**

## 4.0 FINDINGS AND CONCLUSIONS

### 4.1 Spatial Variation in SAV: Changes and Sedimentologic Drivers

The most important factor determining the success of benthic habitat mapping from aerial photography is collecting the photographs under optimal environmental conditions (Finkbeiner et al., 2001). Efforts were made to attain the aerial photographs (Figure 8; NOAA-OCM, 2015; ECSU, unpublished data; APNEP, 2019, unpublished data) when environmental conditions were favorable for mapping SAV (i.e., low turbidity, winds below 5 mph, sun angle between 20° and 35°, no clouds or haze, and during peak growing season; Ferguson and Wood, 1994; Finkbeiner et al., 2001; Kenworthy et al., 2012). However, ideal conditions are difficult to predict, and the turbid low-salinity water in Currituck Sound makes it particularly challenging to identify and map SAV (Ferguson et al., 1989; Ferguson and Wood, 1994; Kenworthy et al., 2012). Ferguson and Wood (1994) noted that the 1990 photography was adversely affected by white caps, turbidity, and sun glint and the resulting SAV polygons (NOAA-OCM, 2015) were conservative estimates of cover. The 2012 imagery collected by APNEP over Currituck Sound and Back Bay was so adversely affected by turbidity and cloud cover that they have excluded those areas from the official mapping project due to the inaccuracies of the SAV delineations (https://www.nconemap.gov/datasets/ncdenr::sav-2012-2014-mapping). Despite some of these limitations, the aerial maps are still valuable for reviewing full-coverage SAV distribution patterns. Moreover, similar SAV and water depth relationships can be identified between the aerial maps and the hydroacoustic surveys conducted in this study that provided more accurate simultaneous measurements of SAV cover and depth (Figure 19). However, due to the limitations of the aerial datasets, we were unable to calculate the error associated with the spatiotemporal changes in SAV distribution calculated from the digitized SAV maps (Figure 9). Thus, discussion on analyses performed using these datasets did not focus on quantified temporal variations. Instead, the datasets were used to gain a broad qualitative understanding of SAV distribution over the last several decades.

Results from the quadrat surveys in this study demonstrated that SAV percent cover was greatest in the southern study area and at the transects closest to the eastern shore. While the lateral distribution was consistent with previous work in Currituck Sound, the longitudinal difference deviated from what was expected. The preferential abundance (i.e., aerial coverage; Table 10) of SAV in the northern half and along the eastern shore was immediately evident in the digitized SAV maps from 1990, 2003, 2008, and 2012 (Figure 8) and corroborated by previous observational field studies in the region (e.g., Dickson, 1958; Sincock et al., 1965; Davis and Carey, 1981; Davis and Brinson, 1983, 1990; Carter and Rybicki, 1994; Hartis, 2013). Following a comprehensive review of historical accounts in the area dating back to 1853 and a series of large field studies from 1958 to 1964, Sincock et al. (1965) asserted that the southern end of Currituck Sound had never been as productive as the northern section and attributed this primarily to the deeper waters in the south. The inverse relationship between water depth and SAV abundance has long been recognized (Dennison et al., 1993; Findlay et al., 2014), so it stands to reason that, all other factors being equal, the shallower northern and eastern areas of Currituck Sound would have greater SAV coverage than the deeper southern and western areas. However, as previously mentioned, the quadrat surveys were limited to depths shallower than 1.3 m. Additionally, the depths sampled during these surveys were approximately the same (i.e., not significantly different at $\alpha = 0.05$) regardless of the locations of the transects (i.e., north, south, east, west, mid). Thus, the consistently greater abundance of SAV in the south and east

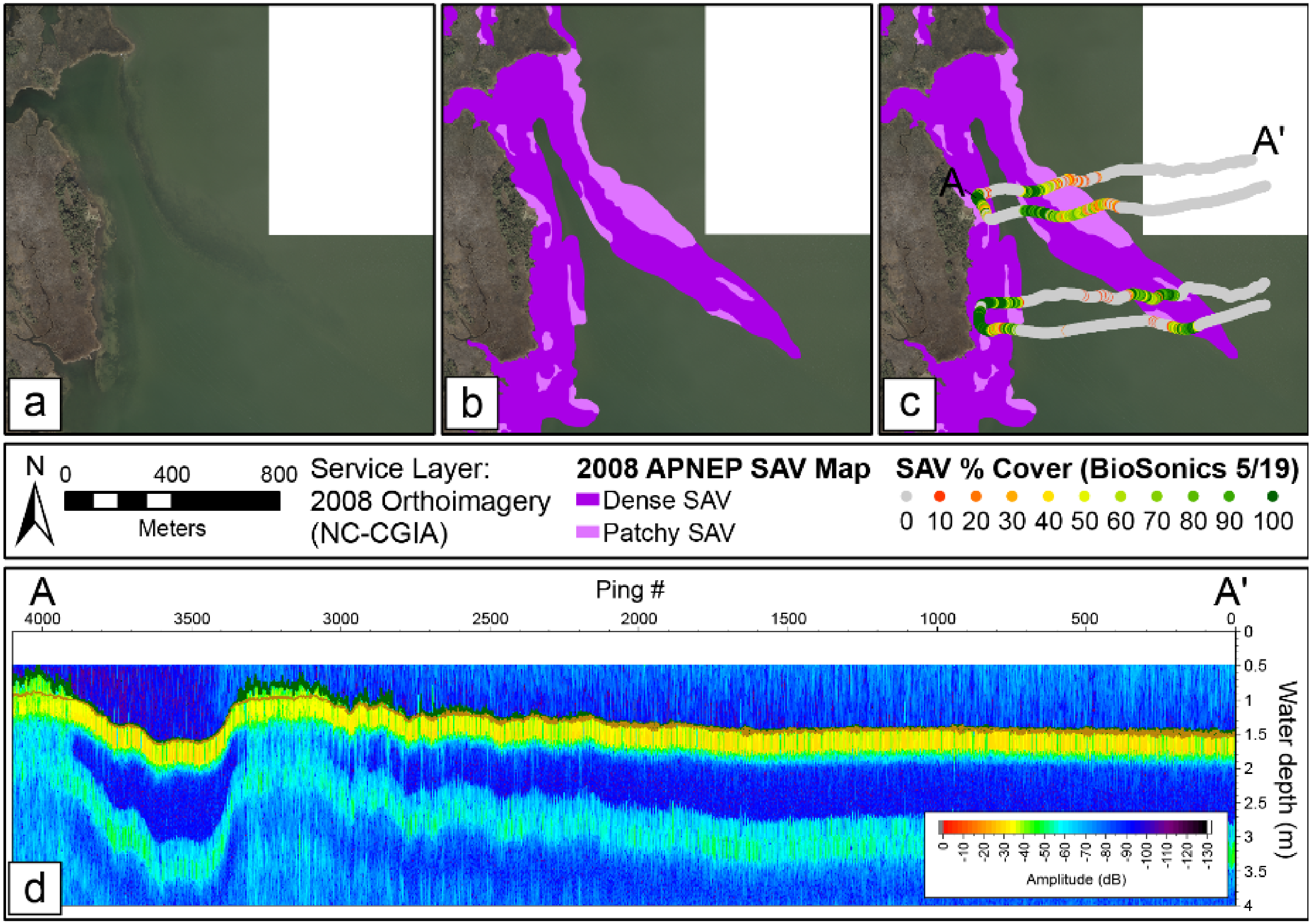


**Figure 19.** (a) 2008 ortho imagery of a portion of the western shore of Currituck Sound showing SAV growing along the shore and on an existing shoal, (b) corresponding APNEP digitization of the SAV where dark purple equals dense SAV and light purple equals patchy SAV, (c) SAV percent cover results from the BioSonics survey conducted in May 2019 for sites SS2 (bottom) and SS3 (top) (dark green = 100% cover, red = 10% cover, gray = no SAV), (d) partial echogram for SS3 starting from the shore (A) and extending offshore (A'), showing the distance to the bottom (brown line) and SAV presence (green line).

suggests that at similar water depths, conditions in these two areas may be more favorable for SAV growth. However, determining the validity of this relationship requires a more robust spatial assessment than the quadrat surveys provided.

To examine this further, the SAV distribution maps were constrained to the established north and south boundaries in this study and overlain by depth contours at 1.0, 1.5, and 2.0 m. The northern and southern study areas contain approximately 7,100 and 6,500 ha of open water, respectively (Table 9). The northern area is characterized by a larger shallow area with 30% of water depths shallower than 1.0 m compared to only 13% of the total area at the same depth range for the southern area (Table 9). SAV cover, as calculated for the four aerial surveys, was consistently greater in the northern study area (Table 10). This also revealed that SAV grows in deeper water in the southern study area (Table 10). The SAV cover in each study area was divided into four depth strata (i.e., <1.0 m, 1.0–1.5 m, 1.5–2.0 m, and >2.0 m) to determine potential differences in abundance between the northern and southern study areas at similar depths. This was done by measuring SAV cover within each depth strata within the corresponding northern or southern boundary and dividing it by the total area in that depth interval and multiplying by 100 to get the percentage, thus, normalizing the SAV cover data from the two study areas (Table 11). This indicated that SAV cover within any given depth interval is generally about the same or greater in the south relative to the north. Comparing the depth-normalized SAV cover between these two areas demonstrated that although the shallower northern study area has greater areal coverage of SAV, when comparing similar depth intervals, the southern study area has more abundant SAV. This implies that for mitigation projects, there may be more suitable sites in the north but choosing a site in the south may yield better results. Although water depth is clearly a primary driver, this also suggests that there are other factors influencing variations in SAV distribution between the northern and southern study areas.

**Table 9. Areal extent of depth intervals in hectares and percent of total area for the northern and southern study areas.**

| | North | | South | |
|---|---|---|---|---|
| Depth Interval | Depth Area (ha) | % of Total Area | Depth Area (ha) | % of Total Area |
| <1.0 m | 2138 | 30 | 848 | 13 |
| 1.0–1.5 m | 1850 | 26 | 1199 | 19 |
| 1.5–2.0 m | 1878 | 27 | 1433 | 22 |
| >2.0 m | 1206 | 17 | 2976 | 46 |
| Total | 7071 | 100 | 6456 | 100 |

**Table 10. SAV cover in hectares per depth interval and percent of total SAV cover for the northern and southern study areas. SAV cover is based on the 1990, 2003, 2008, and 2012 aerial survey datasets (shown in Figure 8).**

| | | North | | South | |
|---|---|---|---|---|---|
| Year | Depth Interval | SAV Cover (ha) | % of Total SAV Cover | SAV Cover (ha) | % of Total SAV Cover |
| 1990 | <1.0 m | 624 | 96 | 196 | 68 |
| | 1.0–1.5 m | 26 | 4 | 92 | 32 |
| | 1.5–2.0 m | 0 | 0 | 0 | 0 |
| | >2.0 m | 0 | 0 | 0 | 0 |
| | Total | 650 | 100 | 289 | 100 |
| 2003 | <1.0 m | 682 | 98 | 272 | 55 |
| | 1.0–1.5 m | 16 | 2 | 106 | 21 |
| | 1.5–2.0 m | 0 | 0 | 112 | 23 |
| | >2.0 m | 0 | 0 | 7 | 1 |
| | Total | 698 | 100 | 497 | 100 |
| 2008 | <1.0 m | 999 | 85 | 475 | 79 |
| | 1.0–1.5 m | 164 | 14 | 125 | 21 |
| | 1.5–2.0 m | 8 | 1 | 1 | 0 |
| | >2.0 m | 0 | 0 | 0 | 0 |
| | Total | 1171 | 100 | 601 | 100 |
| 2012 | <1.0 m | 861 | 97 | 521 | 72 |
| | 1.0–1.5 m | 28 | 3 | 150 | 21 |
| | 1.5–2.0 m | 0 | 0 | 45 | 6 |
| | >2.0 m | 0 | 0 | 6 | 1 |
| | Total | 889 | 100 | 722 | 100 |
| Average of all surveys | <1.0 m | 792 | 94 | 366 | 69 |
| | 1.0–1.5 m | 59 | 6 | 118 | 24 |
| | 1.5–2.0 m | 2 | 0 | 40 | 7 |
| | >2.0 m | 0 | 0 | 3 | 1 |
| | Total | 852 | 100 | 527 | 100 |

**Table 11. SAV cover per depth interval and areal extent of depth intervals in hectares, and percent of depth-interval area containing SAV (i.e., [SAV Cover ÷ Depth Area] × 100) for the northern and southern study areas. SAV cover is based on the 1990, 2003, 2008, and 2012 aerial surveys (shown in Figure 8).**

| | | North | | | South | | |
|---|---|---|---|---|---|---|---|
| Year | Depth Interval | SAV Cover (ha) | Depth Area (ha) | % SAV Cover by Depth Area | SAV Cover (ha) | Depth Area (ha) | % SAV Cover by Depth Area |
| 1990 | <1.0 m | 624 | 2138 | 29 | 196 | 848 | 23 |
| | 1.0–1.5 m | 26 | 1850 | 1 | 92 | 1199 | 8 |
| | 1.5–2.0 m | 0 | 1878 | 0 | 0 | 1433 | 0 |
| | >2.0 m | 0 | 1206 | 0 | 0 | 2976 | 0 |
| 2003 | <1.0 m | 682 | 2138 | 32 | 272 | 848 | 32 |
| | 1.0–1.5 m | 16 | 1850 | 1 | 106 | 1199 | 9 |
| | 1.5–2.0 m | 0 | 1878 | 0 | 112 | 1433 | 8 |
| | >2.0 m | 0 | 1206 | 0 | 7 | 2976 | 0 |
| 2008 | <1.0 m | 999 | 2138 | 47 | 475 | 848 | 56 |
| | 1.0–1.5 m | 164 | 1850 | 9 | 125 | 1199 | 10 |
| | 1.5–2.0 m | 8 | 1878 | 0 | 1 | 1433 | 0 |
| | >2.0 m | 0 | 1206 | 0 | 0 | 2976 | 0 |
| 2012 | <1.0 m | 861 | 2138 | 40 | 521 | 848 | 61 |
| | 1.0–1.5 m | 28 | 1850 | 2 | 150 | 1199 | 13 |
| | 1.5–2.0 m | 0 | 1878 | 0 | 45 | 1433 | 3 |
| | >2.0 m | 0 | 1206 | 0 | 6 | 2976 | 0 |
| Average of all surveys | <1.0 m | 792 | 2138 | 37 | 366 | 848 | 43 |
| | 1.0–1.5 m | 59 | 1850 | 3 | 118 | 1199 | 10 |
| | 1.5–2.0 m | 2 | 1878 | 0 | 40 | 1433 | 3 |
| | >2.0 m | 0 | 1206 | 0 | 3 | 2976 | 0 |

One factor that may account for the greater coverage of SAV observed in the southern study area at similar depths, despite a larger areal extent of shallow depths in the northern study area, is differences in light availability across the Sound (Sincock et al., 1965; Batiuk et al., 2000; Short et al., 2002). Historically, the northern portion of Currituck Sound has reported higher turbidity than the southern end (Dickson, 1958; Sincock et al., 1965; Davis and Brinson, 1983; Carter and Rybicki, 1994; Smith, 2007; Fear, 2008; Fine, 2008). The simultaneous light attenuation data collected for this study support these observations with the northernmost station, CS03, having slightly higher average daily $K_d$ values (i.e., poorer water clarity) than the two stations further south, CS02 and CS01 (Figures 15 and 20). Several possible explanations for this pattern have been proposed in the past; including high turbidity inputs from the three major tributaries, all located in the north; more limited flushing in the north due to restricted mixing across the Big Narrows; reduced susceptibility to sediment resuspension in the south due to sandier sediments and deeper depths; and the higher salinity in the south resulting in increased flocculation and rates of sedimentation compared to those in the north (Sincock et al., 1965; Davis and Carey, 1981; Davis and Brinson, 1983; Carter and Rybicki, 1994; Fear, 2008). Given the shallow depths and relatively long residence time of water in Currituck Sound, water clarity is especially vulnerable to atypical weather such as high winds and heavy rains (Caldwell, 2001; Wagner, 2016). Because the north is characterized by finer sediments (i.e., more susceptible to

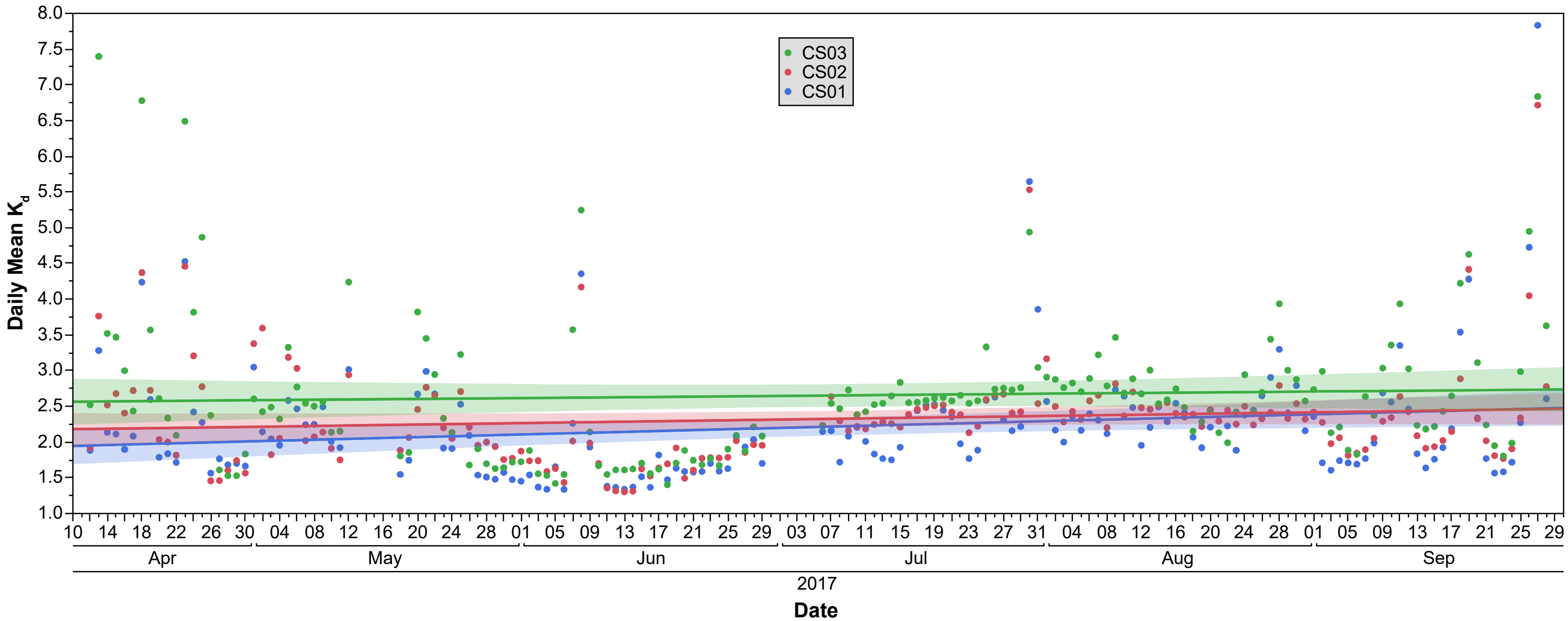


**Figure 20. Daily mean light attenuation ($K_d$) from three stations in Currituck Sound (Figure 15). Plot illustrates similar trends in $K_d$ at all three locations and that station CS03 (northernmost) had a higher $K_d$ (i.e., diminished water clarity) on average than the two stations further south. Although, this is only showing a subset of the data (April 10–September 30 2017), these relationships hold true when looking at the entire time series.**

resuspension) and holds all major tributaries (i.e., increased high-turbidity inputs), it is often disproportionally affected by these events, thus exacerbating the spatial variation (Dickson, 1958; Davis and Carey, 1981; Davis and Brinson, 1990; Carter and Rybicki, 1994; Moorman et al., 2017).

While this may account for north–south spatial variations in SAV, the reasoning behind the observed preferential abundance of SAV along the eastern shore, as evidenced by the aerial and quadrat surveys, is less clear given the data collected. Although few studies have investigated the hydrology in Currituck Sound, the consensus is that the system is generally well-mixed vertically and laterally (i.e., east–west) due to its shallow nature and primarily wind-driven circulation (Sincock et al., 1965; Caldwell, 2001; Fear, 2008; Wagner et al., 2016; Moorman et al., 2017). Most notably, in a study investigating the water quality along the proposed Mid-Currituck Bridge corridor during non-storm and storm conditions, Wagner et al. (2016) found that turbidity and total suspended solids, along with other physical water-quality parameters and constituents, were laterally and vertically uniform but temporally variable. Thus, suggesting that variations in water clarity may not be the cause of east–west spatial variations in SAV. Perhaps the lateral variations in SAV coverage are a function of bathymetry as the western shore generally has a narrower shelf and steeper slope than the eastern shore.

The surveys conducted in 1959, 1960, and 1962 by Sincock et al. (1965) recorded dominant soil type for each gridded quadrat across the Sound to provide a more complete mapping of soil distribution. The soil types used include loam, silt, sand, clay, shell, muck, and peat (Sincock et al., 1965). The study found that sand was the dominant soil type for all of Currituck Sound, but that sand made up a greater proportion of the sediment in the southern end (Sincock et al., 1965). The sediment samples collected in this study were not as widely distributed as those from Sincock et al., but a dominance of sand throughout the two study areas and a greater proportion of sand in the southern study area were also observed. This observation is also supported by Hartis (2013) following a 2010 study where soil was classified similarly to Sincock et al. (1965). Wagner et al. (2016) analyzed the sediments at five locations along the proposed Mid-Currituck Bridge corridor at three different times from 2011–2015. They found that the fine fraction (<63 μm) in sediments was highly variable spatially and temporally, ranging from 1 to 68 weight percent, and that generally, fines were more abundant in the central locations than the nearshore locations (Wagner et al., 2016). More work is needed to understand the modern-day sedimentary processes in Currituck Sound that may help better address the SAV distribution. The few studies on sedimentation in this region suggest that sediment inputs are low and transient and characterized by frequent resuspension and little long-term accretion of fine particles (Wagner et al., 2016).

SAV are known to colonize sediments with a wide range of grain size, particularly in lower salinity environments, suggesting that grain-size is not likely the dominant factor limiting growth (Barko and Smart, 1986; Batiuk et al., 2000; Koch, 2001; Koch et al., 2004). Sediment chemistry on the other hand seems to have a much greater impact on SAV distribution, and organic content is often the most significant limiting factor in sediments (Barko and Smart, 1986; Batiuk et al., 2000; Koch, 2001; Koch et al., 2004). A large number of studies have shown that SAV beds are generally limited to sediments with less than 5% organic matter (Barko and Smart, 1986; Batiuk et al., 2000; Koch, 2001; Koch et al., 2004). In this study, very few sediment samples had greater than 5% organic content and those that did were typically associated with little to no SAV, although the macroalga muskgrass was sometimes identified in these areas. Otherwise, no clear correlation between SAV cover and sediment grain-size or organic content was evident from this study. Sincock et al. (1965) reported that silt soils were the most frequently vegetated throughout the Sound, followed by loam, and both were considerably more vegetated than sand. Although a statistical relationship could not be clearly established, it was generally observed that sites with greater fine fractions were more likely to be unvegetated. This may suggest that a shift has occurred in the preferred sediment grain size colonized by SAV in this system towards coarser sediments. If so, this could point to water-quality changes in the system such as deteriorating water clarity making areas with fewer fine particles (i.e., less potential for sediment resuspension) more suitable for SAV or increased nutrient concentrations resulting in more nutrient availability in and around sands (i.e., no longer limiting SAV growth; Barko and Smart, 1986; Batiuk et al., 2000; Koch, 2001). More data would be necessary to determine if such change has occurred, especially since the relationship between SAV and sediments is often highly species dependent.

Historically, the SAV species found in Currituck Sound have generally remained unchanged, with some notable exceptions (e.g., the introduction of Eurasian watermilfoil), though their relative abundance has varied greatly over the past century. Sago pondweed (*Stuckenia pectinata*) was the dominant species in the early 1900s and reported to be extremely abundant in 1909 (McAtee, 1919) and from 1926 to 1930 (Bourn, 1932). In a series of studies conducted by Sincock et al. (1965) from 1959 to 1962, bushy pondweed and wild celery were the dominant species observed. In 1962, the Ash Wednesday nor'easter struck the Outer Banks and caused several breaks in the barrier island leading to a dramatic increase in the salinity of Currituck Sound (Davis and Brinson, 1990). It is believed the ensuing decreased turbidity (i.e., resulting from increased flocculation and sedimentation) allowed the invasive Eurasian watermilfoil to quickly take over (Davis and Brinson, 1983, 1990). Davis and Brinson (1990) observed widgeon grass and wild celery become increasingly prevalent from 1973 to 1988 and, although still the dominant species at the time, Eurasian watermilfoil began declining around the same time. The top three species observed in 1990 by Ferguson and Wood (1994) were the same as those observed in this study (i.e., widgeon grass, wild celery, and Eurasian watermilfoil).

Widgeon grass and wild celery were the most prevalent SAV species observed along the 27 100-m monitoring transects for all four survey periods and their distribution densities were negatively correlated. Widgeon grass appeared to dominate the southern study area and along the western and eastern shores while wild celery dominated the northern study area and along the middle transects (Figures 13 and 14). Additionally, the lateral variations (i.e., west, mid, and east) within each study area (i.e., north and south) were examined and species seasonality (e.g., peak biomass of widgeon grass occurring earlier in the growing season than wild celery; Kantrud, 1991; McFarland, 2006; Koch et al., 2004) was accounted for by averaging the groups from all four quadrat surveys (Figure 21). From this, it appears that the purported dominance of wild celery in the north (Figure 13) may be a result of the high number of mid transects in the northern compared to the southern study area (i.e., 7:2). One possible explanation for the prevalence of wild celery in the mid areas is wind-wave exposure. Widgeon grass roots are unable to penetrate substrate deeply, thus its belowground biomass lies within the upper 10 cm of sediments making it very susceptible to excess turbulence (Kantrud, 1991; Davis and Brinson, 1990). Wild celery has a greater wave tolerance than widgeon grass (Batiuk et al., 2000; Koch, 2001) and is therefore more likely to dominate in the less protected middle portions of the Sound. Although widgeon grass was more prevalent than wild celery near-shore in the north (Figure 21), the magnitude of difference was reduced from that of the south, which suggests that this longitudinal variation may still exist but perhaps at a smaller spatial scale than what was implied in Figure 13. Differences in salinity or light availability between the northern and southern study areas could possibly account for this variation. Widgeon grass has a higher salinity tolerance and is more light sensitive than wild celery (Davis and Brinson, 1990; Kantrud, 1991; McFarland, 2006), therefore it is more likely to outperform wild celery in the south where salinity tends to be higher and turbidity tends to be lower. Following an inspection of duck food conditions in October 1924, Assistant Biologist of the Bureau of Biological Survey, C.C. Sperry, reported that while abundant in the Sound, wild celery was especially rare toward the southern end and eastern side (Sincock et al., 1965). Suggesting that the patterns observed in this study may be long-standing niche environments.

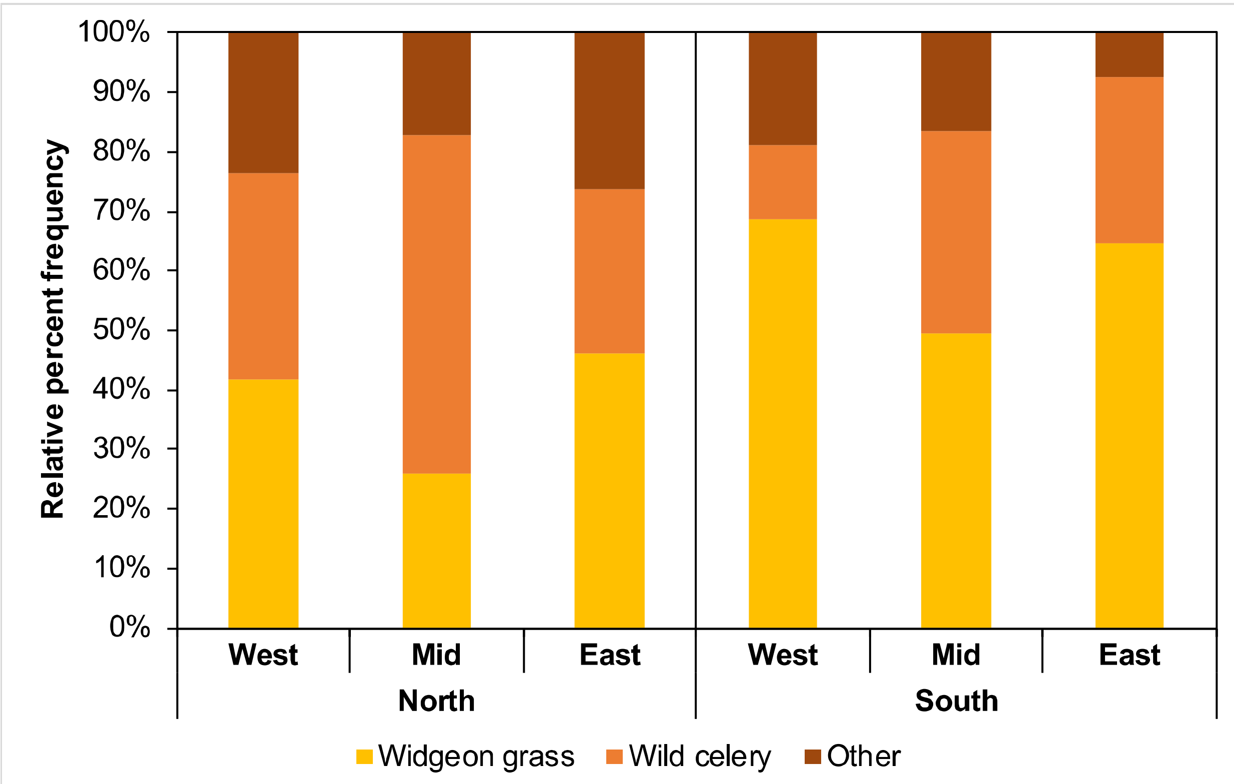


**Figure 21. Relative percent frequency of SAV species for the west, mid, and east transects within the northern and southern study areas and averaged across all times surveyed.**

### 4.2 Water Depth and Light Attenuation Influence on SAV Distribution

Water depth affects several principal factors influencing the establishment and continuation of SAV habitats, such as the amount of light that can reach the bottom (Dennison et al., 1993), wave energy and current velocity, and subsequently, sediment deposition and resuspension (Koch, 2001; Madsen et al., 2001). The historical and modern relationship between SAV frequency and water depth in the region was investigated in order to determine whether any significant changes have occurred over time (Table 12, Figure 22). Maps showing sampling locations of previous studies are shown in Appendix E. Field surveys conducted in 1959 and 1960 by Sincock et al. (1965) showed that SAV was found at maximum depths ($Z_{max}$) of 3.1 and 3.2 m and the peak-depth limit ($Z_{peak}$) was between 1.5–1.8 m and 1.8–2.1 m in 1959 and 1960,

**Table 12. $Z_{peak}$ (~80$^{th}$ percentile) and $Z_{max}$ for all available SAV studies in Currituck Sound leading up to and including this study and ordered by ascending date. Survey methods are listed and categorically color coded: green = quadrat, blue = aerial photography interpretation, and red = hydroacoustic.**

| Date | $Z_{peak}$ | $Z_{max}$ | n | Survey method | Source |
|---|---|---|---|---|---|
| Aug-1959 | 1.5–1.8 (80.0%) | 3.0 | 3922 | Quadrat point sampling | [1]Sincock et al., 1965 |
| Aug-1960 | 1.8–2.1 (83.6%) | 3.2 | 4464 | Quadrat point sampling | [1]Sincock et al., 1965 |
| Jul-1978 | 1.6–1.8 (81.1%) | 3.1 | 74 | Biomass/quadrat (g/m$^2$) | [2]Davis & Carey, 1981 |
| Jul-1988 | 1.4–1.8 (93.5%) | 2.3 | 31 | Biomass/quadrat (g/m$^2$) | [3]Davis & Brinson, 1990 |
| 1990 | 1.0 (80.0%) | 2.6 | 6105 | Aerial photography interpretation | [5]NOAA |
| Oct-2003 | 1.0 (80.0%) | 2.7 | 10130 | Aerial photography interpretation | [6]ECSU |
| Jun-2008 | 0.9 (80.0%) | 2.7 | 17047 | Aerial photography interpretation | [7]APNEP |
| Jul-2010 | 1.4–1.8 (89.3%) | 2.2[a] | 75 | Quadrat rake sampling | [4]Hartis, 2013 |
| Oct-2012 | 0.8 (80.0%) | 2.9 | 20116 | Aerial photography interpretation | [8]APNEP |
| Oct-2017 | 1.06 (80.0%) | 1.79 | 10770 | Hydroacoustic (BioSonics) | [9]This study |
| Oct-2017 | 1.06 (80.0%) | 1.32[b] | 164 | Quadrat survey | [9]This study |
| May-2018 | 1.04 (80.0%) | 1.31[b] | 162 | Quadrat survey | [9]This study |
| Jun-2018 | 1.11 (80.0%) | 1.57 | 11392 | Hydroacoustic (BioSonics) | [9]This study |
| Oct-2018 | 1.05 (80.0%) | 1.32[b] | 162 | Quadrat survey | [9]This study |
| May-2019 | 1.06 (80.0%) | 1.26[b] | 162 | Quadrat survey | [9]This study |
| May-2019 | 1.21 (80.0%) | 1.75 | 12041 | Hydroacoustic (BioSonics) | [9]This study |

[a] Reported maximum depth was 2.9 m but based on one sample; next closest maximum depth was 2.2 m.
[b] Maximum depth surveyed.

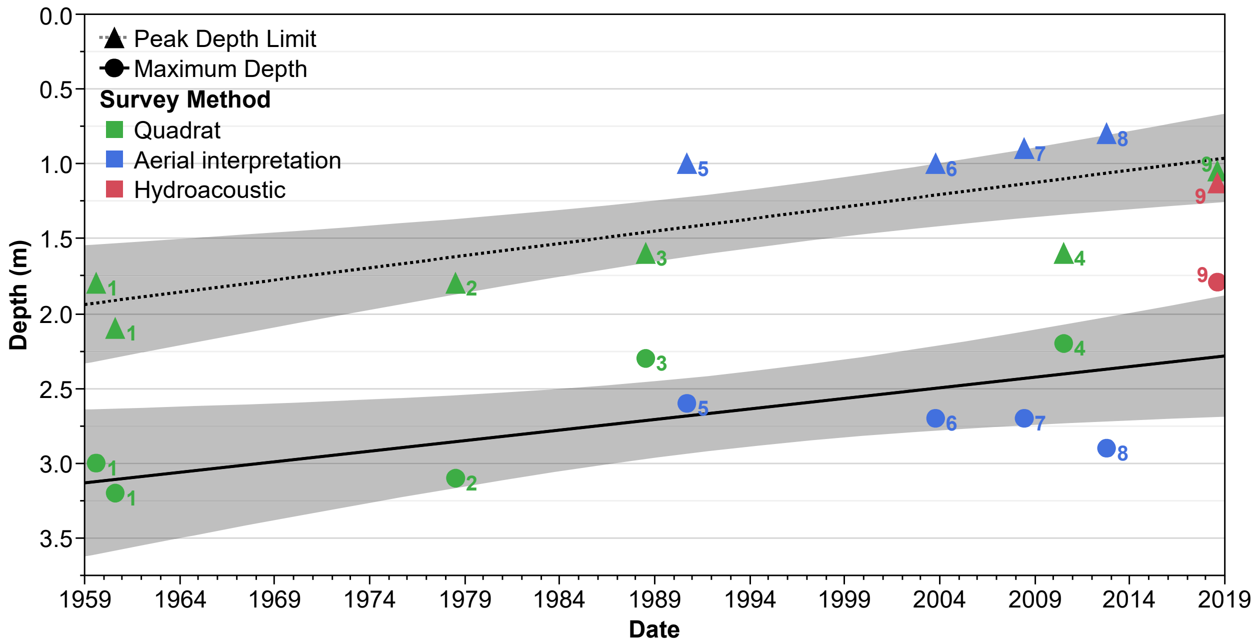


**Figure 22. Time series of $Z_{peak}$ (triangles and dashed trendline) and $Z_{max}$ (circles and solid trendline) for all available SAV studies in Currituck Sound leading up to and including this study. Points are categorically color coded based on survey methods: green = quadrat, blue = aerial photography interpretation, and red = hydroacoustic. Data references (1–9) listed in Table 12.**

respectively. In 1978, Davis and Carey (1981) resampled the transects established by Sincock et al. (1965) and found that $Z_{max}$ was 3.1 m and $Z_{peak}$ was between 1.6–1.8 m. Following the methods from the previous study, Davis and Brinson (1990) resampled the transects in 1988 and found that $Z_{max}$ was 2.3 m and $Z_{peak}$ was 1.4–1.8 m. In 2010, Hartis (2013) measured SAV cover systematically across the sound using the rake method and reported $Z_{max}$ to be 2.9 m and $Z_{peak}$ was once again 1.4–1.8 m. However, the 2.9 m maximum depth was based on a single site and the next closest depth where SAV was present was 2.2 m. This gap in plant presence (i.e., from 2.2 to 2.9 m), the potential errors associated with the rake method in turbid waters (i.e., unknowingly obtaining unattached samples that were uprooted and transported to another location; USEPA, 2006; Zhu et al., 2007), contemporary work in the area, and Hartis' own definition of the littoral-pelagic boundary at 2 m, adds uncertainty to this reported maximum depth. Thus, $Z_{max}$ for the 2010 study was delimited as 2.2 m since it was the maximum continuous depth of SAV presence. The modern-day relationship between SAV and depth was explored primarily through the hydroacoustic surveys conducted in October 2017, June 2018, and May 2019. The average $Z_{peak}$ and $Z_{max}$ from the three hydroacoustic surveys were 1.13 and 1.70 m, respectively. The maximum depth of SAV could not be determined from the data collected during the quadrat surveys because these were restricted to depths shallower than 1.35 m. Looking at only the quadrat sites where SAV was present, $Z_{peak}$ for the four quadrat surveys was approximately 1.05 m, similar to the results from the hydroacoustic surveys conducted in the same time frame.

Creating a time series of all SAV research in Currituck Sound leading up to and including this study shows a general shallowing of both the maximum depth and peak-depth limit at which SAV was found (Figure 22). In the past, these changes have been largely correlated with increased turbidity in the Sound and as a result, turbidity has been cited as a dominant force influencing both short-term and long-term changes in SAV by most major studies in the region (Bourne, 1932; Dickson, 1958; Sincock et al., 1965; Davis and Carey, 1981; Davis and Brinson, 1983, 1990; Carter and Rybicki, 1994). Turbidity alone cannot explain all changes to SAV in Currituck Sound, thus, other factors have been investigated or at least suggested in the literature, including turbulence, temperature, salinity, inorganic nutrients, epiphytic growth, and disease (Davis and Carey, 1981; Davis and Brinson, 1983, 1990; Carter and Rybicki, 1994). While none of these factors can be explicitly ruled out, it is thought that, with the exception of salinity, most have not contributed to significant changes in SAV abundance and distribution (Davis and Carey, 1981; Davis and Brinson, 1983, 1990; Carter and Rybicki, 1994). Lack of data prior to degradation in Currituck Sound as well as insufficient research on SAV in pristine oligohaline estuary environments makes it difficult to differentiate between natural fluctuations in the vegetation and anthropogenically induced changes. However, studies suggest that SAV beds tend to recover quickly from short-term disturbances (e.g., storms; Dickson, 1958; Davis and Carey, 1981).

Light availability has been identified as the key driver controlling the establishment of SAV habitats in most systems (Fonseca et al., 1998; Short et al., 2002; Batiuk et al., 2000; Koch, 2001). The Chesapeake Bay Program, after extensive review of scientific literature, research findings, and application of models, has developed a set of SAV habitat requirements that define the minimal water-quality levels necessary for the growth and survival of SAV across various salinity regimes (Batiuk et al., 1992; Batiuk et al., 2000). The water-column light requirement over the growing season for oligohaline environments was found to be 13%, meaning that when median seasonal PLW is greater than 13%, SAV are expected to thrive (Batiuk et al., 2000).

This value was derived from in-depth review of various studies including laboratory and field studies both in and out of Chesapeake Bay (Batiuk et al., 2000). One field study by Carter and Rybicki (1990) in the tidal fresh Potomac River and oligohaline Potomac Estuary suggested that the minimum light required for SAV growth was 7% and that at 11 to 14.5% light, SAV cover increased from year to year (Batiuk et al., 2000; Batiuk et al., 1992). Other studies looked at the percent light at the maximum depth that various oligohaline SAV species would grow which was found to range from 2 to 62% (Batiuk et al., 2000). Comparing the PLW-depth relationship to results from the hydroacoustic surveys suggests the relationship in Currituck Sound is similar to that established for oligohaline regions of Chesapeake Bay. Assuming a median growing-season $K_d$ of 1.99 $m^{-1}$, the calculated PLW at a depth of 1.79 m (i.e., $Z_{max}$ as determined from the hydroacoustic surveys) is 2.8%. Meaning that in Currituck Sound, at least 2.8% of light must reach the bottom for SAV to survive. However, the majority (80%) of SAV was found at depths shallower than 1.21 m (i.e., $Z_{peak}$), suggesting that SAV requires >9% light for denser cover.

The revised report published by the Chesapeake Bay Program (Batiuk et al., 2000) differentiated between two light requirements: the minimum light (primary) and water-column light (secondary) requirements. The water-column light requirement is based on calculating the PLW and is considered less robust than the minimum light requirement that is based on calculating the percent light at the leaf (PLL), considering the attenuation from epiphytic attachment (Batiuk et al., 2000). Calculating PLL, however, requires two additional variables, epiphyte biomass and the epiphytic light attenuation coefficient, which are derived from data on total suspended solids, dissolved inorganic nitrogen, and dissolved inorganic phosphorous (Batiuk et al., 2000). Since this data were not available, PLW was used as a substitute. When comparing the calculated results of PLW and PLL, light attenuation by epiphytic material appeared to be particularly important in the fresh and oligohaline regions of Chesapeake Bay due to the high nutrient and total suspended solids concentrations (Batiuk et al., 2000). However, in practice, SAV was sometimes found inhabiting areas where PLL was as low as 1–3%, much lower than the established 9% minimum light requirement. Additionally, during the 1978 and 1988 studies, Davis and Brinson (1990) noted that while epiphytes were likely a primary cause of stress on wild celery in the Pamlico River, epiphytic growth was largely absent or non-detectable on wild celery in Currituck Sound. Thus, epiphytes may not be critical in this system and while future inclusion of epiphytic effects on light attenuation may be worthwhile, the use of PLW is likely a good surrogate.

The water-quality data collected in this study indicated the relatively high light attenuation observed in this system primarily resulted from high concentrations of dissolved organic matter (fDOM). However, $K_d$ was largely affected by short-term changes in turbidity and chlorophyll, suggesting that the resuspension of sediments and microphytobenthos can significantly alter light conditions in the Sound on short timescales. As expected in this shallow system, resuspension was prevalent during storms, however, the resultant turbidity spikes generally returned to baseline conditions quickly (e.g., <2 days). This might imply that infrequent, short-term fluctuations in turbidity will have little long-term influence on SAV. However, the effects of changes in water quality are often cumulative, thus, numerous short-term turbidity spikes, even seemingly minor ones, have the potential to severely impact SAV on both shorter and longer timescales.

## 5.0 FUTURE MANAGEMENT IMPLICATIONS

The hydroacoustic and in-water quadrat surveys conducted in this study provided a broad understanding of modern-day SAV distribution that, especially when put into context with previous work in the region, can be invaluable for implementing effective management strategies. Moving forward, modifying these methods to better address the observed distribution patterns of SAV may be advantageous, particularly for assessing changes in SAV cover at different scales. Considering spatial scale is critical in selecting a sampling method and resolution that can adequately represent the habitat being investigated (Fonseca et al., 1998). Observations made during the quadrat surveys revealed that the SAV habitat in Currituck Sound is mainly characterized by patchy SAV beds. Thus, small variabilities in the sampling locations can result in significant differences in the measured SAV cover. Currents, wind, and GPS error made it difficult for data to be collected in precisely the same locations both between survey types (i.e., hydroacoustic and quadrat) and among survey dates. As a result, the quadrat data could not be used to assess the accuracy of the hydroacoustic surveys and short term (i.e., seasonal and annual) changes in SAV cover could not be confidently assessed for either survey type. Given the spatial heterogeneity of the SAV beds, measuring changes at smaller spatial and temporal scales (e.g., at the site level and seasonal) would require increased sampling resolution (Kenworthy et al., 2012). To do this most efficiently, Kenworthy et al. (2012) suggests compiling all available data on SAV distribution and the physical processes affecting the patterns of distribution (e.g., light, waves, salinity, and sedimentary processes) to predict the expected distribution and develop a map of potential SAV habitat using the data. The resulting sites should be prioritized for future research, restoration, and/or mitigation (Kenworthy et al., 2012).

Although preserving existing SAV beds is ideal both ecologically and economically, mitigating to compensate for permanent losses caused by anthropogenic activity is an increasingly popular management practice. Mitigation, while proven to be a successful tool, can have many pitfalls and comprehensive planning is vital to the success of these projects (Fonseca et al., 1998). The most important decision in the mitigation planning process is site selection since SAV survivorship in an unsuitable area could, at best, be costly and ineffective and, at worst, result in additional SAV losses (Fonseca et al. 1998). The results of this study provide a preliminary assessment of possible mitigation areas in Currituck Sound for the Mid-Currituck Bridge or other future projects. Ideally, SAV plantings should occur at the impacted sites once the issues that led to SAV loss have been remedied; however, this is not always possible. For instance, NCDOT estimates that the Mid-Currituck Bridge will shade 1.4 ha of existing SAV beds and 2.5 ha of potential SAV habitats (defined as areas with water depths ≤1.8 m by the Coastal Area Management Act) meaning 1.4 ha of SAV beds could be lost, but replanting in this immediate area would be inadvisable as light availability will be impacted (NCDOT, 2019).

The success of SAV plantings is highly dependent on how well a site satisfies multiple criteria including historical SAV distribution, current SAV distribution, proximity to existing SAV beds, sediment characteristics, wave exposure, water depth, water quality, and bioturbation (Fonseca et al., 1998; Short et al., 2002). Areas that have consistently remained unvegetated in the past should be avoided whenever possible since it is unlikely that they will be able to support vegetation (Fonseca et al., 1998). Currently vegetated areas should immediately be rejected, and care should be taken to ensure this definition considers both continuous and patchy beds; therefore, areas close enough to be naturally revegetated by existing SAV beds should also be avoided (Fonseca et al., 1998; Short et al., 2002). Although not typically the principle factor limiting growth, sediment grain-size and organic content should be considered particularly in context of the species selected for replanting (Fonseca et al., 1998; Short et al., 2002; Batiuk et al., 2000; Koch et al., 2004). Existing SAV beds should be used as indicators of the thresholds of wave exposure and water depth for SAV in the system (Fonseca et al., 1998; Short et al., 2002). Depth limits on SAV are largely a function of various water-quality parameters (e.g., TSS, chlorophyll-a, DIN, DIP, CDOM, etc.) affecting light availability (Fonseca et al., 1998; Short et al., 2002; Batiuk et al., 2000). Lastly, areas with prolific infauna should be avoided since excess bioturbation of sediments can devastate vegetation (Fonseca et al., 1998; Short et al., 2002).

For the purposes of this study, the historical and current SAV distribution, sediment characteristics, wave exposure, water depth, and water quality in Currituck Sound were examined. The aerial SAV maps (Figure 8; NOAA-OCM, 2015; ECSU, unpublished data; APNEP, 2019, unpublished data) and review of past field studies in the Sound (Sincock et al., 1965; Davis and Carey, 1981; Davis and Brinson, 1990; Hartis, 2013) provided an understanding of historical SAV distribution. Data on current SAV distribution was collected but spatially limited to the sites where the hydroacoustic and quadrat surveys were conducted. Sediments were found to be primarily sandy with low organic matter and little spatial variability. No statistical relationship between SAV cover and sediment characteristics were discovered from the sites surveyed; however, a review of existing literature shows that high organic matter can limit SAV growth (although the actual limit varies among species) and peaty sediments are unsuitable for SAV growth (Batiuk et al., 2000; Koch et al., 2004), a relationship that was anecdotally observed in the quadrat surveys. Areas of high, medium, and low wave exposure were identified with WEMo and compared to historical SAV data to inform the placement of the field survey locations. The depth of existing SAV beds was measured from the hydroacoustic and quadrat surveys. Lastly, the median seasonal $K_d$ coupled with the most comprehensive bathymetric dataset available were used to model the spatial distribution of potential SAV habitats based on water-column light requirements (i.e., PLW) and depth. This model, supported by the SAV-depth relationship established from the hydroacoustic and quadrat surveys as well as the Chesapeake Bay habitat requirements for oligohaline environments, provided a preliminary understanding of current light availability for the Currituck.

By integrating the depth-light model developed in this study with historical and current SAV coverage data, areas that meet some of the preliminary conditions for a suitable mitigation site (i.e., shallow water depths with enough light available, previously vegetated, and currently unvegetated) were identified. Given an understanding of SAV depth distribution and light availability in this system, water depth areas were differentiated by their likelihood of sustaining planted SAV. The hashed gray portion of Figure 23a represents the regions that are beyond 1.8 m in depth and receive less than 2.8% light, thus, not at all likely to support SAV. The green regions in Figure 23a receive enough light to sustain SAV and are further subdivided by their potential for successful SAV growth and survival. Areas shallower than 1.0 m (i.e., receiving 13.7% or more light) were deemed very likely to sustain planted vegetation (shown as the darkest green in Figure 23a), areas between 1.0 and 1.5 m (i.e., receiving between 13.7 and 5.1% light) were moderately likely (shown as the medium green in Figure 23a), and areas between 1.5 m and 1.8 m (i.e., receiving between 5.1% and 2.8% light) were the least likely (shown as the lightest green in Figure 23a). Inverting the combined 1990, 2003, 2008, and 2012 aerial SAV distribution datasets provides a synopsis of the areas that have always been unvegetated (shown in semi-transparent black in Figure 23b). Lastly, the most current SAV dataset, APNEP's 2012 map (unpublished data), was used to demonstrate the presently vegetated areas (shown in blue in

Figure 23c). The suitable mitigation areas (remaining green portions in Figure 23c) are those left after eliminating the areas that have consistently been unvegetated, are currently vegetated, or are not at all likely to sustain SAV due to depth and insufficient light.

However, due to the limitations of the bathymetric data and aerial SAV maps, as previously discussed, and the lack of modern synoptic SAV data in Currituck Sound since the 2012 APNEP aerial survey (unpublished data), site selection based on these data alone would be imprudent. Instead, this model should be used to identify regions where focusing additional data collection efforts would be most appropriate. Considering the challenges of photointerpretation in waters where light attenuation with depth is high and the time constraints of other mapping methods at a regional scale, prioritizing key areas of interest is essential for ensuring future work is efficient and effective (Kenworthy et al., 2012; Finkbeiner et al., 2001). Additional data collection should focus on finer scale mapping of existing SAV and bathymetry. This study has shown that in Currituck Sound, the primary factor limiting SAV distribution is water depth, thus, prior to choosing a mitigation site, it is vital that additional bathymetry is collected in the places where lacking. This is especially true near and in between the marsh islands (e.g., the Big Narrows) since the availability of protected sections (i.e., low wave energy) and historical SAV distribution suggest this could be a favorable area for mitigation. Ideally, further studies would be conducted to support some of the other parameters that affect suitability for SAV growth and survival (e.g., TSS, chlorophyll-a, DIN, DIP, CDOM, epiphytes, bioturbation), but practically, site selection could focus on water depth, proximity to existing vegetation, and avoidance of peat and sediments with high organic content. Given the heterogenous nature of SAV in the Currituck Sound, finding unvegetated areas that will not impact the natural fluctuations of existing beds could be challenging, especially when trying to meet the rest of the criteria. Consequently, if no suitable site is found, managers may have to turn to other, potentially more costly, approaches such as site engineering or water-quality restoration.

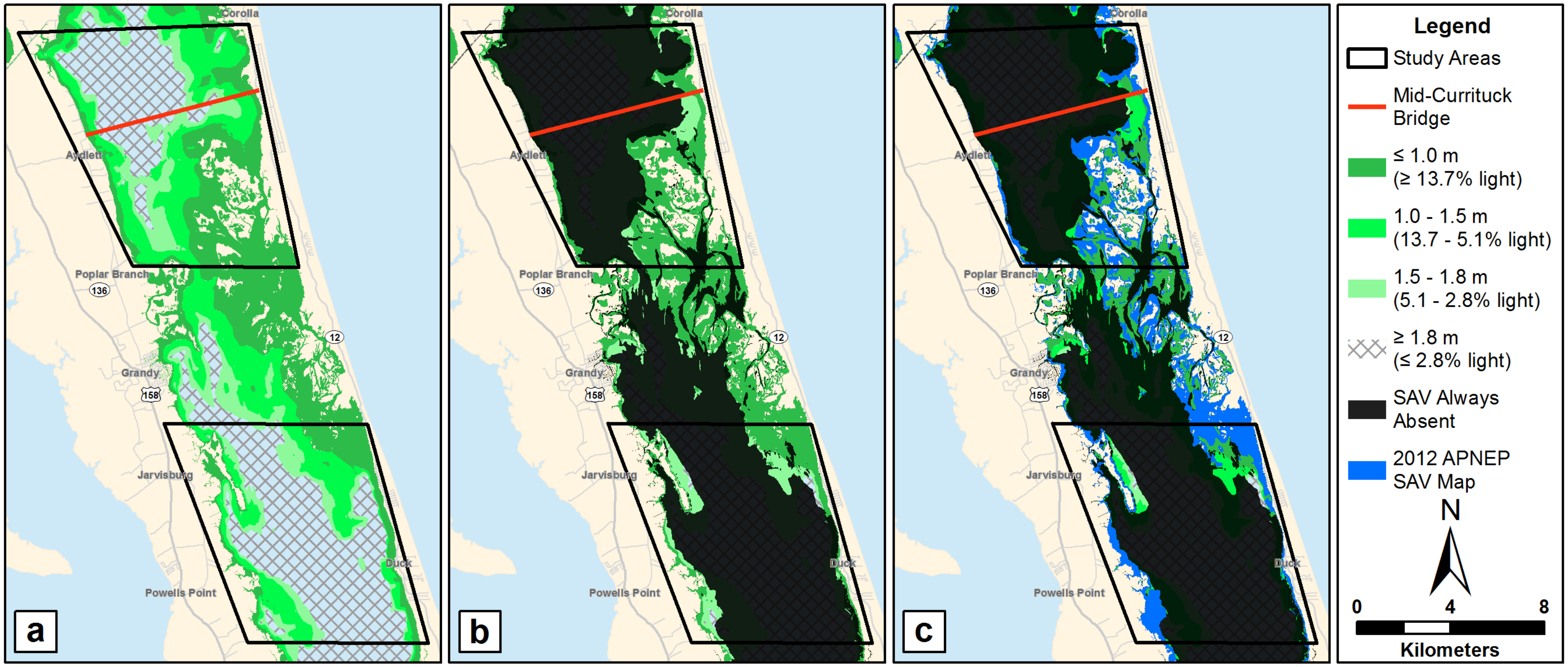


**Figure 23. Visualization of the site selection process for SAV mitigation or for prioritizing data collection by eliminating the areas that (a) are not at all likely to support SAV (hashed gray polygon) due to excess depth (i.e. >1.8 m) and insufficient light (i.e., <2.8%), (b) have never supported SAV (black polygon) unless the site will be engineered to support vegetation, and (c) are currently vegetated (blue polygon). The remaining green areas in (c) are those with the greatest potential for successful mitigation and can be further categorized based on depth and the amount of light reaching the bottom. The regions that are most likely to support SAV are symbolized as the darkest green and those that are least likely to support SAV are shown as the lightest green.**

## 6.0 SUMMARY

The past and present relationship between water depth and SAV cover was examined in several ways: (1) historical SAV cover maps, (2) hydroacoustic surveys (BioSonics), (3) quadrat transect surveys, (4) modeling using light attenuation data, and (5) comparisons with historical ground surveys. While individually these approaches are limited by either the quality of the data available or the associated spatial or temporal scales, together, the results suggest that in Currituck Sound, SAV are not present beyond a water depth of 1.8 m and are preferentially located at depths shallower than 1.0 m. Assuming a median growing-season $K_d$ of 1.99 $m^{-1}$ (as measured for the combined 2016 and 2017 growing seasons), the calculated minimum water-column light requirement is 2.8% and water-column light requirement for peak growth is ≥13.7%. Sediments were dominated by sand (average weight percent >90%) and had very low organic content (average percent LOI ~1.0%). While some spatial and temporal variations in sediment composition were identified, no statistical relationships between SAV cover and sediment characteristics were observed. Light availability with water depth proved to be the dominant factor limiting SAV growth and distribution in Currituck Sound. Therefore, the light and depth thresholds identified in this study are key to developing a sound management and mitigation plan.

## REFERENCES


Albemarle-Pamlico National Estuary Partnership (APNEP), 2019. Submerged Aquatic Vegetation (SAV) 2006-2008 Mapping Effort – Revised. https://www.nconemap.gov/datasets/f6cf4ca894f34026aeeec060570a62c5_0?geometry=-81.859%2C33.811%2C-71.444%2C36.945

Albemarle-Pamlico National Estuary Partnership (APNEP), unpublished data. Submerged Aquatic Vegetation (SAV) 2012-2014 Mapping Effort: Currituck Sound and Back Bay.

Barko, J.W., Smart, R.M., 1986. Sediment-related mechanisms of growth limitation in submersed macrophytes. Ecology 67,1328-1340.

Batiuk, R.A., Bergstrom, P., Kemp, M., Koch, E., Murray, L., Stevenson, J.C., Bartleson, R., Carter, V., Rybicki, N.B., Landwehr, J.M. and Gallegos, C., Karrh, L., Naylor, M., Wilcox, D., Moore, K.A., Ailstock, S., Teichberg, M., 2000. Chesapeake Bay Submerged Aquatic Vegetation Water Quality and Habitat-Based Requirements and Restoration Targets: A Second Technical Synthesis. CBP/TRS 245/00 EPA 903-R-00-014. U.S. EPA Chesapeake Bay Program, Annapolis, Maryland.

Batiuk, R.A., Orth, R.J., Moore, K.A., Stevenson, J.C., Dennison, W.C., Staver, L., Carter, V., Rybicki, N.B., Hickman, R., Kollar, S., Bieber, S., 1992. Chesapeake Bay Submerged Aquatic Vegetation Habitat Requirements and Restoration Targets: A Technical Synthesis. CBP/TRS 83/92. U.S. EPA Chesapeake Bay Program, Annapolis, Maryland.

Beck, M.W., Heck, K.L., Jr., Able, K.W., Childers, D.L., Eggleston, D.B., Gillanders, B.M., Halpern, B., Hays, C.G., Hoshino, K., Minello, T.J., Orth, R.J., Sheridan, P.F., Weinstein, M.P., 2001. The identification, conservation, and management of estuarine and marine nurseries for fish and invertebrates. Bioscience 51 (8), 633-641.

Benner, C. S., Knutson, P. L., Broehu, B. A., and Hurme, A. K., 1982. Vegetative erosion control in an oligohaline environment Currituck Sound, NC. Wetlands 2, 105-117.

BioSonics, Inc., 2013. Visual Acquisition MX: User Guide 6.1. Seattle, WA: BioSonics, Inc.

BioSonics, Inc., 2016. Visual Habitat: User Guide. Seattle, WA: BioSonics, Inc.

Bourne, W.S. 1932. Ecological and physiological studies on certain aquatic angiosperms. Contrib. Boyce Thompson Inst. 4, 425-496.

Caldwell, W.S., 2001. Hydrologic and Salinity Characteristics of Currituck Sound and Selected Tributaries in North Carolina and Virginia, 1998–99. Water-Resources Investigations Report 01–4097.

Carter, V., Rybicki, N.B., 1990. Light attenuation and submersed macrophyte distribution in the tidal Potomac River and estuary. Estuaries 13 (4), 441-452.

Carter, V., Rybicki, N.B., 1994. Invasions and declines of submersed macrophytes in the tidal Potomac River and Estuary, the Currituck Sound-Back Bay system, and the Pamlico River Estuary. Lake and Reservoir Management 10 (1), 39-48.

Chambers, P.A., Kalff, J., 1985. Depth distribution and biomass of submersed aquatic macrophyte communities in relation to Secchi depth. Canadian Journal of Fisheries and Aquatic Sciences 42, 701-709.

Davis, G.J., Brinson, M.M., 1983. Trends in submerged macrophyte communities of the Currituck Sound: 1909-1979. Journal of Aquatic Plant Management 21, 83-87.

Davis, G.J., and Brinson, M.M., 1990. A survey of submersed aquatic vegetation of the Currituck Sound and the western Albemarle-Pamlico estuarine system: N.C. Albemarle-Pamlico Estuarine Study.

Davis, G.J., Carey, D.F., Jr., 1981. Trends in submerged macrophyte communities of the Currituck Sound: 1977-1979. Journal of Aquatic Plant Management 19, 3-8.

Dennison, W.C., Orth, R.J., Moore, K.A, Stevenson, J.C., Carter, V., Kollar, S., Bergstrom, P.W., Batiuk, R.A., 1993. Assessing water quality with submersed aquatic vegetation: Habitat requirements as barometers of Chesapeake Bay health. Bioscience 43, 86-94.

Dickson, A.W., 1958. Some ecological observations in Currituck Sound. Mimeo. Rep., North Carolina Wildlife Resources Commission, Raleigh. 11 pp.

Elizabeth City State University (ECSU), unpublished data. ECSU Currituck SAV 10-16-03.

Fear, J., 2008. A Comprehensive Site Profile for the North Carolina National Estuarine Research Reserve. North Carolina National Estuarine Research Reserve, 321 pp.

Ferguson, R.L., Rivera, J.A., Wood, L.L., 1989. Submerged aquatic vegetation in the Albemarle-Pamlico estuarine system. National Marine Fisheries Service, NOAA, Beaufort Laboratory, Beaufort, NC. Project No. 88-10.

Ferguson, R.L., L.L. Wood. 1994. Rooted Vascular Beds in the Albemarle-Pamlico Estuarine System. US Environmental Protection Agency, National Estuary Program, NC Department of Environment, Health, and Natural Resources. Report No. 94-02.

Findlay, S.E.G., Strayer, D.L., Smith, S.D. and Curri, N., 2014. Magnitude and patterns of change in submerged aquatic vegetation of the tidal freshwater Hudson River. Estuaries and Coasts 37 (5), 1233-1242.

Fine, J.M., 2008. Documentation of data collection in Currituck Sound, North Carolina and Virginia, 2006–2007. U.S. Geological Survey Open-File Report 2008–1147.

Finkbeiner, M., Stevenson, B., Seaman, R., 2001. Guidance for benthic habitat mapping: an aerial photographic approach. Monograph, NOAA, Coastal Services Center, Charleston, SC.

Fonseca, M.S., Kenworthy, J., Thayer, G.W., 1998. Guidelines for the conservation and restoration of seagrasses in the united states and adjacent waters. NOAA Coastal Ocean Program Decision Analysis Series No. 12.

Forstall, R.L., 1996. Population of States and Counties of the United States: 1790 to 1990, U.S. Bureau of the Census, Washington, DC.

Forte, M., 2007. Interferometric Sonar for Identifying Submerged Aquatic Vegetation in a Shallow Estuary. U.S. Army Corps of Engineers Field Research Facility, Duck, NC.

Fourqurean, J.W., Duarte, C.M., Kennedy, H., Marbà, N., Holmer, M., Mateo, M.A., Apostolaki, E.T., Kendrick, G.A., Krausse-Jensen, D., McGlathery, S.O., 2012. Seagrass ecosystems as a globally significant carbon stock. Nature Geoscience. doi:10.1038/NGEO1477

Ganju, N.K., Miselis, J.L., Aretxabaleta, A.L., 2014. Physical and biogeochemical controls on light attenuation in a eutrophic, back-barrier estuary. Biogeosciences 11 (24), 7193-7205.

Greiner, J.T., McGlathery, K.J., Gunnell, J., McKee, B.A., 2013. Seagrass restoration enhances “blue carbon” sequestration in coastal waters. PLOS ONE 8 (8), e72469.

Hartis, B.M., 2013. Mapping, Monitoring and Modeling Submersed Aquatic Vegetation Species and Communities. Dissertation, North Carolina State University, Fisheries, Wildlife, and Conservation Biology.

Heiri, O., Lotter, A.F., Lemcke, G., 2001. Loss on ignition as a method for estimating organic and carbonate content in sediments: reproducibility and comparability of results. Journal of Paleolimnology 25, 101-110.

Kantrud, H., 1991. Widgeongrass (Ruppia maritima L.): A Literature Review. U.S. Fish and Wildlife Service Fish and Wildlife Research 10, 58 pp.

Keddy, P.A., 1982. Quantifying within-lake gradients of wave energy: interrelationships of wave energy, substrate particle size and shoreline plants in Axe Lake, Ontario. Aquatic Botany 14, 41-58.

Kemp, W.M., Batiuk, R.A., Batleson, R., Bergstrom, P., Carter, V., Gallegos, C.L., Hunley, W., Karrh, L., Koch, E.W., Landwehr, J.M., Moore, K.A., Murray, L., Naylor, M., Rybicki, N.B., Stevenson, J.C., Wilcox, D., 2004. Habitat requirements for submerged aquatic vegetation in Chesapeake Bay: Water quality, light regime, and physical-chemical factors. Estuaries, 27 (3), 363-377.

Kemp, W.M., Boynton, W.R., Adolf, J.E., Boesch, D.F., Boicourt, W.C., Brush, G., Cornwell, J.C., Fisher, T.R., Glibert, P.M., Hagy, J.D., Harding, L.W., Houde, E.D., Kimmel, D.G., Miller, W.D., Newell, R.I.E., Roman, M.R., Smith, E.M., Stevenson, J.C., 2005. Eutrophication of Chesapeake Bay: historical trends and ecological interactions. Marine Ecology Progress Series 303, 1-29.

Kenworthy, W.J., Buckel, C.A., Carpenter, D.E., Eggleston, D.B., Field, D., Krahforst, C.S., Luczkovich, J.J., Plaia, G.R., 2012. Development of submerged aquatic vegetation monitoring protocols in North Carolina. Development of Submerged Aquatic Vegetation Monitoring Protocols in North Carolina. Final Report to the North Carolina Coastal recreational Fisheries License Fund. Sep 21, 2012.

Kenworthy, W.J., Fonseca, M.S., 1996. Light requirements of seagrasses Halodule wrightii and Syringodium filiforme derived from the relationship between diffuse light attenuation and maximum depth distribution. Estuaries 19, 740-750.

Koch, E.W., 2001. Beyond light: physical, geological, and geochemical parameters as possible submersed aquatic vegetation habitat requirements. Estuaries 24 (1), 43117.

Koch, E.W., Engelhardt, K.A.M., Bortz, J.K., Murphy, R.F., Thur, R.M., Yee, K.A., Sellner, K.G. 2004. SAV Restoration Handbook: a guide for restoring SAV on DoD installations; US Department of Defense.

Madsen, J.D., Chambers, P.A., James, W.F., Koch, E.W., Westlake, D.F., 2001. The interaction between water movement, sediment dynamics and submersed macrophytes. Hydrobiologia 444, 71-84.

Malhotra, A., Fonseca, M. S., 2007. WEMo (Wave Exposure Model): Formulation, Procedures and Validation. NOAA Technical Memorandum NOS NCCOS #65. 28 pp.

Mallinson, D.J., Culver, S.J., Riggs, S.R., Walsh, J.P., Ames, D.V., Smith, C.W., 2008. Past, Present and Future Inlets of the Outer Banks Barrier Islands, North Carolina. East Carolina University Printing Press, Greenville, NC, 22 pp.

McAtee, W. L. 1919. Notes on the flora of Churches Island, North Carolina. J. Elisha Mitchell Sci. Society 35, 61-75.

McFarland, D.G., 2006. Reproductive ecology of Vallisneria americana Michaux. ERDC TN-SAV-06-4. U.S. Army Engineer Research and Development Center, Vicksburg, MS

McGlathery, K.J., Sundbäck, K., Anderson, I.C., 2007. Eutrophication in shallow coastal bays and lagoons: the role of plants in the coastal filter. Marine Ecology Progress Series 348, 1-18.

McKay, S.K., Wilson, C.R., Piatkowski, D., 2012. Currituck Sound estuary restoration: a case study in objective setting. ERDC TN-EMRRP-EBA-17. U.S. Army Engineer Research and Development Center, Vicksburg, MS.

McLeod, E., Chmura, G.L., Bouillon, S., Salm, R., Björk, M., Duarte, C.M., Lovelock, C.E., Schlesinger, W.H., Silliman, B.R., 2011. A blueprint for blue carbon: toward an improved

understanding of the role of vegetated coastal habitats in sequestering $CO_2$. Frontiers in Ecology and the Environment 9 (10), 552-560.
Middleboe, A.L., Markager, S., 1997. Depth limits and minimum light requirements of freshwater macrophytes. Freshwater Biology 37, 553-568.
Moore, K.A., 2004. Influence of seagrasses on water quality in shallow regions of the lower Chesapeake Bay. Journal of Coastal Research SI45, 162-178.
Moorman, M.C., Augspurger, T., Stanton, J.D. and Smith, A., 2017. Where's the grass? Disappearing submerged aquatic vegetation and declining water quality in Lake Mattamuskeet. Journal of Fish and Wildlife Management 8 (2), 401-417.
Moran, K.L., Mallinson, D.J., Culver, S.J., Leorri, E., and Mulligan, R.P., 2015. Late Holocene evolution of Currituck Sound, North Carolina, USA: environmental change driven by sea-level rise, storms, and barrier island morphology. J. Coast. Res. 31 (4), 827-841.
National Oceanic and Atmospheric Administration (NOAA) Office of Coastal Management (OCM), 2015. North Carolina Seagrass Submersed Rooted Vasculars 1990 Geodatabase. https://inport.nmfs.noaa.gov/inport/item/47910/printable-form
North Carolina Department of Environment, Health, and Natural Resources (NCDEHNR), U.S. Environmental Protection Agency (EPA), 1994. Comprehensive Conservation and Management Plan. Technical Document. National Estuary Program, Albemarle-Pamlico Estuarine Study. https://files.nc.gov/apnep/documents/files/apes/9314.pdf
North Carolina Department of Transportation (NCDOT), 2012. Administrative Action Final Environmental Impact Statement: Mid-Currituck Bridge Study, Currituck and Dare Counties, North Carolina. https://connect.ncdot.gov/projects/MidCurrituckBridgeDocuments/Final%20Environmental%20Impact%20Statement%20January%202012.pdf
North Carolina Department of Transportation (NCDOT), 2019. Reevaluation of Final Environmental Impact Statement Study Report: Mid-Currituck Bridge Study, Currituck and Dare Counties, North Carolina. https://www.ncdot.gov/projects/mid-currituck-bridge/Documents/reevaluation-feis.pdf
Orth, R.J., Carruthers, T.J.B., Dennison, W.C., Duarte, C.M., Fourqurean, J.W., Heck, K.L., Hughes, A.R., Kendrick, G.A., Kenworthy, W.J., Olyarnik, S., Short, F.T., Waycott, M., Williams, S.L., 2006. A Global Crisis for Seagrass Ecosystems: Bioscience, 56, 987-996.
Pedersen, T.M., Gallegos, C.L., Nielsen, S.L., 2012. Influence of near-bottom re-suspended sediment on benthic light availability. Estuarine, Coastal and Shelf Science 106, 93-101.
Piepho, M., 2017. Assessing maximum depth distribution, vegetated area, and production of submerged macrophytes in shallow, turbid coastal lagoons of the southern Baltic Sea. Hydrobiologia 794, 303-316.
Poppe, L.J., Eliason, A.H., Fredericks, J.J., Rendigs, R.R., Blackwood D., and Polloni, C.F. 2000. U. S. Geological Survey Open-File Report 00-358.
Rideout, R.R., 1990. A comprehensive environmental management plan for the Currituck Sound drainage basin: background investigations. N.C. Albemarle-Pamlico Estuarine Study Project No. 90-19.
Riggs, S.R., Bray, J.R., Wyrick, R.A., Klingman, C.R., Hamilton, J.C., Ames, D.V., Watson, J.S., 1993. Sedimentation and Sediment Quality in the North Landing River, Currituck County Estuarine System, North Carolina and Virginia. US Environmental Protection Agency, National Estuary Program, NC Department of Environment, Health, and Natural Resources. Report No. 92-22.

Sheldon, R.B., Boylen, C.W., 1977. Maximum depth inhabited by aquatic vascular plants. American Midland Naturalist 97, 248-254.
Short, F.T., Davis, R.C., Kopp, B.S., Short, C.A., Burdick, D.M., 2002. Site-selection model for optimal transplantation of eelgrass Zostera marina in the northeastern US. Marine Ecology Progress Series 227, 253-267.
Short, F.T., Neckles, H., 1999. The effects of global climate change on seagrasses. Aquatic Botany 63, 169–196.
Short, F.T., Wyllie-Echeverria, S., 1996. Natural and human-induced disturbance of seagrasses. Environmental Conservation 23 (1), 17-27.
Sincock, J.L., Johnston, K.H., Coggin, R.W., Wollits, R.W., Kerwin, J.A., Dickson, A.W., Crowell, T., Grandy III, J., Davis, J.R., McCartney, R., 1965. Back Bay – Currituck Sound data report. U.S. Fish and Wildlife Service, North Carolina Wildlife Resources Commission, and Virginia Commission of Game and Inland Fisheries. 1600 pp.
Smith, C., 2007, Written Comm., Citizen Water-Quality Monitoring Group, unpublished data.
Tokoro, T., Hosokawa, S., Miyoshi, E., Tada, K., Watanabe, K., Montani, S., Kayanne, H. and Kuwae, T., 2014. Net uptake of atmospheric CO 2 by coastal submerged aquatic vegetation. Global Change Biology 20, 1873-1884.
U.S. Army Corps of Engineers (USACE), 2010. Currituck Sound ecosystem restoration feasibility study. Interagency Briefing: Read-Ahead Materials, Wilmington District (SAW).
U.S. Army Corps of Engineers (USACE), 2011. Feasibility Scoping, Meeting: 2 September 2011. Wilmington District, NC.
U.S. Army Corps of Engineers (USACE), 2012. Currituck Sound Ecosystem Restoration Project, Currituck, North Carolina Integrated Feasibility Report and Environmental Impact Statement. U.S. Army Engineer District, Wilmington.
U.S. Environmental Protection Agency (USEPA). 2006. Volunteer Estuary Monitoring: A Methods Manual. EPA-842-B-06-003. Office of Water, Washington, DC. 396 pp.
Wadelynn Geospatial LLC, unpublished data.
Wagner, C., Fitzgerald, S., and Antolino, D., 2016. Characterization of Water-Quality and Bed-Sediment Conditions in Currituck Sound, North Carolina, Prior to the Mid-Currituck Bridge Construction, 2011–15. U.S.G.S. Open-File Report 2015–1208, 84 pp.
Ward, L.G., Kemp, W.M., Boynton, W.R., 1984. The influence of waves and seagrass communities on suspended particulates in an estuarine embayment. Mar. Geol. 59, 85-103.
Waycott, M., Duarte, C.M., Carruthers, T.J.B., Orth, R.J., Dennison, W.C., Olyarnik, S., Calladine, A., Fourqurean, J.W., Heck, K.L., Hughes, A.R., Kendrick, G.A., Kenworthy, W.J., Short, F.T., Williams, S.L., Paine, R.T., 2009. Accelerating Loss of Seagrasses across the Globe Threatens Coastal Ecosystems: Proceedings of the National Academy of Sciences of the United States of America, v. 106, p. 12377-12381.
Wicker, A.M., Endres, K.M., 1995. Relationship between waterfowl and American coot abundance with submersed macrophytic vegetation in Currituck Sound, North Carolina. Estuaries, 18 (2), 428-431.
Zhu, B., Fitzgerald, D.G., Mayer, C.M., Rudstam, L.G., Mills, E.L. 2006. Alteration of ecosystem function by zebra mussels in Oneida Lake, NY: Impacts on submerged macrophytes. Ecosystems 9, 1017-1028.
Zhu, B., Fitzgerald, D.G., Hoskins, S.B., Rudstam, L.G., Mayer, C.M., Mills, E.L., 2007. Quantification of historical changes of submerged aquatic vegetation cover in two bays of

Lake Ontario with three complementary methods. Journal of Great Lakes Research 33 (1), 122-135.
Zimmerman, R.C., Cabello-Pasini, A., Alberte, R.S., 1994. Modeling daily production of aquatic macrophytes from irradiance measurements: A comparative analysis. Marine Ecology Progress Series 114, 185-196.

# APPENDICES

## Appendix A. Extreme Wind Events

The objective of this task is to determine the frequency (and return interval), duration, and intensity of wind events that qualify as extremes (e.g., top 1% of events) and evaluate responses corresponding to quarterly surveys using wind speed data over the most recent 10-year period. For this assessment, hourly observations from four NOAA National Data Buoy Center sites along the North Carolina coast (Duck [DUKN7], Oregon Inlet [ORIN7], Cape Hatteras [HCGN7] and Cape Lookout [CLKN7]) were downloaded and compiled. The number of years of data ranged from 6 for Cape Hatteras to 32 for Cape Lookout. The full dataset of wind events consisted of all of the recorded datasets of wind event records from each monitoring station. The complete wind event dataset was then copied to a secure network location for storage and backup purposes. A working copy of the dataset was then loaded to a Microsoft SQL Server database. The 95$^{th}$, 99$^{th}$ and 99.9$^{th}$ percentile wind speeds for each site across all years was then computed using Proc Univariate (SAS 2009; **Table A1**) to develop cumulative frequency distributions.

Table A1. Wind speed thresholds for the 95$^{th}$, 99$^{th}$, and 99.9$^{th}$ percentile of hourly wind speed events from each of the North Carolina coastal stations examined (Duck [DUKN7], Oregon Inlet [ORIN7], Cape Hatteras [HCGN7] and Cape Lookout [CLKN7]). Top panel are wind speeds in KPH. Bottom panel are wind speeds in MPH.

| Site | 95$^{th}$ | 99$^{th}$ | 99.9$^{th}$ |
|---|---|---|---|
| **DUKN7** | 41.3 | 53.5 | 71.0 |
| **ORIN7** | 35.2 | 43.0 | 54.5 |
| **HCGN7** | 40.7 | 51.6 | 70.1 |
| **CLKN7** | 39.2 | 49.7 | 65.9 |

| | | | |
|---|---|---|---|
| **DUKN7** | 25.7 | 33.2 | 44.1 |
| **ORIN7** | 21.9 | 26.7 | 33.9 |
| **HCGN7** | 25.3 | 32.1 | 43.6 |
| **CLKN7** | 24.4 | 30.9 | 40.9 |

Using a time lag of 8 hours between events, the data for each site were examined for the number of events that lasted more than one hour for each of the percentile wind speeds. The duration of individual events by station and wind speed threshold (percentiles 95, 99, 99.9) was then computed. The working copy of the dataset was then modified to include a number of additional database fields to be used in identifying individual wind events, flagging records as belonging to the 95$^{th}$, 99$^{th}$ and 99.9$^{th}$ percentile, and for grouping these records together to form extended wind events. Threshold values for each percentile category based upon wind speed values were established for each wind station's dataset utilizing SAS software (**Table A1**). Utilizing these values, each wind event record was then flagged as positive for each of the percentile categories where an event's wind speed met or exceeded that percentile category's threshold value. This process was carried out utilizing a script written in T-SQL. Once each wind event record was flagged for all corresponding percentile categories, the individual wind events were grouped by station, date recorded and hour of the event examined to determine if the events were part of an extended wind event. Extended wind events for the purpose of this study were designated as any grouping of 4 consecutive hourly wind speed observations at or above the threshold or more individual wind events where any 2 consecutive wind events were not separated by more than 8 hours. The grouping of wind event records was computed separately for each wind station as well as by each percentile category for each station. The duration of each wind event was numerically sequenced during this process by flagging each individual wind event as belonging to said wind event. This process was completed for each percentile category. Separate datasets were then created for each percentile category per wind monitoring station. The total number of events, frequency of events (f) per year, and the return interval (1/f) computed for each site and percentile wind speed threshold (**Table A2**). This exercise reveals that wind events reaching the various percentile levels decreased dramatically from 95 to the 99.9$^{th}$ percentile. Frequency and return interval were similar for the various percentiles among sites (**Table A2**).

Table A3. The number of events, number per year, and return intervals for each percentile wind event by North Carolina coastal stations examined (Duck [DUKN7], Oregon Inlet [ORIN7], Cape Hatteras [HCGN7] and Cape Lookout [CLKN7]). Values in bold are means.

| Event Percentile Wind Speed | Station | Number of Events | Frequency (number of events per year) | Average Interval Between Events in Years | Average Interval Between Events in Days |
|---|---|---|---|---|---|
| 95 | CLKN7 | 910 | 28.4 | 0.04 | 13 |
| 95 | DUKN7 | 250 | 31.3 | 0.03 | 12 |
| 95 | HCGN7 | 188 | 31.3 | 0.03 | 12 |
| 95 | ORIN7 | 297 | 37.1 | 0.03 | 10 |
| | | | **32.0** | **0.03** | **12** |
| | | | | | |
| 99 | CLKN7 | 203 | 6.3 | 0.16 | 58 |
| 99 | DUKN7 | 54 | 6.85 | 0.15 | 54 |
| 99 | HCGN7 | 49 | 8.2 | 0.12 | 45 |
| 99 | ORIN7 | 65 | 8.1 | 0.12 | 45 |
| | | | **7.4** | **0.14** | **50** |
| | | | | | |
| 99.9 | CLKN7 | 18 | 0.6 | 1.78 | 649 |
| 99.9 | DUKN7 | 6 | 0.8 | 1.33 | 487 |
| 99.9 | HCGN7 | 6 | 1.0 | 1.00 | 365 |
| 99.9 | ORIN7 | 9 | 1.1 | 0.89 | 324 |
| | | | **0.9** | **1.25** | **456** |

However, the direction from which events occurred was different among sites. Sites CLKNY, HCGN7 and DUKN7 were all similar in that these extreme events tended to occur from the north. However, one site, ORIN7 was different in that many events also occurred from the south direction (**Figure A1** [95$^{th}$ percentiles], **Figure A2** [99$^{th}$ percentiles], **Figure A3** [99.9$^{th}$ percentiles]). These data indicate that while most sites along the North Carolina coast are similar in their wind field extreme event characteristics, some areas, such as Oregon Inlet, may have a disproportionate effect of wind events from the south contributing to extreme events.

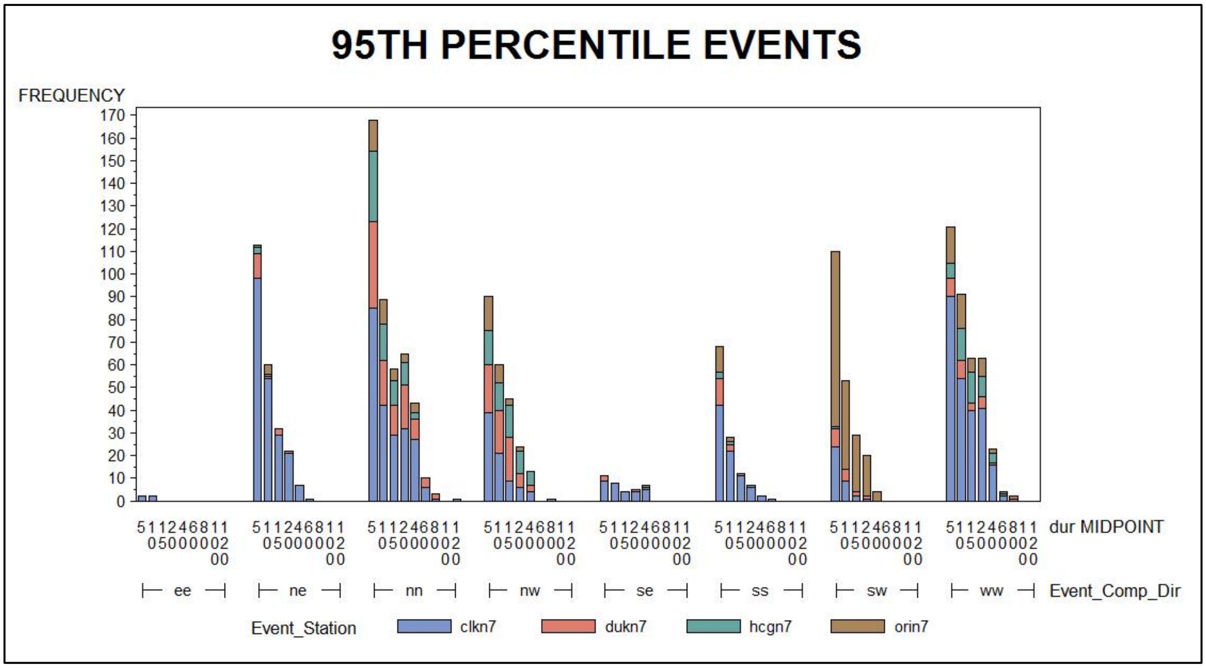


Figure A1. Percentage of 95$^{th}$ percentile wind events by North Carolina coastal stations examined (Duck [DUKN7], Oregon Inlet [ORIN7], Cape Hatteras [HCGN7] and Cape Lookout [CLKN7]), compass direction and duration bin.

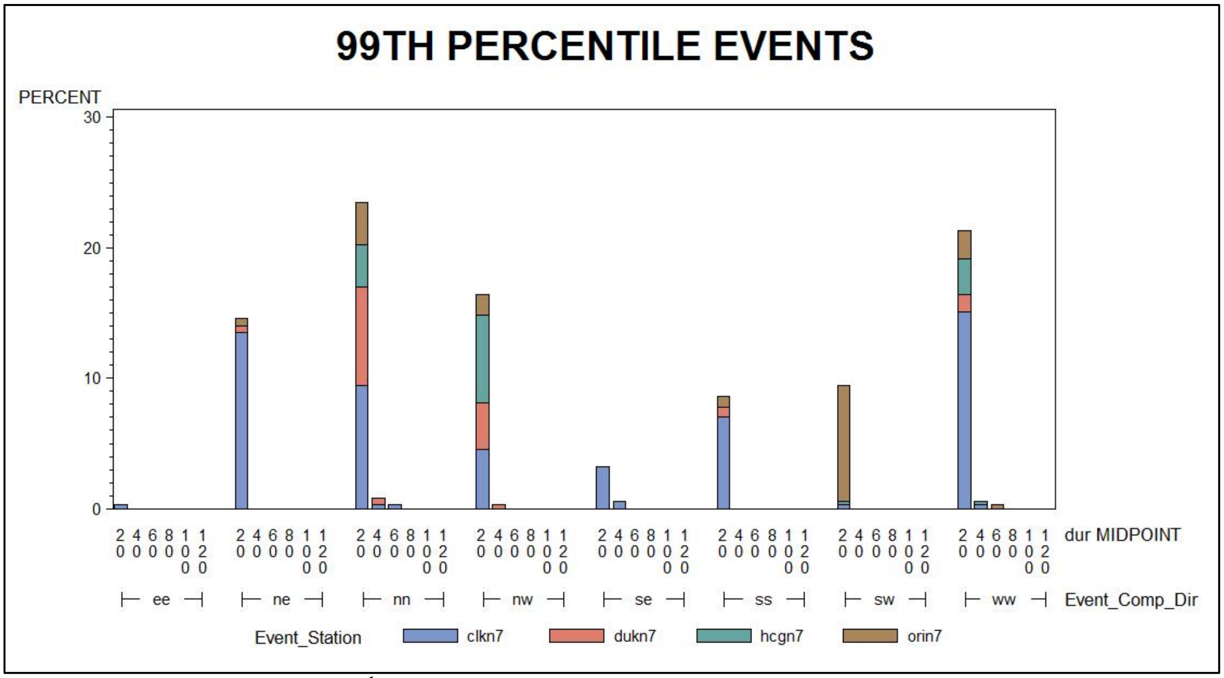


Figure A2. Percentage of 99th percentile wind events by North Carolina coastal stations examined (Duck [DUKN7], Oregon Inlet [ORIN7], Cape Hatteras [HCGN7] and Cape Lookout [CLKN7]), compass direction and duration bin.

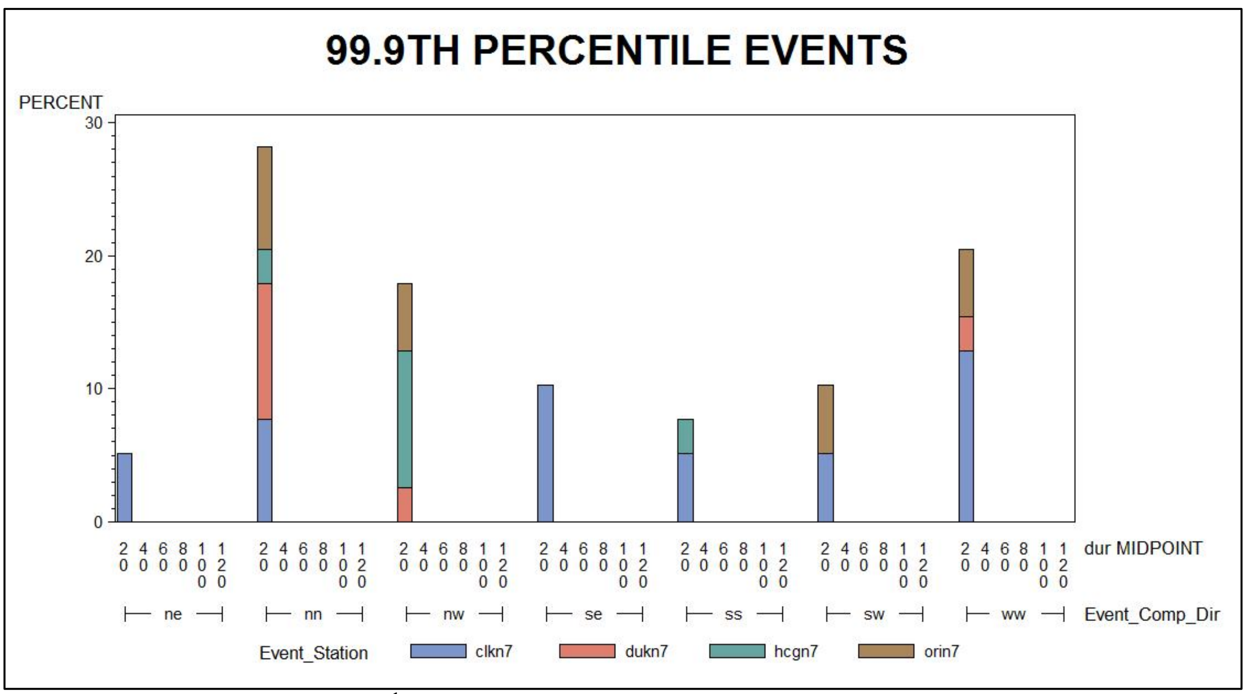


Figure A3. Percentage of 99.9th percentile wind events by North Carolina coastal stations examined (Duck [DUKN7], Oregon Inlet [ORIN7], Cape Hatteras [HCGN7] and Cape Lookout [CLKN7]), compass direction and duration bin.

## Appendix B. Statistical Analyses Result Reports (JMP Pro 14)

**Sediments – Weight % Sand, Silt, and Clay and % LOI**
**Quadrat Survey 1 – October 2017**
**Fit Group**
**Oneway Analysis of Weight % Sand By Study Area**

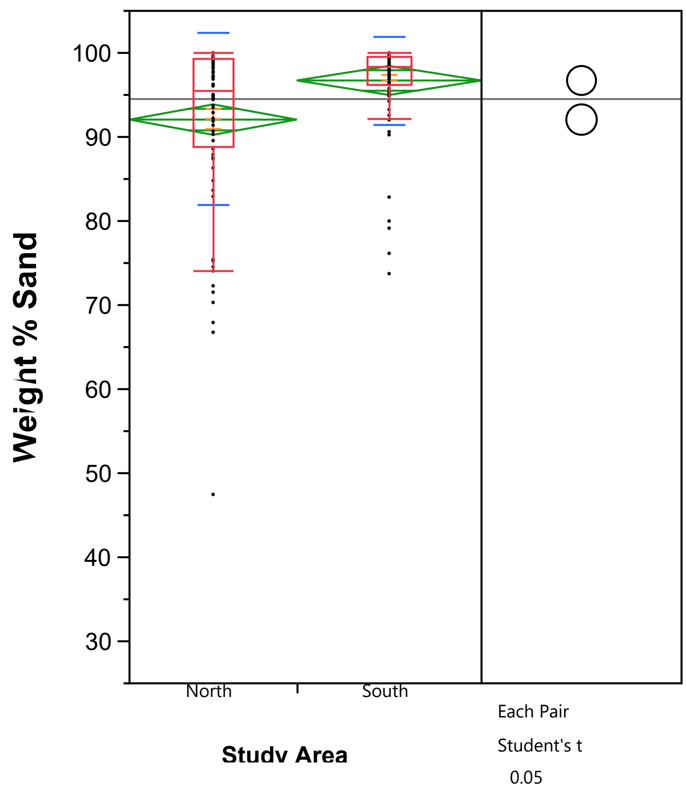


### Quantiles

| Level | Minimum | 10% | 25% | Median | 75% | 90% | Maximum |
|---|---|---|---|---|---|---|---|
| North | 47.5 | 74.4 | 88.8 | 95.6 | 99.3 | 100.0 | 100.0 |
| South | 73.7 | 92.3 | 96.3 | 98.4 | 99.5 | 100.0 | 100.0 |

### Means and Std Deviations

| Level | Number | Mean | Std Dev | Std Err Mean | Lower 95% | Upper 95% |
|---|---|---|---|---|---|---|
| North | 76 | 92.1 | 10.2 | 1.2 | 89.7 | 94.4 |
| South | 84 | 96.7 | 5.2 | 0.6 | 95.6 | 97.8 |

### Means Comparisons
### Comparisons for each pair using Student's t
### Confidence Quantile

| t | Alpha |
|---|---|
| 1.975 | 0.05 |

### Connecting Letters Report

| Level | | | Mean |
|---|---|---|---|
| South | A | | 96.7 |
| North | | B | 92.1 |

Levels not connected by same letter are significantly different.

### Detailed Comparisons Report
### Comparing South with North

| | | | |
|---|---|---|---|
| Difference | 4.654 | t Ratio | 3.678622 |
| Std Err Dif | 1.265 | DF | 158 |
| Upper CL Dif | 7.152 | Prob > \|t\| | 0.0003* |
| Lower CL Dif | 2.155 | Prob > t | 0.0002* |
| Confidence | 0.95 | Prob < t | 0.9998 |

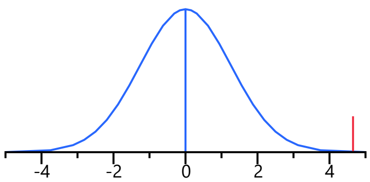


### Nonparametric Comparisons For Each Pair Using Wilcoxon Method

| q* | Alpha |
|---|---|
| 1.960 | 0.05 |

| Level | - Level | Score Mean Difference | Std Err Dif | Z | p-Value | Hodges-Lehmann | Lower CL | Upper CL |
|---|---|---|---|---|---|---|---|---|
| South | North | 22.6 | 7.3 | 3.094 | 0.0020* | 1.872 | 0.543 | 3.646 |

## Oneway Analysis of Weight % Silt By Study Area

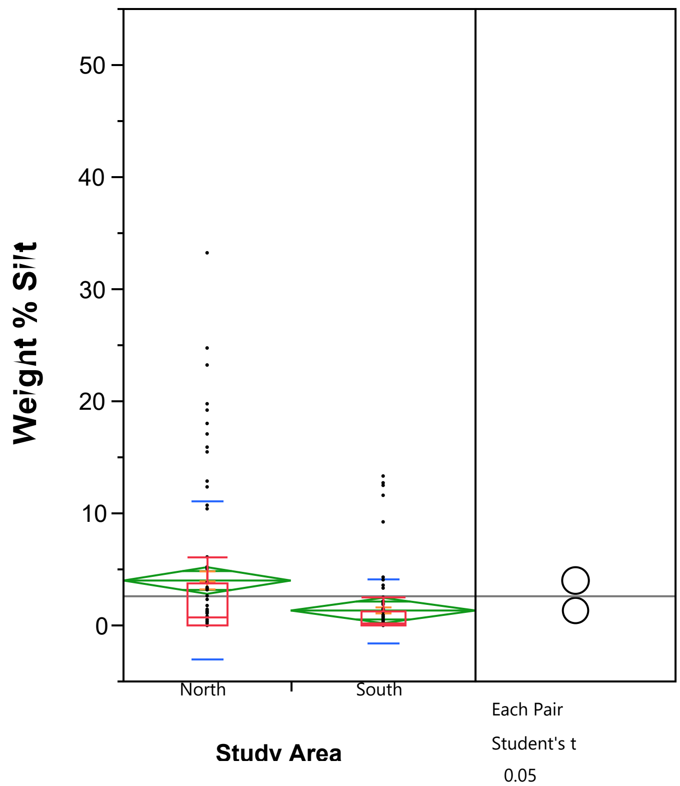


## Quantiles

| Level | Minimum | 10% | 25% | Median | 75% | 90% | Maximum |
|---|---|---|---|---|---|---|---|
| North | 0.0 | 0.0 | 0.0 | 0.8 | 3.7 | 16.3 | 33.2 |
| South | 0.0 | 0.0 | 0.0 | 0.2 | 1.2 | 3.5 | 13.3 |

## Means and Std Deviations

| Level | Number | Mean | Std Dev | Std Err Mean | Lower 95% | Upper 95% |
|---|---|---|---|---|---|---|
| North | 76 | 4.0 | 7.0 | 0.8 | 2.4 | 5.6 |
| South | 84 | 1.3 | 2.9 | 0.3 | 0.7 | 2.0 |

## Means Comparisons
## Comparisons for each pair using Student's t
## Confidence Quantile

| t | Alpha |
|---|---|
| 1.975 | 0.05 |

## Connecting Letters Report

| Level | | | Mean |
|---|---|---|---|
| North | A | | 4.0 |
| South | | B | 1.3 |

Levels not connected by same letter are significantly different.

## Detailed Comparisons Report
## Comparing South with North

| | | | |
|---|---|---|---|
| Difference | -2.676 | t Ratio | -3.21904 |
| Std Err Dif | 0.831 | DF | 158 |
| Upper CL Dif | -1.034 | Prob > \|t\| | 0.0016* |
| Lower CL Dif | -4.318 | Prob > t | 0.9992 |
| Confidence | 0.95 | Prob < t | 0.0008* |

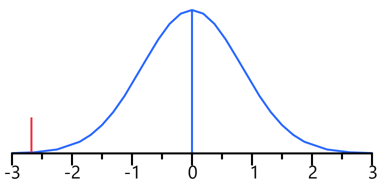


## Nonparametric Comparisons For Each Pair Using Wilcoxon Method

| q* | Alpha |
|---|---|
| 1.960 | 0.05 |

| Level | - Level | Score Mean Difference | Std Err Dif | Z | p-Value | Hodges-Lehmann | Lower CL | Upper CL |
|---|---|---|---|---|---|---|---|---|
| South | North | -14.8 | 7.3 | -2.041 | 0.0412* | -0.272 | -0.813 | 0.000 |

## Oneway Analysis of Weight % Clay By Study Area

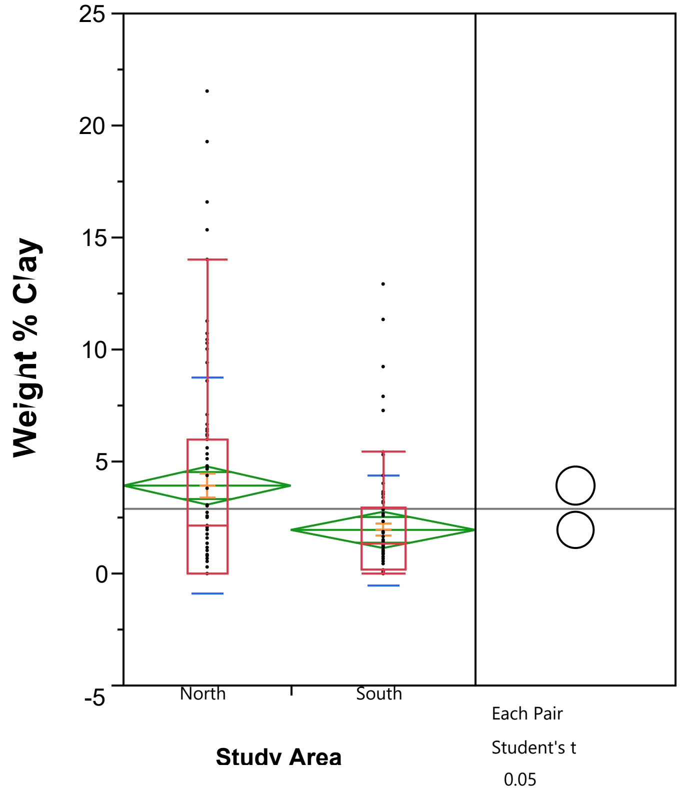


## Quantiles

| Level | Minimum | 10% | 25% | Median | 75% | 90% | Maximum |
|---|---|---|---|---|---|---|---|
| North | 0.0 | 0.0 | 0.0 | 2.1 | 6.0 | 10.5 | 21.5 |
| South | 0.0 | 0.0 | 0.2 | 1.3 | 2.9 | 4.2 | 12.9 |

## Means and Std Deviations

| Level | Number | Mean | Std Dev | Std Err Mean | Lower 95% | Upper 95% |
|---|---|---|---|---|---|---|
| North | 76 | 3.9 | 4.8 | 0.6 | 2.8 | 5.0 |
| South | 84 | 1.9 | 2.4 | 0.3 | 1.4 | 2.5 |

## Means Comparisons
## Comparisons for each pair using Student's t
## Confidence Quantile

| t | Alpha |
|---|---|
| 1.975 | 0.05 |

## Connecting Letters Report

| Level | | | Mean |
|---|---|---|---|
| North | A | | 3.9 |
| South | | B | 1.9 |

Levels not connected by same letter are significantly different.

### Detailed Comparisons Report
### Comparing South with North

| | | | |
|---|---|---|---|
| Difference | -1.978 | t Ratio | -3.32528 |
| Std Err Dif | 0.595 | DF | 158 |
| Upper CL Dif | -0.803 | Prob > \|t\| | 0.0011* |
| Lower CL Dif | -3.152 | Prob > t | 0.9995 |
| Confidence | 0.95 | Prob < t | 0.0005* |

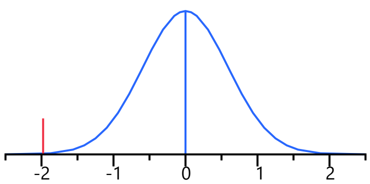


### Nonparametric Comparisons For Each Pair Using Wilcoxon Method

| q* | Alpha |
|---|---|
| 1.960 | 0.05 |

| Level | - Level | Score Mean Difference | Std Err Dif | Z | p-Value | Hodges-Lehmann | Lower CL | Upper CL |
|---|---|---|---|---|---|---|---|---|
| South | North | -13.7 | 7.3 | -1.880 | 0.0601 | -0.727 | -1.745 | 0.000 |

## Oneway Analysis of % LOI By Study Area

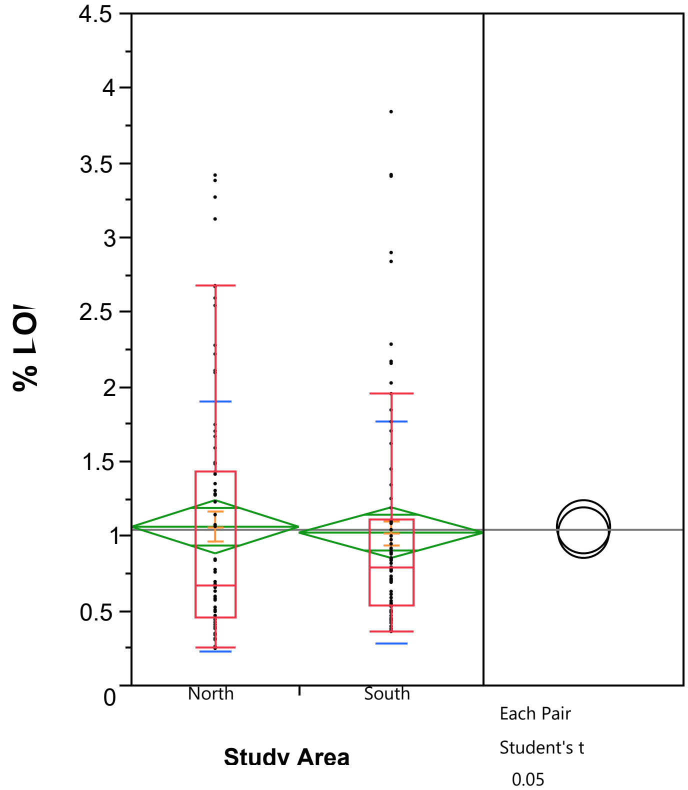


## Quantiles

| Level | Minimum | 10% | 25% | Median | 75% | 90% | Maximum |
|---|---|---|---|---|---|---|---|
| North | 0.2 | 0.4 | 0.4 | 0.7 | 1.4 | 2.6 | 3.4 |
| South | 0.4 | 0.4 | 0.5 | 0.8 | 1.1 | 2.1 | 3.8 |

## Means and Std Deviations

| Level | Number | Mean | Std Dev | Std Err Mean | Lower 95% | Upper 95% |
|---|---|---|---|---|---|---|
| North | 76 | 1.1 | 0.8 | 0.1 | 0.9 | 1.3 |
| South | 84 | 1.0 | 0.7 | 0.1 | 0.9 | 1.2 |

## Means Comparisons
## Comparisons for each pair using Student's t
## Confidence Quantile

| t | Alpha |
|---|---|
| 1.975 | 0.05 |

## Connecting Letters Report

| Level | | Mean |
|---|---|---|
| North | A | 1.1 |
| South | A | 1.0 |

Levels not connected by same letter are significantly different.

**Detailed Comparisons Report**
**Comparing South with North**

| | | | |
|---|---|---|---|
| Difference | -0.039 | t Ratio | -0.31582 |
| Std Err Dif | 0.124 | DF | 158 |
| Upper CL Dif | 0.206 | Prob > \|t\| | 0.7526 |
| Lower CL Dif | -0.285 | Prob > t | 0.6237 |
| Confidence | 0.95 | Prob < t | 0.3763 |

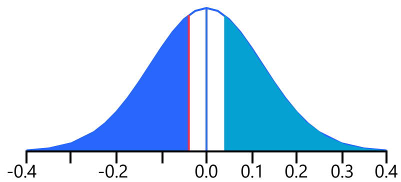


## Nonparametric Comparisons For Each Pair Using Wilcoxon Method

| q* | Alpha |
|---|---|
| 1.960 | 0.05 |

| Level | - Level | Score Mean Difference | Std Err Dif | Z | p-Value | Hodges-Lehmann | Lower CL | Upper CL |
|---|---|---|---|---|---|---|---|---|
| South | North | 6.1 | 7.3 | 0.832 | 0.4054 | 0.049 | -0.083 | 0.181 |

**Quadrat Survey 2 – May 2018**

**Fit Group**

**Oneway Analysis of Weight % Sand By Study Area**

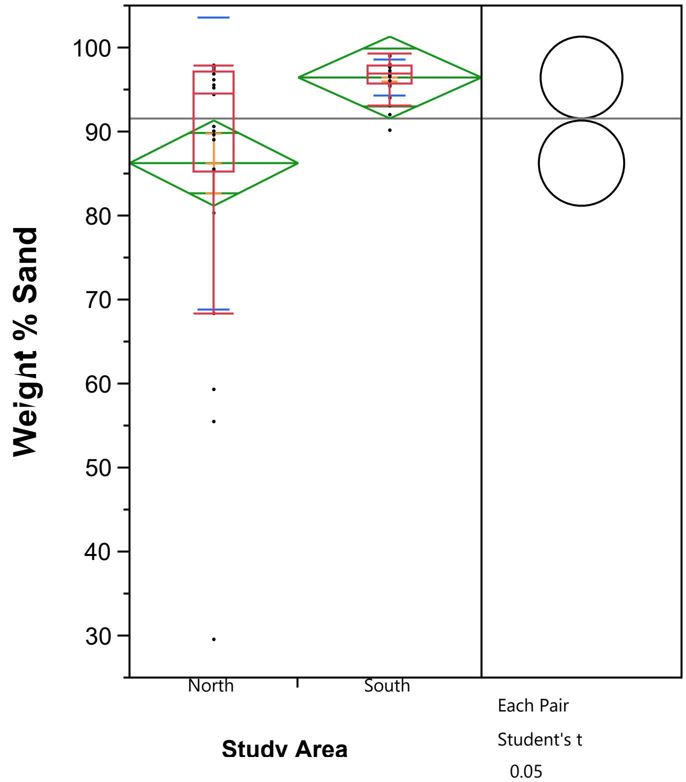


## Quantiles

| Level | Minimum | 10% | 25% | Median | 75% | 90% | Maximum |
|---|---|---|---|---|---|---|---|
| North | 29.6 | 57.0 | 85.3 | 94.4 | 97.2 | 97.6 | 97.9 |
| South | 90.2 | 92.6 | 95.6 | 96.8 | 97.9 | 99.0 | 99.2 |

## Means and Std Deviations

| Level | Number | Mean | Std Dev | Std Err Mean | Lower 95% | Upper 95% |
|---|---|---|---|---|---|---|
| North | 23 | 86.2 | 17.3 | 3.6 | 78.7 | 93.7 |
| South | 25 | 96.4 | 2.2 | 0.4 | 95.5 | 97.3 |

## Means Comparisons

## Comparisons for each pair using Student's t

## Confidence Quantile

| t | Alpha |
|---|---|
| 2.013 | 0.05 |

## Connecting Letters Report

| Level | | Mean |
|---|---|---|
| South | A | 96.4 |
| North | B | 86.2 |

Levels not connected by same letter are significantly different.

### Detailed Comparisons Report
### Comparing South with North

| | | | |
|---|---|---|---|
| Difference | 10.194 | t Ratio | 2.916106 |
| Std Err Dif | 3.496 | DF | 46 |
| Upper CL Dif | 17.231 | Prob > \|t\| | 0.0055* |
| Lower CL Dif | 3.157 | Prob > t | 0.0027* |
| Confidence | 0.95 | Prob < t | 0.9973 |

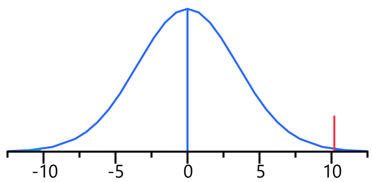


### Nonparametric Comparisons For Each Pair Using Wilcoxon Method

| q* | Alpha |
|---|---|
| 1.960 | 0.05 |

| Level | - Level | Score Mean Difference | Std Err Dif | Z | p-Value | Hodges-Lehmann | Lower CL | Upper CL |
|---|---|---|---|---|---|---|---|---|
| South | North | 11.6 | 4.0 | 2.869 | 0.0041* | 2.810 | 0.592 | 8.171 |

## Oneway Analysis of Weight % Silt By Study Area

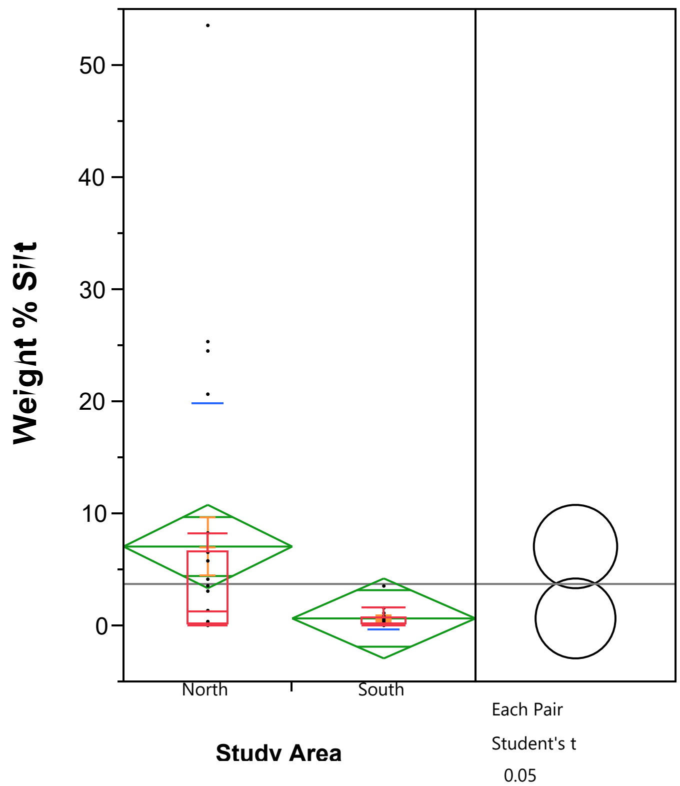


## Quantiles

| Level | Minimum | 10% | 25% | Median | 75% | 90% | Maximum |
|---|---|---|---|---|---|---|---|
| North | 0.0 | 0.0 | 0.2 | 1.3 | 6.5 | 25.0 | 53.5 |
| South | 0.0 | 0.0 | 0.1 | 0.2 | 0.7 | 2.4 | 3.6 |

## Means and Std Deviations

| Level | Number | Mean | Std Dev | Std Err Mean | Lower 95% | Upper 95% |
|---|---|---|---|---|---|---|
| North | 23 | 7.0 | 12.8 | 2.7 | 1.5 | 12.6 |
| South | 25 | 0.6 | 1.0 | 0.2 | 0.2 | 1.0 |

## Means Comparisons
## Comparisons for each pair using Student's t
## Confidence Quantile

| t | Alpha |
|---|---|
| 2.013 | 0.05 |

## Connecting Letters Report

| Level | | | Mean |
|---|---|---|---|
| North | A | | 7.0 |
| South | | B | 0.6 |

Levels not connected by same letter are significantly different.

## Detailed Comparisons Report
## Comparing South with North

| | | | |
|---|---|---|---|
| Difference | -6.413 | t Ratio | -2.50506 |
| Std Err Dif | 2.560 | DF | 46 |
| Upper CL Dif | -1.260 | Prob > \|t\| | 0.0158* |
| Lower CL Dif | -11.566 | Prob > t | 0.9921 |
| Confidence | 0.95 | Prob < t | 0.0079* |

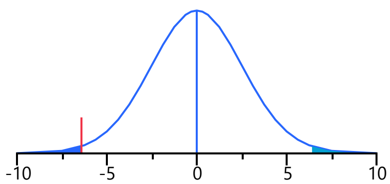


## Nonparametric Comparisons For Each Pair Using Wilcoxon Method

| q* | Alpha |
|---|---|
| 1.960 | 0.05 |

| Level | - Level | Score Mean Difference | Std Err Dif | Z | p-Value | Hodges-Lehmann | Lower CL | Upper CL |
|---|---|---|---|---|---|---|---|---|
| South | North | -9.9 | 4.0 | -2.437 | 0.0148* | -0.517 | -3.545 | -0.067 |

## Oneway Analysis of Weight % Clay By Study Area

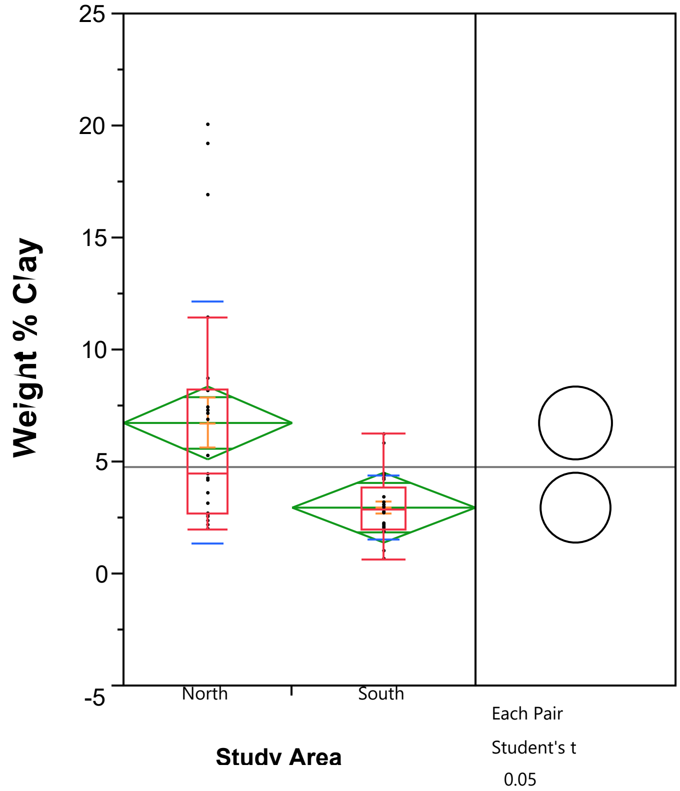


## Quantiles

| Level | Minimum | 10% | 25% | Median | 75% | 90% | Maximum |
|---|---|---|---|---|---|---|---|
| North | 2.0 | 2.1 | 2.6 | 4.5 | 8.2 | 18.3 | 20.1 |
| South | 0.7 | 0.9 | 2.0 | 2.9 | 3.8 | 5.0 | 6.2 |

## Means and Std Deviations

| Level | Number | Mean | Std Dev | Std Err Mean | Lower 95% | Upper 95% |
|---|---|---|---|---|---|---|
| North | 23 | 6.7 | 5.4 | 1.1 | 4.4 | 9.1 |
| South | 25 | 2.9 | 1.4 | 0.3 | 2.4 | 3.5 |

## Means Comparisons
## Comparisons for each pair using Student's t
## Confidence Quantile

| t | Alpha |
|---|---|
| 2.013 | 0.05 |

## Connecting Letters Report

| Level | | | Mean |
|---|---|---|---|
| North | A | | 6.7 |
| South | | B | 2.9 |

Levels not connected by same letter are significantly different.

### Detailed Comparisons Report
### Comparing South with North

| | | | |
|---|---|---|---|
| Difference | -3.781 | t Ratio | -3.37693 |
| Std Err Dif | 1.120 | DF | 46 |
| Upper CL Dif | -1.527 | Prob > \|t\| | 0.0015* |
| Lower CL Dif | -6.035 | Prob > t | 0.9993 |
| Confidence | 0.95 | Prob < t | 0.0007* |

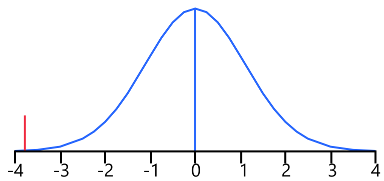


### Nonparametric Comparisons For Each Pair Using Wilcoxon Method

| q* | Alpha |
|---|---|
| 1.960 | 0.05 |

| Level | - Level | Score Mean Difference | Std Err Dif | Z | p-Value | Hodges-Lehmann | Lower CL | Upper CL |
|---|---|---|---|---|---|---|---|---|
| South | North | -11.8 | 4.0 | -2.910 | 0.0036* | -2.118 | -4.391 | -0.628 |

## Oneway Analysis of % LOI By Study Area

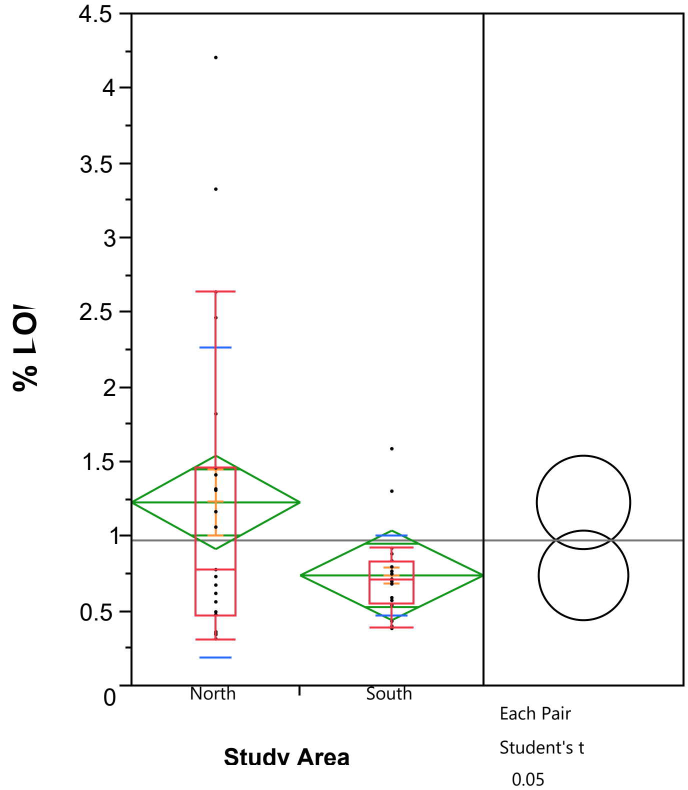


## Quantiles

| Level | Minimum | 10% | 25% | Median | 75% | 90% | Maximum |
|---|---|---|---|---|---|---|---|
| North | 0.3 | 0.3 | 0.5 | 0.8 | 1.5 | 3.0 | 4.2 |
| South | 0.4 | 0.4 | 0.5 | 0.7 | 0.8 | 1.1 | 1.6 |

## Means and Std Deviations

| Level | Number | Mean | Std Dev | Std Err Mean | Lower 95% | Upper 95% |
|---|---|---|---|---|---|---|
| North | 23 | 1.2 | 1.0 | 0.2 | 0.8 | 1.7 |
| South | 25 | 0.7 | 0.3 | 0.1 | 0.6 | 0.8 |

## Means Comparisons
## Comparisons for each pair using Student's t
## Confidence Quantile

| t | Alpha |
|---|---|
| 2.013 | 0.05 |

## Connecting Letters Report

| Level | | | Mean |
|---|---|---|---|
| North | A | | 1.2 |
| South | | B | 0.7 |

Levels not connected by same letter are significantly different.

## Detailed Comparisons Report
## Comparing South with North

| | | | |
|---|---|---|---|
| Difference | -0.489 | t Ratio | -2.27036 |
| Std Err Dif | 0.215 | DF | 46 |
| Upper CL Dif | -0.055 | Prob > \|t\| | 0.0279* |
| Lower CL Dif | -0.922 | Prob > t | 0.9860 |
| Confidence | 0.95 | Prob < t | 0.0140* |

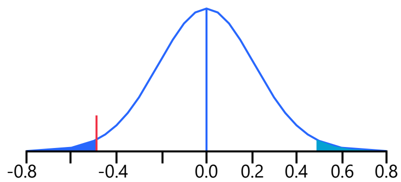


## Nonparametric Comparisons For Each Pair Using Wilcoxon Method

| q* | Alpha |
|---|---|
| 1.960 | 0.05 |

| Level | - Level | Score Mean Difference | Std Err Dif | Z | p-Value | Hodges-Lehmann | Lower CL | Upper CL |
|---|---|---|---|---|---|---|---|---|
| South | North | -3.3 | 4.0 | -0.826 | 0.4091 | -0.142 | -0.619 | 0.128 |

**Quadrat Survey 3 – October 2018**
**Fit Group**
**Oneway Analysis of Weight % Sand By Study Area**

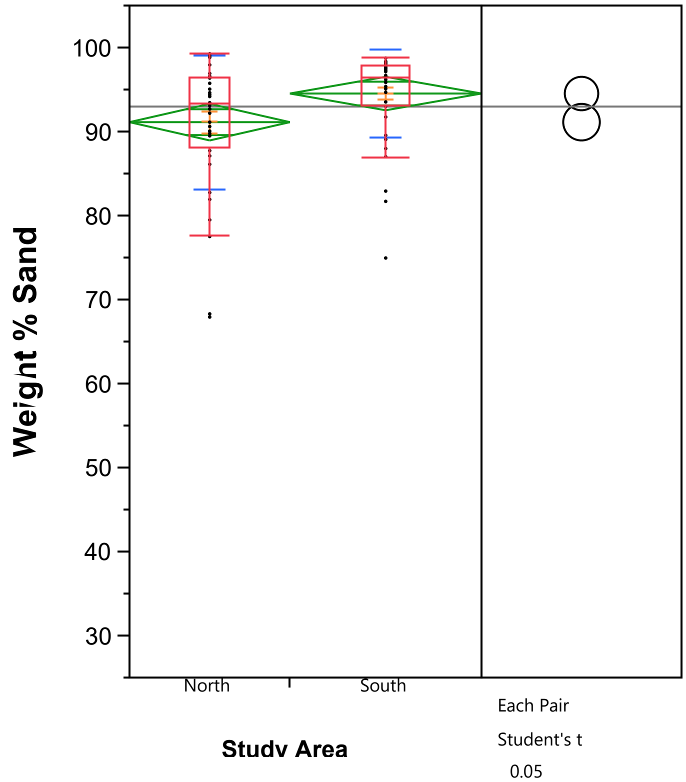


**Quantiles**

| Level | Minimum | 10% | 25% | Median | 75% | 90% | Maximum |
|---|---|---|---|---|---|---|---|
| North | 67.9 | 78.9 | 88.2 | 93.3 | 96.5 | 98.8 | 99.3 |
| South | 74.9 | 87.4 | 93.0 | 96.5 | 97.8 | 98.3 | 98.7 |

**Means and Std Deviations**

| Level | Number | Mean | Std Dev | Std Err Mean | Lower 95% | Upper 95% |
|---|---|---|---|---|---|---|
| North | 36 | 91.1 | 7.9 | 1.3 | 88.4 | 93.8 |
| South | 43 | 94.5 | 5.1 | 0.8 | 92.9 | 96.1 |

**Means Comparisons**
**Comparisons for each pair using Student's t**
**Confidence Quantile**

| t | Alpha |
|---|---|
| 1.991 | 0.05 |

**Connecting Letters Report**

| Level | | | Mean |
|---|---|---|---|
| South | A | | 94.5 |
| North | | B | 91.1 |

Levels not connected by same letter are significantly different.

## Detailed Comparisons Report
## Comparing South with North

| | | | |
|---|---|---|---|
| Difference | 3.407 | t Ratio | 2.298345 |
| Std Err Dif | 1.483 | DF | 77 |
| Upper CL Dif | 6.360 | Prob > \|t\| | 0.0243* |
| Lower CL Dif | 0.455 | Prob > t | 0.0121* |
| Confidence | 0.95 | Prob < t | 0.9879 |

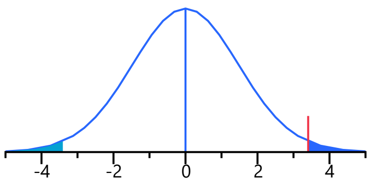


## Nonparametric Comparisons For Each Pair Using Wilcoxon Method

| q* | Alpha |
|---|---|
| 1.960 | 0.05 |

| Level | - Level | Score Mean Difference | Std Err Dif | Z | p-Value | Hodges-Lehmann | Lower CL | Upper CL |
|---|---|---|---|---|---|---|---|---|
| South | North | 11.3 | 5.2 | 2.180 | 0.0292* | 2.104 | 0.220 | 4.494 |

## Oneway Analysis of Weight % Silt By Study Area

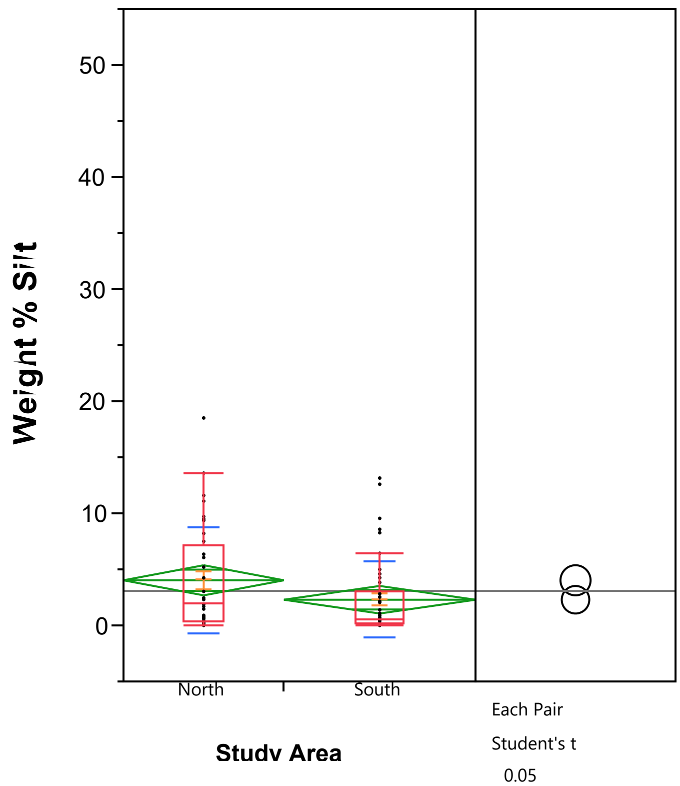


## Quantiles

| Level | Minimum | 10% | 25% | Median | 75% | 90% | Maximum |
|---|---|---|---|---|---|---|---|
| North | 0.0 | 0.2 | 0.4 | 1.9 | 7.2 | 11.2 | 18.5 |
| South | 0.0 | 0.0 | 0.1 | 0.6 | 3.1 | 8.5 | 13.1 |

## Means and Std Deviations

| Level | Number | Mean | Std Dev | Std Err Mean | Lower 95% | Upper 95% |
|---|---|---|---|---|---|---|
| North | 36 | 4.0 | 4.7 | 0.8 | 2.4 | 5.6 |
| South | 43 | 2.3 | 3.4 | 0.5 | 1.2 | 3.4 |

## Means Comparisons
## Comparisons for each pair using Student's t
## Confidence Quantile

| t | Alpha |
|---|---|
| 1.991 | 0.05 |

## Connecting Letters Report

| Level | | Mean |
|---|---|---|
| North | A | 4.0 |
| South | A | 2.3 |

Levels not connected by same letter are significantly different.

## Detailed Comparisons Report
## Comparing South with North

| | | | |
|---|---|---|---|
| Difference | -1.735 | t Ratio | -1.89571 |
| Std Err Dif | 0.915 | DF | 77 |
| Upper CL Dif | 0.087 | Prob > \|t\| | 0.0618 |
| Lower CL Dif | -3.557 | Prob > t | 0.9691 |
| Confidence | 0.95 | Prob < t | 0.0309* |

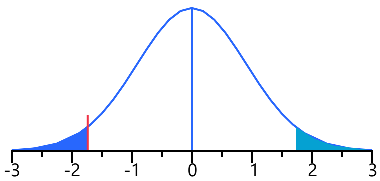


## Nonparametric Comparisons For Each Pair Using Wilcoxon Method

| q* | Alpha |
|---|---|
| 1.960 | 0.05 |

| Level | - Level | Score Mean Difference | Std Err Dif | Z | p-Value | Hodges-Lehmann | Lower CL | Upper CL |
|---|---|---|---|---|---|---|---|---|
| South | North | -12.0 | 5.2 | -2.323 | 0.0202* | -0.600 | -1.994 | -0.086 |

## Oneway Analysis of Weight % Clay By Study Area

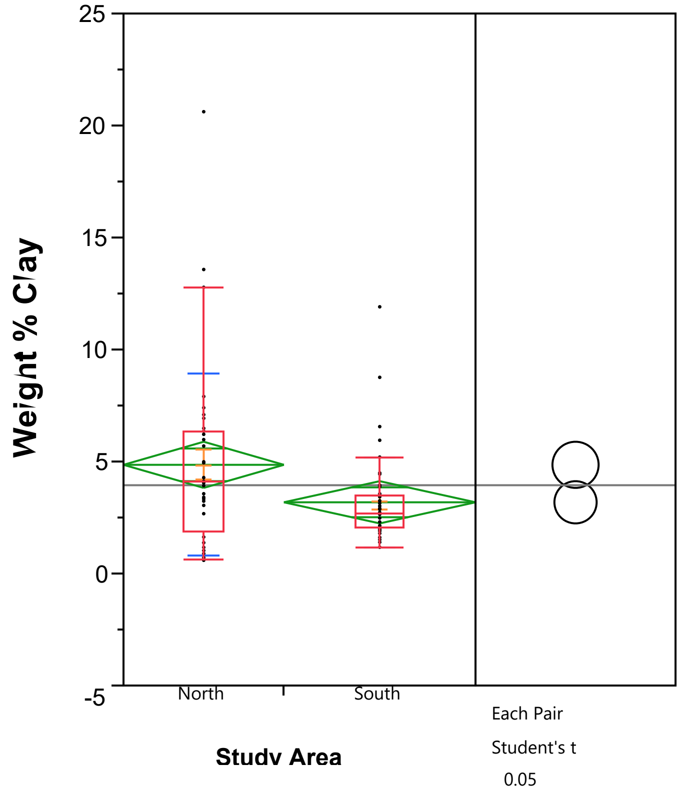


## Quantiles

| Level | Minimum | 10% | 25% | Median | 75% | 90% | Maximum |
|---|---|---|---|---|---|---|---|
| North | 0.6 | 0.8 | 1.9 | 4.1 | 6.3 | 9.4 | 20.6 |
| South | 1.2 | 1.6 | 2.1 | 2.7 | 3.4 | 5.6 | 11.9 |

## Means and Std Deviations

| Level | Number | Mean | Std Dev | Std Err Mean | Lower 95% | Upper 95% |
|---|---|---|---|---|---|---|
| North | 36 | 4.9 | 4.0 | 0.7 | 3.5 | 6.2 |
| South | 43 | 3.2 | 2.0 | 0.3 | 2.6 | 3.8 |

## Means Comparisons
## Comparisons for each pair using Student's t
## Confidence Quantile

| t | Alpha |
|---|---|
| 1.991 | 0.05 |

## Connecting Letters Report

| Level | | | Mean |
|---|---|---|---|
| North | A | | 4.9 |
| South | | B | 3.2 |

Levels not connected by same letter are significantly different.

### Detailed Comparisons Report
### Comparing South with North

| | | | |
|---|---|---|---|
| Difference | -1.673 | t Ratio | -2.38476 |
| Std Err Dif | 0.701 | DF | 77 |
| Upper CL Dif | -0.276 | Prob > \|t\| | 0.0196* |
| Lower CL Dif | -3.069 | Prob > t | 0.9902 |
| Confidence | 0.95 | Prob < t | 0.0098* |

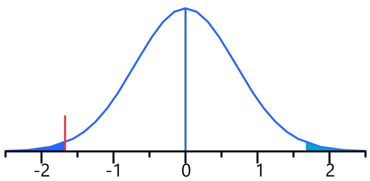


### Nonparametric Comparisons For Each Pair Using Wilcoxon Method

| q* | Alpha |
|---|---|
| 1.960 | 0.05 |

| Level | - Level | Score Mean Difference | Std Err Dif | Z | p-Value | Hodges-Lehmann | Lower CL | Upper CL |
|---|---|---|---|---|---|---|---|---|
| South | North | -11.6 | 5.2 | -2.230 | 0.0258* | -1.267 | -2.189 | -0.202 |

## Oneway Analysis of % LOI By Study Area

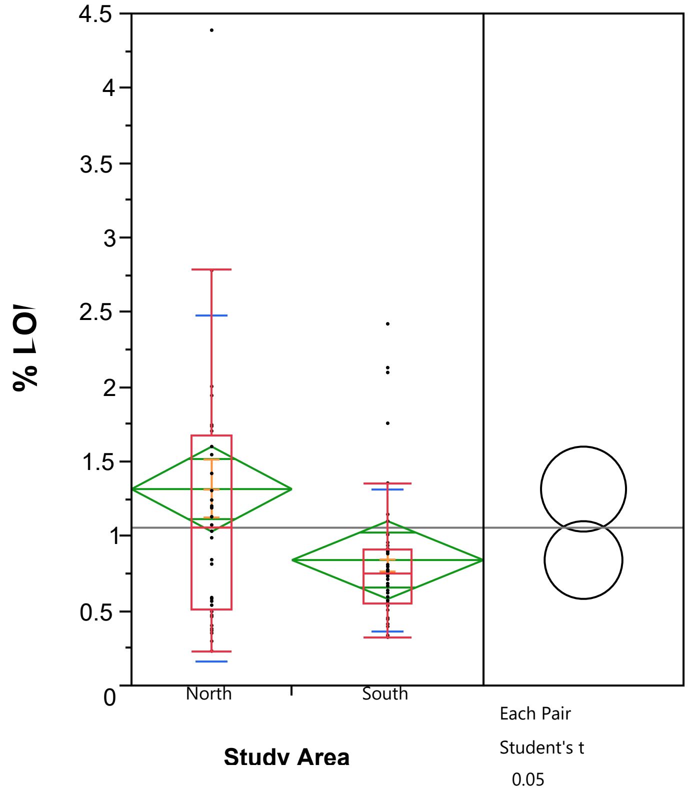


## Quantiles

| Level | Minimum | 10% | 25% | Median | 75% | 90% | Maximum |
|---|---|---|---|---|---|---|---|
| North | 0.2 | 0.4 | 0.5 | 1.1 | 1.7 | 3.3 | 4.8 |
| South | 0.3 | 0.4 | 0.6 | 0.7 | 0.9 | 1.6 | 2.4 |

## Means and Std Deviations

| Level | Number | Mean | Std Dev | Std Err Mean | Lower 95% | Upper 95% |
|---|---|---|---|---|---|---|
| North | 36 | 1.3 | 1.2 | 0.2 | 0.9 | 1.7 |
| South | 43 | 0.8 | 0.5 | 0.1 | 0.7 | 1.0 |

## Means Comparisons
## Comparisons for each pair using Student's t
## Confidence Quantile

| t | Alpha |
|---|---|
| 1.991 | 0.05 |

## Connecting Letters Report

| Level | | | Mean |
|---|---|---|---|
| North | A | | 1.3 |
| South | | B | 0.8 |

Levels not connected by same letter are significantly different.

## Detailed Comparisons Report
## Comparing South with North

| | | | |
|---|---|---|---|
| Difference | -0.475 | t Ratio | -2.45335 |
| Std Err Dif | 0.194 | DF | 77 |
| Upper CL Dif | -0.090 | Prob > \|t\| | 0.0164* |
| Lower CL Dif | -0.861 | Prob > t | 0.9918 |
| Confidence | 0.95 | Prob < t | 0.0082* |

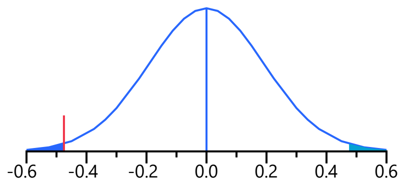


## Nonparametric Comparisons For Each Pair Using Wilcoxon Method

| q* | Alpha |
|---|---|
| 1.960 | 0.05 |

| Level | - Level | Score Mean Difference | Std Err Dif | Z | p-Value | Hodges-Lehmann | Lower CL | Upper CL |
|---|---|---|---|---|---|---|---|---|
| South | North | -7.9 | 5.2 | -1.531 | 0.1258 | -0.220 | -0.540 | 0.053 |

**Quadrat Survey 4 – May 2019**
**Fit Group**
**Oneway Analysis of Weight % Sand By Study Area**

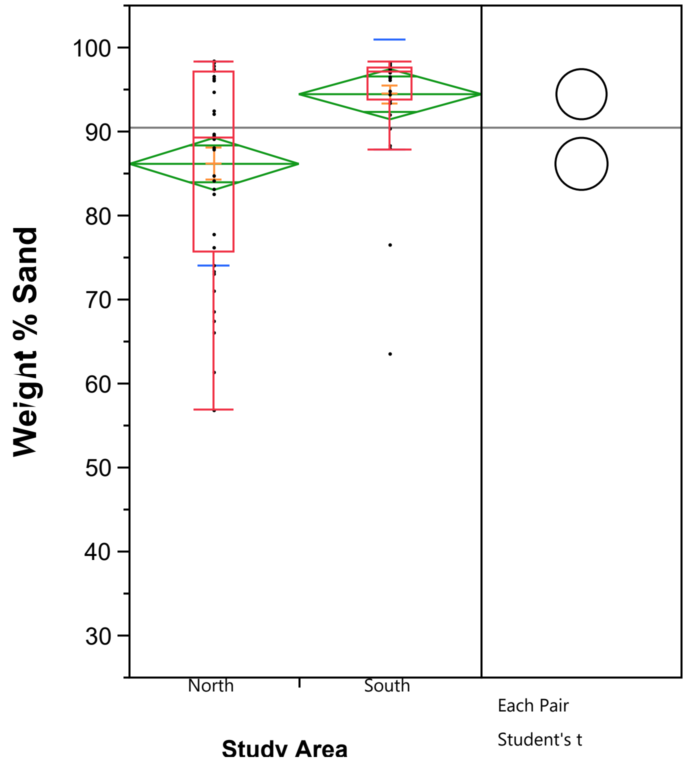


## Quantiles

| Level | Minimum | 10% | 25% | Median | 75% | 90% | Maximum |
|---|---|---|---|---|---|---|---|
| North | 56.8 | 67.3 | 75.6 | 89.3 | 97.2 | 97.9 | 98.4 |
| South | 63.5 | 88.3 | 93.7 | 97.1 | 97.6 | 98.1 | 98.2 |

## Means and Std Deviations

| Level | Number | Mean | Std Dev | Std Err Mean | Lower 95% | Upper 95% |
|---|---|---|---|---|---|---|
| North | 38 | 86.2 | 12.1 | 2.0 | 82.2 | 90.1 |
| South | 41 | 94.4 | 6.5 | 1.0 | 92.4 | 96.5 |

## Means Comparisons
## Comparisons for each pair using Student's t
## Confidence Quantile

| t | Alpha |
|---|---|
| 1.991 | 0.05 |

## Connecting Letters Report

| Level | | | Mean |
|---|---|---|---|
| South | A | | 94.4 |
| North | | B | 86.2 |

Levels not connected by same letter are significantly different.

### Detailed Comparisons Report
### Comparing South with North

| | | | |
|---|---|---|---|
| Difference | 8.291 | t Ratio | 3.83496 |
| Std Err Dif | 2.162 | DF | 77 |
| Upper CL Dif | 12.597 | Prob > \|t\| | 0.0003* |
| Lower CL Dif | 3.986 | Prob > t | 0.0001* |
| Confidence | 0.95 | Prob < t | 0.9999 |

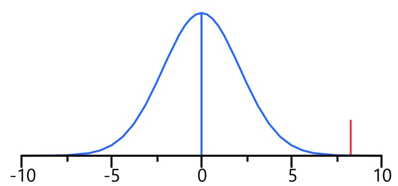


### Nonparametric Comparisons For Each Pair Using Wilcoxon Method

| q* | Alpha |
|---|---|
| 1.960 | 0.05 |

| Level | - Level | Score Mean Difference | Std Err Dif | Z | p-Value | Hodges-Lehmann | Lower CL | Upper CL |
|---|---|---|---|---|---|---|---|---|
| South | North | 17.0 | 5.2 | 3.292 | 0.0010* | 5.494 | 0.921 | 9.874 |

## Oneway Analysis of Weight % Silt By Study Area

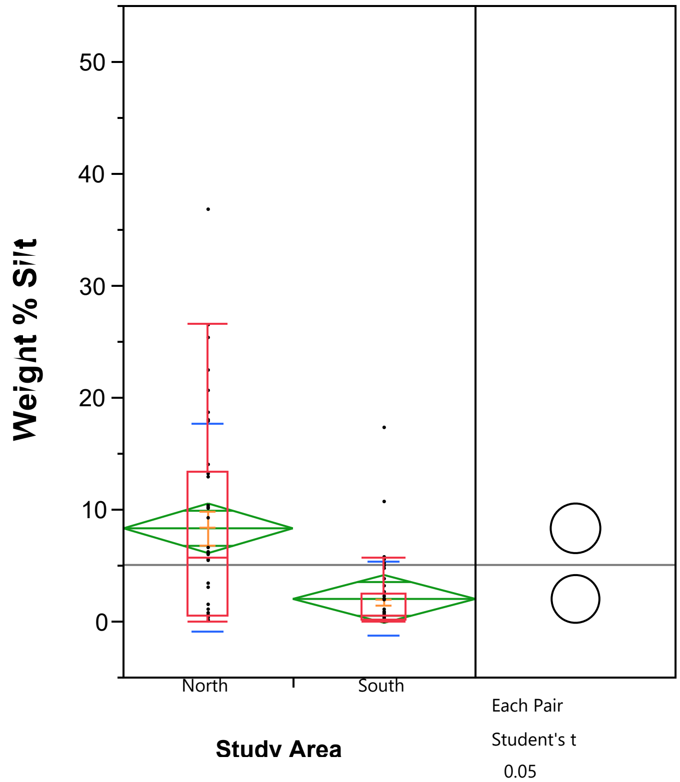


## Quantiles

| Level | Minimum | 10% | 25% | Median | 75% | 90% | Maximum |
|---|---|---|---|---|---|---|---|
| North | 0.1 | 0.1 | 0.6 | 5.8 | 13.4 | 22.8 | 36.8 |
| South | 0.0 | 0.1 | 0.2 | 0.5 | 2.6 | 5.5 | 17.4 |

## Means and Std Deviations

| Level | Number | Mean | Std Dev | Std Err Mean | Lower 95% | Upper 95% |
|---|---|---|---|---|---|---|
| North | 38 | 8.3 | 9.3 | 1.5 | 5.3 | 11.4 |
| South | 41 | 2.0 | 3.3 | 0.5 | 1.0 | 3.1 |

## Means Comparisons
## Comparisons for each pair using Student's t
## Confidence Quantile

| t | Alpha |
|---|---|
| 1.991 | 0.05 |

## Connecting Letters Report

| Level | | | Mean |
|---|---|---|---|
| North | A | | 8.3 |
| South | | B | 2.0 |

Levels not connected by same letter are significantly different.

## Detailed Comparisons Report
## Comparing South with North

| | | | |
|---|---|---|---|
| Difference | -6.309 | t Ratio | -4.08409 |
| Std Err Dif | 1.545 | DF | 77 |
| Upper CL Dif | -3.233 | Prob > \|t\| | 0.0001* |
| Lower CL Dif | -9.385 | Prob > t | 0.9999 |
| Confidence | 0.95 | Prob < t | <.0001* |

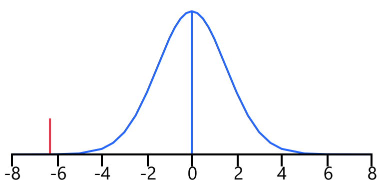


## Nonparametric Comparisons For Each Pair Using Wilcoxon Method

| q* | Alpha |
|---|---|
| 1.960 | 0.05 |

| Level | - Level | Score Mean Difference | Std Err Dif | Z | p-Value | Hodges-Lehmann | Lower CL | Upper CL |
|---|---|---|---|---|---|---|---|---|
| South | North | -17.4 | 5.2 | -3.361 | 0.0008* | -3.502 | -6.485 | -0.464 |

## Oneway Analysis of Weight % Clay By Study Area

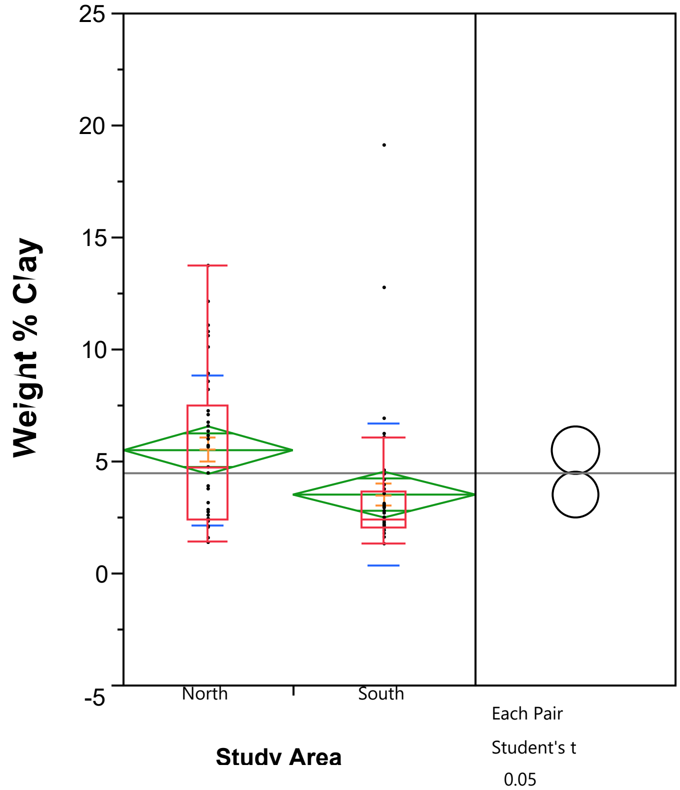


## Quantiles

| Level | Minimum | 10% | 25% | Median | 75% | 90% | Maximum |
|---|---|---|---|---|---|---|---|
| North | 1.4 | 2.0 | 2.4 | 4.8 | 7.5 | 10.8 | 13.8 |
| South | 1.3 | 1.7 | 2.1 | 2.4 | 3.7 | 6.2 | 19.1 |

## Means and Std Deviations

| Level | Number | Mean | Std Dev | Std Err Mean | Lower 95% | Upper 95% |
|---|---|---|---|---|---|---|
| North | 38 | 5.5 | 3.4 | 0.5 | 4.4 | 6.6 |
| South | 41 | 3.5 | 3.2 | 0.5 | 2.5 | 4.5 |

## Means Comparisons
## Comparisons for each pair using Student's t
## Confidence Quantile

| t | Alpha |
|---|---|
| 1.991 | 0.05 |

## Connecting Letters Report

| Level | | | Mean |
|---|---|---|---|
| North | A | | 5.5 |
| South | | B | 3.5 |

Levels not connected by same letter are significantly different.

## Detailed Comparisons Report
## Comparing South with North

| | | | |
|---|---|---|---|
| Difference | -1.982 | t Ratio | -2.68028 |
| Std Err Dif | 0.740 | DF | 77 |
| Upper CL Dif | -0.510 | Prob > \|t\| | 0.0090* |
| Lower CL Dif | -3.455 | Prob > t | 0.9955 |
| Confidence | 0.95 | Prob < t | 0.0045* |

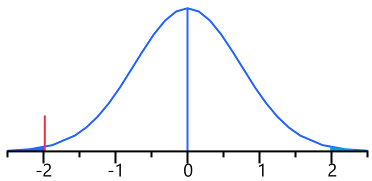


## Nonparametric Comparisons For Each Pair Using Wilcoxon Method

| q* | Alpha |
|---|---|
| 1.960 | 0.05 |

| Level | - Level | Score Mean Difference | Std Err Dif | Z | p-Value | Hodges-Lehmann | Lower CL | Upper CL |
|---|---|---|---|---|---|---|---|---|
| South | North | -15.8 | 5.2 | -3.066 | 0.0022* | -1.799 | -3.340 | -0.443 |

## Oneway Analysis of % LOI By Study Area

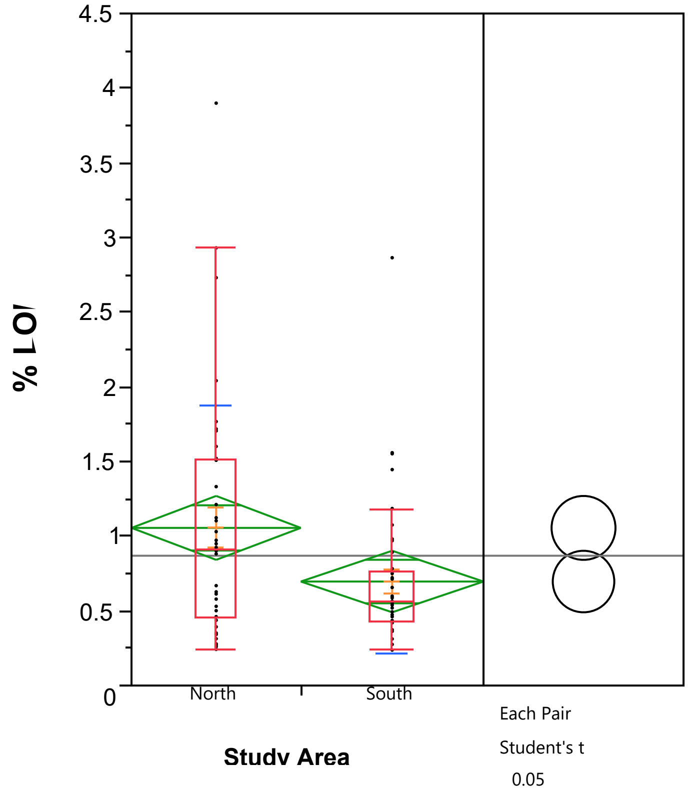


### Quantiles

| Level | Minimum | 10% | 25% | Median | 75% | 90% | Maximum |
|---|---|---|---|---|---|---|---|
| North | 0.2 | 0.3 | 0.5 | 0.9 | 1.5 | 2.1 | 3.9 |
| South | 0.2 | 0.3 | 0.4 | 0.6 | 0.8 | 1.4 | 2.9 |

### Means and Std Deviations

| Level | Number | Mean | Std Dev | Std Err Mean | Lower 95% | Upper 95% |
|---|---|---|---|---|---|---|
| North | 38 | 1.1 | 0.8 | 0.1 | 0.8 | 1.3 |
| South | 41 | 0.7 | 0.5 | 0.1 | 0.5 | 0.8 |

### Means Comparisons
### Comparisons for each pair using Student's t
### Confidence Quantile

| t | Alpha |
|---|---|
| 1.991 | 0.05 |

### Connecting Letters Report

| Level | | | Mean |
|---|---|---|---|
| North | A | | 1.1 |
| South | | B | 0.7 |

Levels not connected by same letter are significantly different.

### Detailed Comparisons Report
### Comparing South with North

| | | | |
|---|---|---|---|
| Difference | -0.359 | t Ratio | -2.40779 |
| Std Err Dif | 0.149 | DF | 77 |
| Upper CL Dif | -0.062 | Prob > \|t\| | 0.0184* |
| Lower CL Dif | -0.656 | Prob > t | 0.9908 |
| Confidence | 0.95 | Prob < t | 0.0092* |

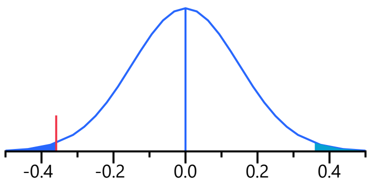


### Nonparametric Comparisons For Each Pair Using Wilcoxon Method

| q* | Alpha |
|---|---|
| 1.960 | 0.05 |

| Level | - Level | Score Mean Difference | Std Err Dif | Z | p-Value | Hodges-Lehmann | Lower CL | Upper CL |
|---|---|---|---|---|---|---|---|---|
| South | North | -10.2 | 5.2 | -1.967 | 0.0491* | -0.210 | -0.481 | 0.005 |

**% SAV Cover**
**Quadrat Survey 1 – October 2017**
**Oneway Analysis of SAV Cover By Study Area**

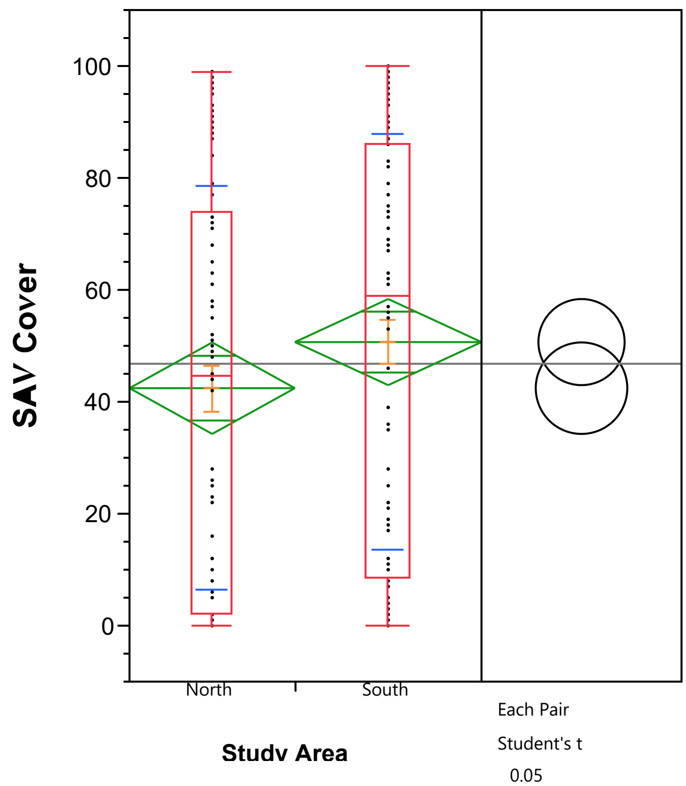


## Quantiles

| Level | Minimum | 10% | 25% | Median | 75% | 90% | Maximum |
|---|---|---|---|---|---|---|---|
| North | 0 | 0 | 2 | 45 | 74 | 93 | 99 |
| South | 0 | 2 | 9 | 59 | 86 | 97 | 100 |

## Means and Std Deviations

| Level | Number | Mean | Std Dev | Std Err Mean | Lower 95% | Upper 95% |
|---|---|---|---|---|---|---|
| North | 78 | 42 | 36 | 4 | 34 | 51 |
| South | 88 | 51 | 37 | 4 | 43 | 59 |

## Means Comparisons
## Comparisons for each pair using Student's t
## Confidence Quantile

| t | Alpha |
|---|---|
| 1.975 | 0.05 |

## Connecting Letters Report

| Level | | Mean |
|---|---|---|
| South | A | 51 |
| North | A | 42 |

Levels not connected by same letter are significantly different.

### Detailed Comparisons Report
### Comparing South with North

| | | | |
|---|---|---|---|
| Difference | 8.235 | t Ratio | 1.448305 |
| Std Err Dif | 5.686 | DF | 164 |
| Upper CL Dif | 19.461 | Prob > \|t\| | 0.1494 |
| Lower CL Dif | -2.992 | Prob > t | 0.0747 |
| Confidence | 0.95 | Prob < t | 0.9253 |

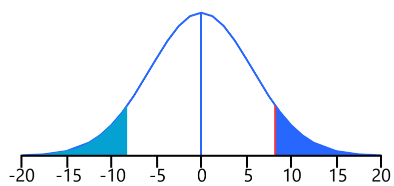


### Nonparametric Comparisons For Each Pair Using Wilcoxon Method

| q* | Alpha |
|---|---|
| 1.960 | 0.05 |

| Level | - Level | Score Mean Difference | Std Err Dif | Z | p-Value | Hodges-Lehmann | Lower CL | Upper CL |
|---|---|---|---|---|---|---|---|---|
| South | North | 13 | 7 | 1.798 | 0.0722 | 6.000 | 0.000 | 18.000 |

## Quadrat Survey 2 – May 2018
## Oneway Analysis of SAV Cover By Study Area

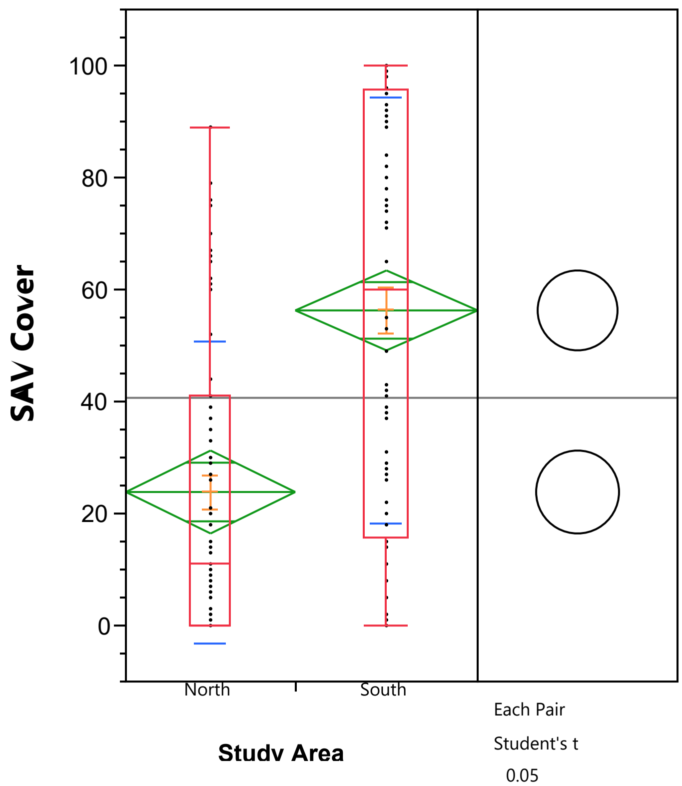


### Quantiles

| Level | Minimum | 10% | 25% | Median | 75% | 90% | Maximum |
|---|---|---|---|---|---|---|---|
| North | 0 | 0 | 0 | 11 | 41 | 67 | 89 |
| South | 0 | 2 | 16 | 60 | 96 | 100 | 100 |

### Means and Std Deviations

| Level | Number | Mean | Std Dev | Std Err Mean | Lower 95% | Upper 95% |
|---|---|---|---|---|---|---|
| North | 78 | 24 | 27 | 3 | 18 | 30 |
| South | 84 | 56 | 38 | 4 | 48 | 65 |

### Means Comparisons
### Comparisons for each pair using Student's t
### Confidence Quantile

| t | Alpha |
|---|---|
| 1.975 | 0.05 |

### Connecting Letters Report

| Level | | | Mean |
|---|---|---|---|
| South | A | | 56 |
| North | | B | 24 |

Levels not connected by same letter are significantly different.

### Detailed Comparisons Report
### Comparing South with North

| | | | |
|---|---|---|---|
| Difference | 32.428 | t Ratio | 6.227374 |
| Std Err Dif | 5.207 | DF | 160 |
| Upper CL Dif | 42.712 | Prob > \|t\| | <.0001* |
| Lower CL Dif | 22.144 | Prob > t | <.0001* |
| Confidence | 0.95 | Prob < t | 1.0000 |

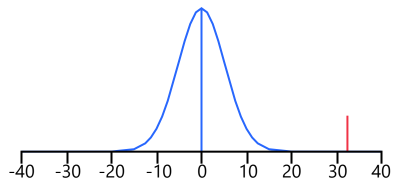


### Nonparametric Comparisons For Each Pair Using Wilcoxon Method

| q* | Alpha |
|---|---|
| 1.960 | 0.05 |

| Level | - Level | Score Mean Difference | Std Err Dif | Z | p-Value | Hodges-Lehmann | Lower CL | Upper CL |
|---|---|---|---|---|---|---|---|---|
| South | North | 41 | 7 | 5.628 | <.0001* | 31.000 | 19.000 | 43.000 |

**Quadrat Survey 3 – October 2018**
**Oneway Analysis of SAV Cover By Study Area**

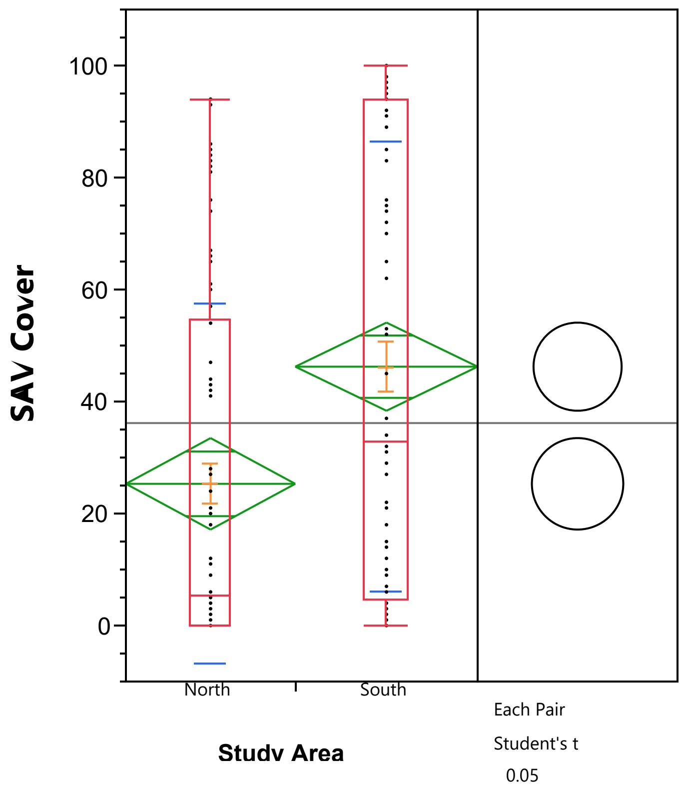


## Quantiles

| Level | Minimum | 10% | 25% | Median | 75% | 90% | Maximum |
|---|---|---|---|---|---|---|---|
| North | 0 | 0 | 0 | 6 | 55 | 83 | 94 |
| South | 0 | 0 | 5 | 33 | 94 | 100 | 100 |

## Means and Std Deviations

| Level | Number | Mean | Std Dev | Std Err Mean | Lower 95% | Upper 95% |
|---|---|---|---|---|---|---|
| North | 78 | 25 | 32 | 4 | 18 | 33 |
| South | 84 | 46 | 40 | 4 | 37 | 55 |

## Means Comparisons
## Comparisons for each pair using Student's t
## Confidence Quantile

| t | Alpha |
|---|---|
| 1.975 | 0.05 |

## Connecting Letters Report

| Level | | | Mean |
|---|---|---|---|
| South | A | | 46 |
| North | | B | 25 |

Levels not connected by same letter are significantly different.

## Detailed Comparisons Report
## Comparing South with North

| | | | |
|---|---|---|---|
| Difference | 20.918 | t Ratio | 3.642086 |
| Std Err Dif | 5.744 | DF | 160 |
| Upper CL Dif | 32.261 | Prob > \|t\| | 0.0004* |
| Lower CL Dif | 9.576 | Prob > t | 0.0002* |
| Confidence | 0.95 | Prob < t | 0.9998 |

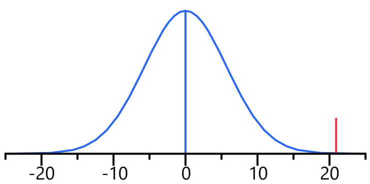


## Nonparametric Comparisons For Each Pair Using Wilcoxon Method

| q* | Alpha |
|---|---|
| 1.960 | 0.05 |

| Level | - Level | Score Mean Difference | Std Err Dif | Z | p-Value | Hodges-Lehmann | Lower CL | Upper CL |
|---|---|---|---|---|---|---|---|---|
| South | North | 28 | 7 | 3.808 | 0.0001* | 13.000 | 4.000 | 27.000 |

**Quadrat Survey 4 – May 2019**
**Oneway Analysis of SAV Cover By Study Area**

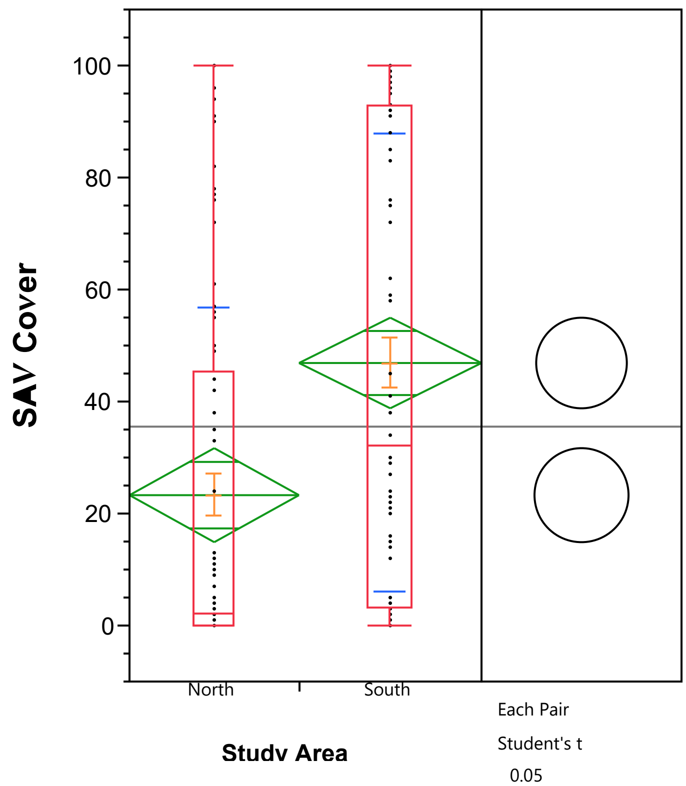


## Quantiles

| Level | Minimum | 10% | 25% | Median | 75% | 90% | Maximum |
|---|---|---|---|---|---|---|---|
| North | 0 | 0 | 0 | 2 | 45 | 83 | 100 |
| South | 0 | 0 | 3 | 32 | 93 | 100 | 100 |

## Means and Std Deviations

| Level | Number | Mean | Std Dev | Std Err Mean | Lower 95% | Upper 95% |
|---|---|---|---|---|---|---|
| North | 78 | 23 | 34 | 4 | 16 | 31 |
| South | 84 | 47 | 41 | 4 | 38 | 56 |

## Means Comparisons
## Comparisons for each pair using Student's t
## Confidence Quantile

| t | Alpha |
|---|---|
| 1.975 | 0.05 |

## Connecting Letters Report

| Level | | | Mean |
|---|---|---|---|
| South | A | | 47 |
| North | | B | 23 |

Levels not connected by same letter are significantly different.

### Detailed Comparisons Report
### Comparing South with North

| | | | |
|---|---|---|---|
| Difference | 23.599 | t Ratio | 3.997443 |
| Std Err Dif | 5.903 | DF | 160 |
| Upper CL Dif | 35.258 | Prob > \|t\| | <.0001* |
| Lower CL Dif | 11.940 | Prob > t | <.0001* |
| Confidence | 0.95 | Prob < t | 1.0000 |

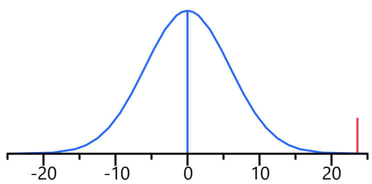


### Nonparametric Comparisons For Each Pair Using Wilcoxon Method

| q* | Alpha |
|---|---|
| 1.960 | 0.05 |

| Level | - Level | Score Mean Difference | Std Err Dif | Z | p-Value | Hodges-Lehmann | Lower CL | Upper CL |
|---|---|---|---|---|---|---|---|---|
| South | North | 31 | 7 | 4.277 | <.0001* | 16.000 | 5.000 | 27.000 |

**% SAV Cover**
**Quadrat Survey 1 – October 2017**
**Oneway Analysis of SAV Cover By Group**

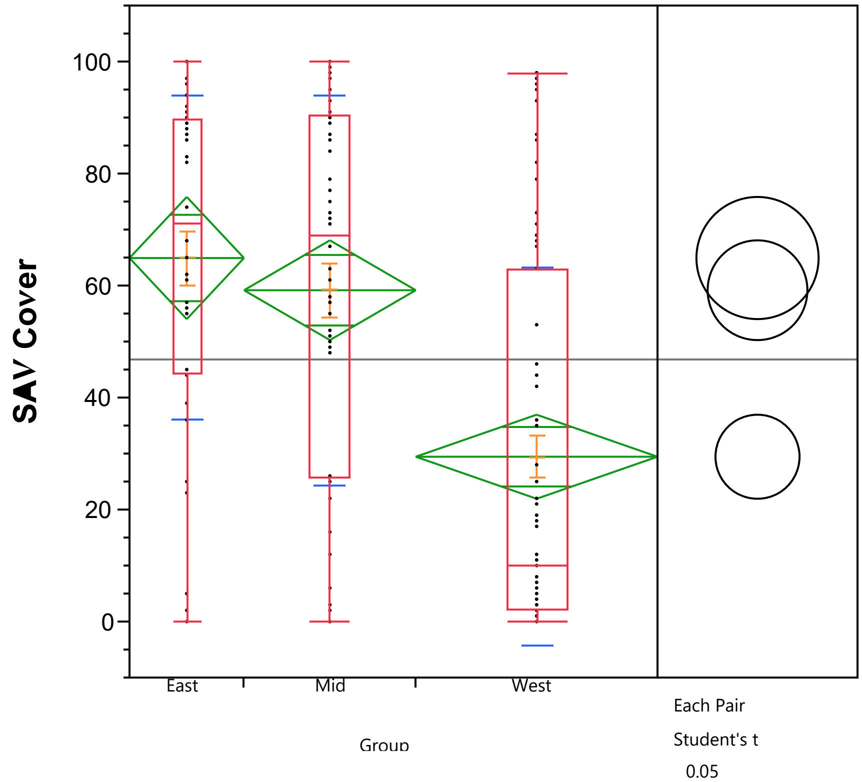


## Quantiles

| Level | Minimum | 10% | 25% | Median | 75% | 90% | Maximum |
|---|---|---|---|---|---|---|---|
| East | 0 | 18 | 44 | 71 | 90 | 96 | 100 |
| Mid | 0 | 1 | 26 | 69 | 90 | 99 | 100 |
| West | 0 | 0 | 2 | 10 | 63 | 86 | 98 |

## Means and Std Deviations

| Level | Number | Mean | Std Dev | Std Err Mean | Lower 95% | Upper 95% |
|---|---|---|---|---|---|---|
| East | 36 | 65 | 29 | 5 | 55 | 75 |
| Mid | 54 | 59 | 35 | 5 | 50 | 69 |
| West | 76 | 29 | 34 | 4 | 22 | 37 |

## Means Comparisons
## Comparisons for each pair using Student's t
## Confidence Quantile

| t | Alpha |
|---|---|
| 1.975 | 0.05 |

## Connecting Letters Report

| Level | | | Mean |
|---|---|---|---|
| East | A | | 65 |
| Mid | A | | 59 |
| West | | B | 29 |

Levels not connected by same letter are significantly different.

## Detailed Comparisons Report

## Comparing Mid with East

| | | | |
|---|---|---|---|
| Difference | -5.750 | t Ratio | -0.80636 |
| Std Err Dif | 7.131 | DF | 163 |
| Upper CL Dif | 8.331 | Prob > \|t\| | 0.4212 |
| Lower CL Dif | -19.831 | Prob > t | 0.7894 |
| Confidence | 0.95 | Prob < t | 0.2106 |

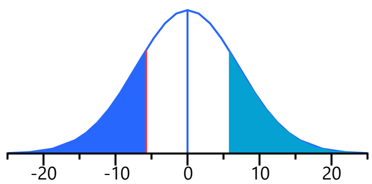


## Comparing West with East

| | | | |
|---|---|---|---|
| Difference | -35.482 | t Ratio | -5.29173 |
| Std Err Dif | 6.705 | DF | 163 |
| Upper CL Dif | -22.242 | Prob > \|t\| | <.0001* |
| Lower CL Dif | -48.723 | Prob > t | 1.0000 |
| Confidence | 0.95 | Prob < t | <.0001* |

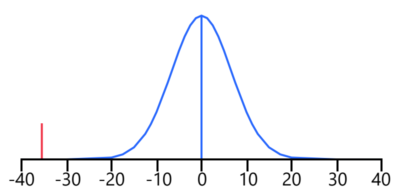


## Comparing West with Mid

| | | | |
|---|---|---|---|
| Difference | -29.732 | t Ratio | -5.04078 |
| Std Err Dif | 5.898 | DF | 163 |
| Upper CL Dif | -18.085 | Prob > \|t\| | <.0001* |
| Lower CL Dif | -41.380 | Prob > t | 1.0000 |
| Confidence | 0.95 | Prob < t | <.0001* |

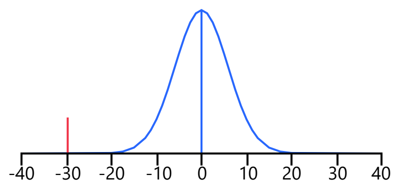


## Nonparametric Comparisons For Each Pair Using Wilcoxon Method

| q* | Alpha |
|---|---|
| 1.960 | 0.05 |

| Level | - Level | Score Mean Difference | Std Err Dif | Z | p-Value | Hodges-Lehmann | Lower CL | Upper CL |
|---|---|---|---|---|---|---|---|---|
| Mid | East | -3 | 6 | -0.461 | 0.6445 | -2.000 | -17.000 | 8.000 |
| West | Mid | -29 | 7 | -4.298 | <.0001* | -32.000 | -51.000 | -16.000 |
| West | East | -31 | 7 | -4.677 | <.0001* | -42.000 | -55.000 | -25.000 |

## Quadrat Survey 2 – May 2018
## Oneway Analysis of SAV Cover By Group

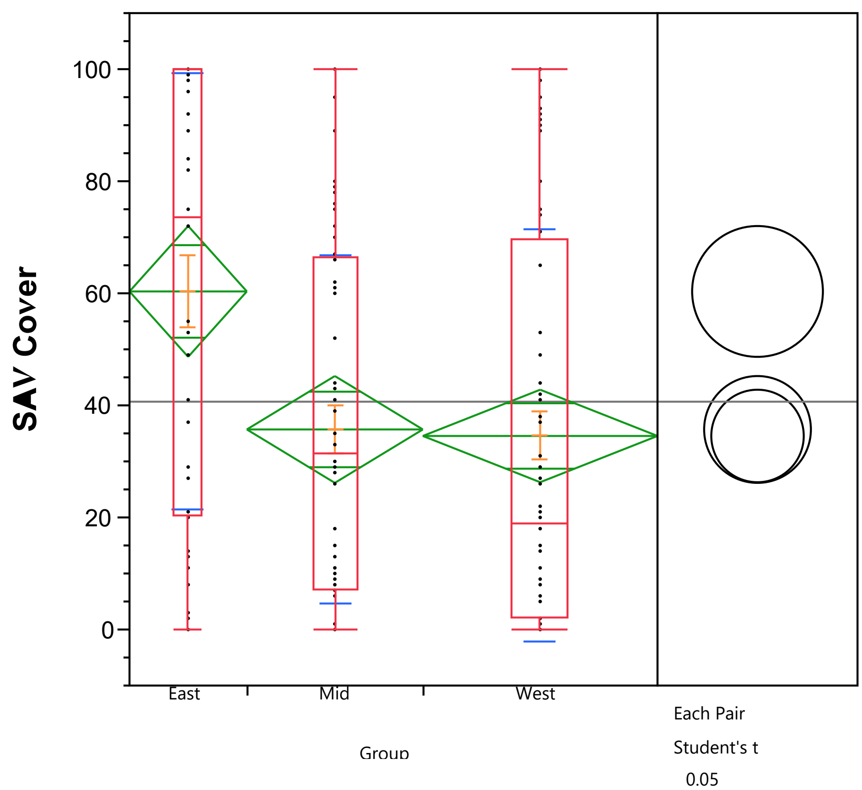


## Quantiles

| Level | Minimum | 10% | 25% | Median | 75% | 90% | Maximum |
|---|---|---|---|---|---|---|---|
| East | 0 | 3 | 20 | 74 | 100 | 100 | 100 |

| Level | Minimum | 10% | 25% | Median | 75% | 90% | Maximum |
|---|---|---|---|---|---|---|---|
| Mid | 0 | 0 | 7 | 32 | 66 | 79 | 100 |
| West | 0 | 0 | 2 | 19 | 70 | 97 | 100 |

### Means and Std Deviations

| Level | Number | Mean | Std Dev | Std Err Mean | Lower 95% | Upper 95% |
|---|---|---|---|---|---|---|
| East | 36 | 60 | 39 | 6 | 47 | 73 |
| Mid | 54 | 36 | 31 | 4 | 27 | 44 |
| West | 72 | 35 | 37 | 4 | 26 | 43 |

### Means Comparisons
### Comparisons for each pair using Student's t
### Confidence Quantile

| t | Alpha |
|---|---|
| 1.975 | 0.05 |

### Connecting Letters Report

| Level | | | Mean |
|---|---|---|---|
| East | A | | 60 |
| Mid | | B | 36 |
| West | | B | 35 |

Levels not connected by same letter are significantly different.

### Detailed Comparisons Report
### Comparing Mid with East

| | | | |
|---|---|---|---|
| Difference | -24.630 | t Ratio | -3.22717 |
| Std Err Dif | 7.632 | DF | 159 |
| Upper CL Dif | -9.557 | Prob > \|t\| | 0.0015* |
| Lower CL Dif | -39.703 | Prob > t | 0.9992 |
| Confidence | 0.95 | Prob < t | 0.0008* |

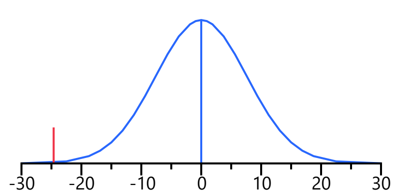


### Comparing West with East

| | | | |
|---|---|---|---|
| Difference | -25.792 | t Ratio | -3.56223 |
| Std Err Dif | 7.240 | DF | 159 |
| Upper CL Dif | -11.492 | Prob > \|t\| | 0.0005* |
| Lower CL Dif | -40.091 | Prob > t | 0.9998 |
| Confidence | 0.95 | Prob < t | 0.0002* |

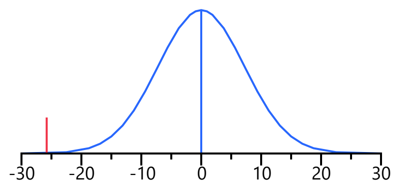


### Comparing West with Mid

| | | | |
|---|---|---|---|
| Difference | -1.162 | t Ratio | -0.18198 |
| Std Err Dif | 6.385 | DF | 159 |
| Upper CL Dif | 11.449 | Prob > \|t\| | 0.8558 |
| Lower CL Dif | -13.773 | Prob > t | 0.5721 |
| Confidence | 0.95 | Prob < t | 0.4279 |

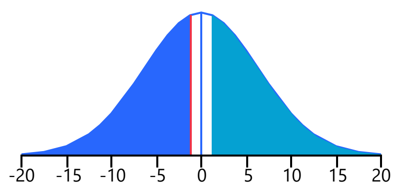


### Nonparametric Comparisons For Each Pair Using Wilcoxon Method

| q* | Alpha |
|---|---|
| 1.960 | 0.05 |

| Level | - Level | Score Mean Difference | Std Err Dif | Z | p-Value | Hodges-Lehmann | Lower CL | Upper CL |
|---|---|---|---|---|---|---|---|---|
| West | Mid | -3 | 7 | -0.386 | 0.6994 | 0.000 | -11.000 | 6.000 |
| Mid | East | -18 | 6 | -3.272 | 0.0011* | -24.000 | -40.000 | -10.000 |
| West | East | -22 | 6 | -3.468 | 0.0005* | -22.000 | -47.000 | -7.000 |

## Quadrat Survey 3 – October 2018
## Oneway Analysis of SAV Cover By Group

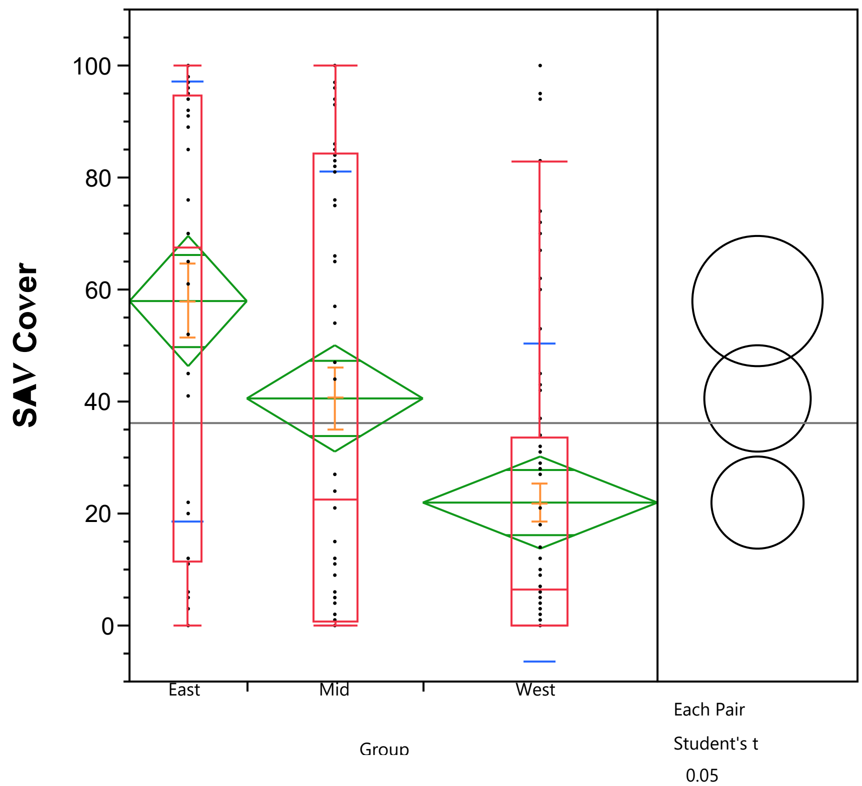


### Quantiles

| Level | Minimum | 10% | 25% | Median | 75% | 90% | Maximum |
|---|---|---|---|---|---|---|---|
| East | 0 | 3 | 11 | 68 | 95 | 100 | 100 |
| Mid | 0 | 0 | 1 | 23 | 84 | 99 | 100 |
| West | 0 | 0 | 0 | 7 | 34 | 72 | 100 |

### Means and Std Deviations

| Level | Number | Mean | Std Dev | Std Err Mean | Lower 95% | Upper 95% |
|---|---|---|---|---|---|---|
| East | 36 | 58 | 39 | 7 | 45 | 71 |
| Mid | 54 | 41 | 40 | 5 | 30 | 52 |
| West | 72 | 22 | 29 | 3 | 15 | 29 |

### Means Comparisons
### Comparisons for each pair using Student's t
### Confidence Quantile

| t | Alpha |
|---|---|
| 1.975 | 0.05 |

## Connecting Letters Report

| Level | | | | Mean |
|---|---|---|---|---|
| East | A | | | 58 |
| Mid | | B | | 41 |
| West | | | C | 22 |

Levels not connected by same letter are significantly different.

## Detailed Comparisons Report
## Comparing Mid with East

| | | | |
|---|---|---|---|
| Difference | -17.389 | t Ratio | -2.28715 |
| Std Err Dif | 7.603 | DF | 159 |
| Upper CL Dif | -2.373 | Prob > \|t\| | 0.0235* |
| Lower CL Dif | -32.405 | Prob > t | 0.9882 |
| Confidence | 0.95 | Prob < t | 0.0118* |

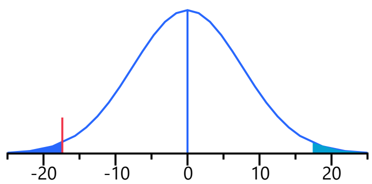


## Comparing West with East

| | | | |
|---|---|---|---|
| Difference | -35.986 | t Ratio | -4.98927 |
| Std Err Dif | 7.213 | DF | 159 |
| Upper CL Dif | -21.741 | Prob > \|t\| | <.0001* |
| Lower CL Dif | -50.231 | Prob > t | 1.0000 |
| Confidence | 0.95 | Prob < t | <.0001* |

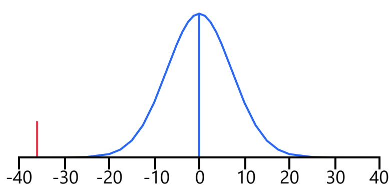


## Comparing West with Mid

| | | | |
|---|---|---|---|
| Difference | -18.597 | t Ratio | -2.92363 |
| Std Err Dif | 6.361 | DF | 159 |
| Upper CL Dif | -6.034 | Prob > \|t\| | 0.0040* |
| Lower CL Dif | -31.160 | Prob > t | 0.9980 |
| Confidence | 0.95 | Prob < t | 0.0020* |

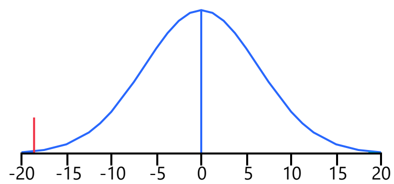


**Nonparametric Comparisons For Each Pair Using Wilcoxon Method**

| q* | Alpha |
|---|---|
| 1.960 | 0.05 |

| Level | - Level | Score Mean Difference | Std Err Dif | Z | p-Value | Hodges-Lehmann | Lower CL | Upper CL |
|---|---|---|---|---|---|---|---|---|
| Mid | East | -13 | 6 | -2.309 | 0.0210* | -11.000 | -36.000 | -1.000 |
| West | Mid | -14 | 7 | -2.221 | 0.0263* | -6.000 | -24.000 | 0.000 |
| West | East | -29 | 6 | -4.625 | <.0001* | -40.000 | -61.000 | -16.000 |

**Quadrat Survey 4 – May 2019**
**Oneway Analysis of SAV Cover By Group**

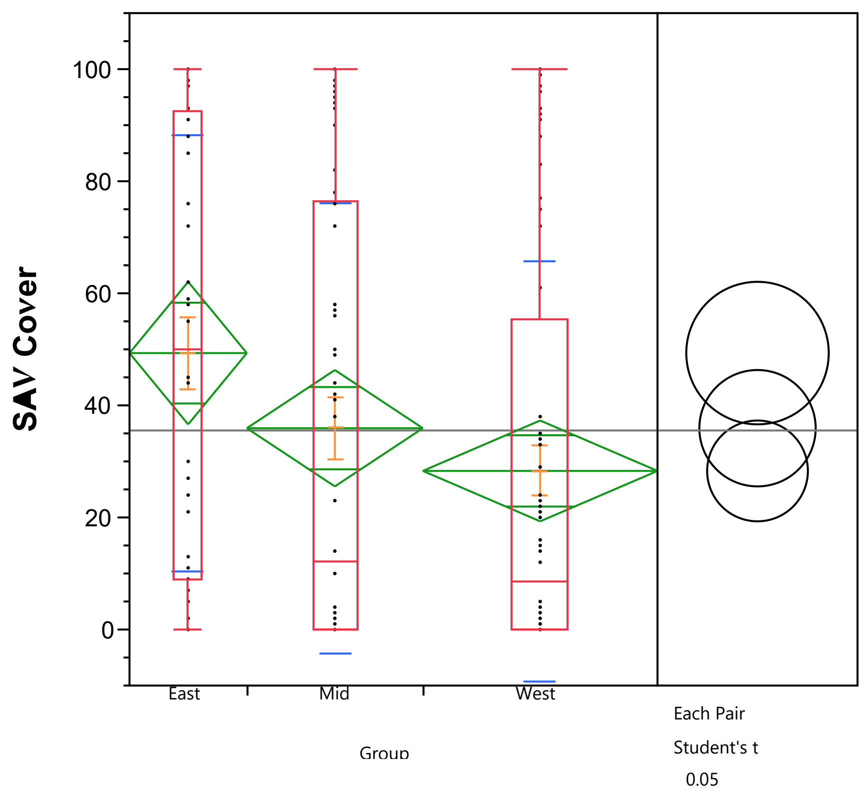


**Quantiles**

| Level | Minimum | 10% | 25% | Median | 75% | 90% | Maximum |
|---|---|---|---|---|---|---|---|
| East | 0 | 1 | 9 | 50 | 93 | 99 | 100 |

| Level | Minimum | 10% | 25% | Median | 75% | 90% | Maximum |
|---|---|---|---|---|---|---|---|
| Mid | 0 | 0 | 0 | 12 | 77 | 98 | 100 |
| West | 0 | 0 | 0 | 9 | 55 | 97 | 100 |

### Means and Std Deviations

| Level | Number | Mean | Std Dev | Std Err Mean | Lower 95% | Upper 95% |
|---|---|---|---|---|---|---|
| East | 36 | 49 | 39 | 6 | 36 | 62 |
| Mid | 54 | 36 | 40 | 5 | 25 | 47 |
| West | 72 | 28 | 37 | 4 | 20 | 37 |

### Means Comparisons
### Comparisons for each pair using Student's t
### Confidence Quantile

| t | Alpha |
|---|---|
| 1.975 | 0.05 |

### Connecting Letters Report

| Level | | | Mean |
|---|---|---|---|
| East | A | | 49 |
| Mid | A | B | 36 |
| West | | B | 28 |

Levels not connected by same letter are significantly different.

### Detailed Comparisons Report
### Comparing Mid with East

| | | | |
|---|---|---|---|
| Difference | -13.407 | t Ratio | -1.61253 |
| Std Err Dif | 8.315 | DF | 159 |
| Upper CL Dif | 3.014 | Prob > \|t\| | 0.1088 |
| Lower CL Dif | -29.829 | Prob > t | 0.9456 |
| Confidence | 0.95 | Prob < t | 0.0544 |

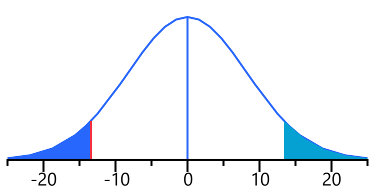


### Comparing West with East

| | | | |
|---|---|---|---|
| Difference | -21.028 | t Ratio | -2.66584 |
| Std Err Dif | 7.888 | DF | 159 |
| Upper CL Dif | -5.449 | Prob > \|t\| | 0.0085* |
| Lower CL Dif | -36.606 | Prob > t | 0.9958 |
| Confidence | 0.95 | Prob < t | 0.0042* |

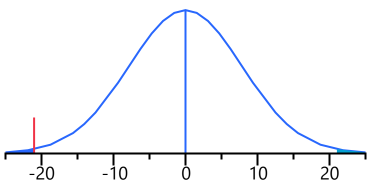


### Comparing West with Mid

| | | | |
|---|---|---|---|
| Difference | -7.620 | t Ratio | -1.09544 |
| Std Err Dif | 6.956 | DF | 159 |
| Upper CL Dif | 6.119 | Prob > \|t\| | 0.2750 |
| Lower CL Dif | -21.359 | Prob > t | 0.8625 |
| Confidence | 0.95 | Prob < t | 0.1375 |

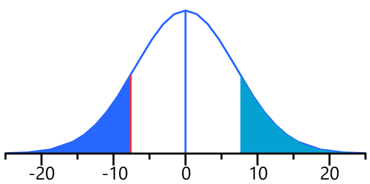


### Nonparametric Comparisons For Each Pair Using Wilcoxon Method

| q* | Alpha |
|---|---|
| 1.960 | 0.05 |

| Level | - Level | Score Mean Difference | Std Err Dif | Z | p-Value | Hodges-Lehmann | Lower CL | Upper CL |
|---|---|---|---|---|---|---|---|---|
| West | Mid | -4 | 6 | -0.628 | 0.5302 | 0.000 | -6.000 | 0.000 |
| Mid | East | -12 | 6 | -2.233 | 0.0255* | -9.000 | -27.000 | 0.000 |
| West | East | -19 | 6 | -3.074 | 0.0021* | -13.000 | -40.000 | -4.000 |

## Appendix C. *In Situ* Monitoring Data Collection and Continuity


**Figure C1. Summary of daily data collected at the five platforms (locations shown in Figure 15) from January 2016 to January 2018.**


**Figure C2. Summary of daily data collected with the two instrumented landers (locations shown in Figure 15) from May 2018 to September 2019. Boxes represent deployment periods (5 total) and gaps in between are instrument turnaround (e.g., data download, battery replacement, and cleaning). No data were collected in the winter months to avoid instrument damage.**

## Appendix D. *In Situ* Monitoring Daily-Average Time Series

### Platform CS01 Daily Averages

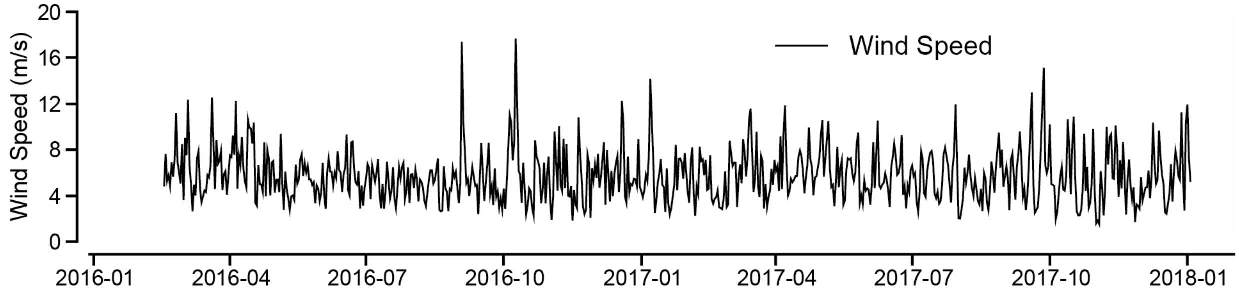


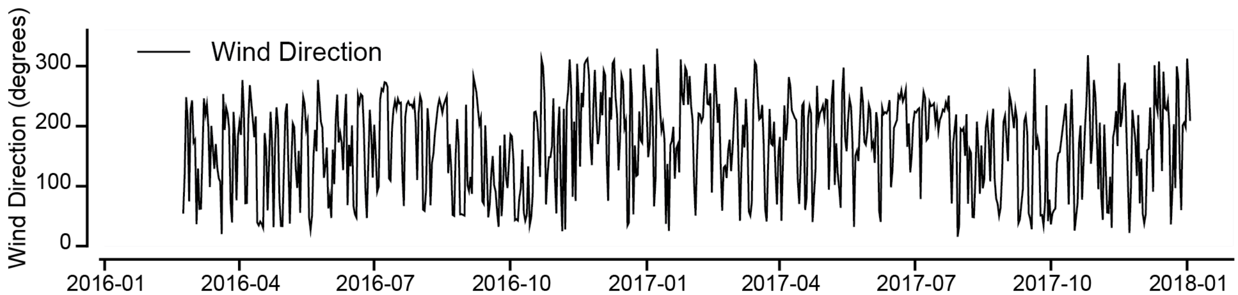


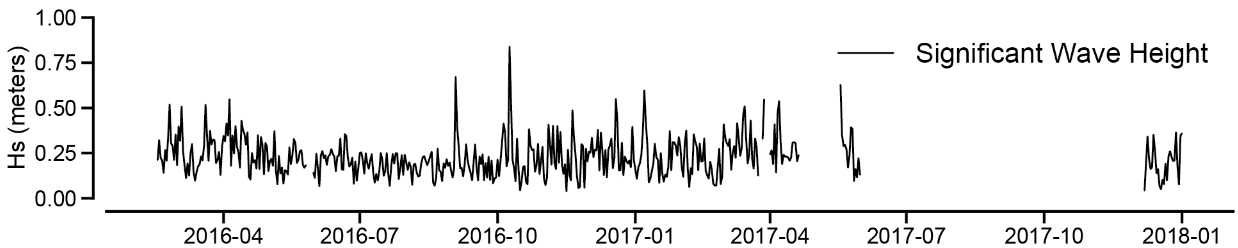


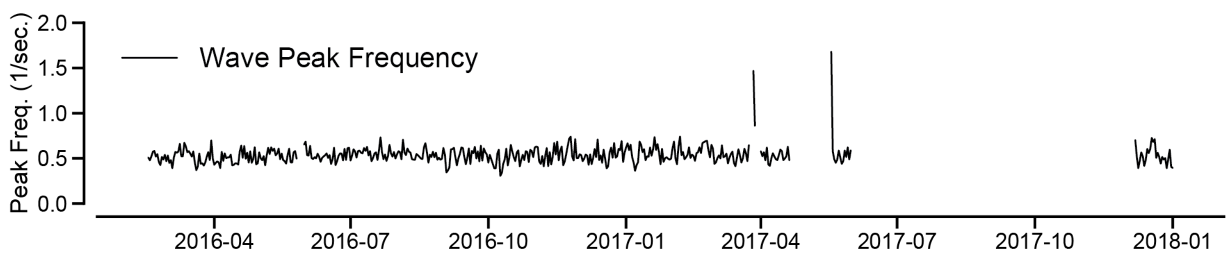


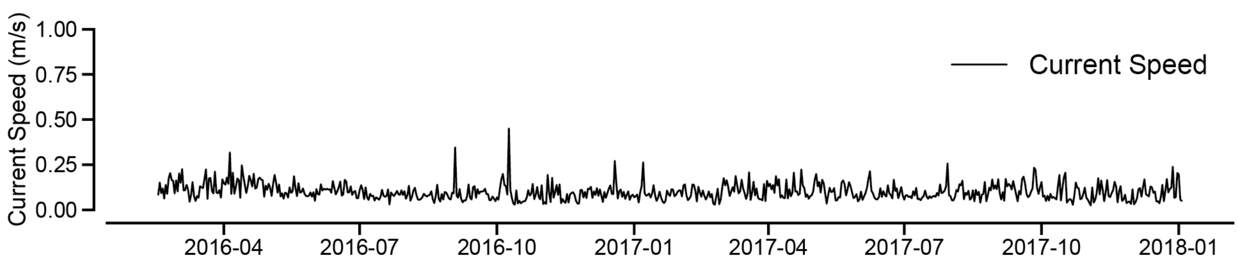

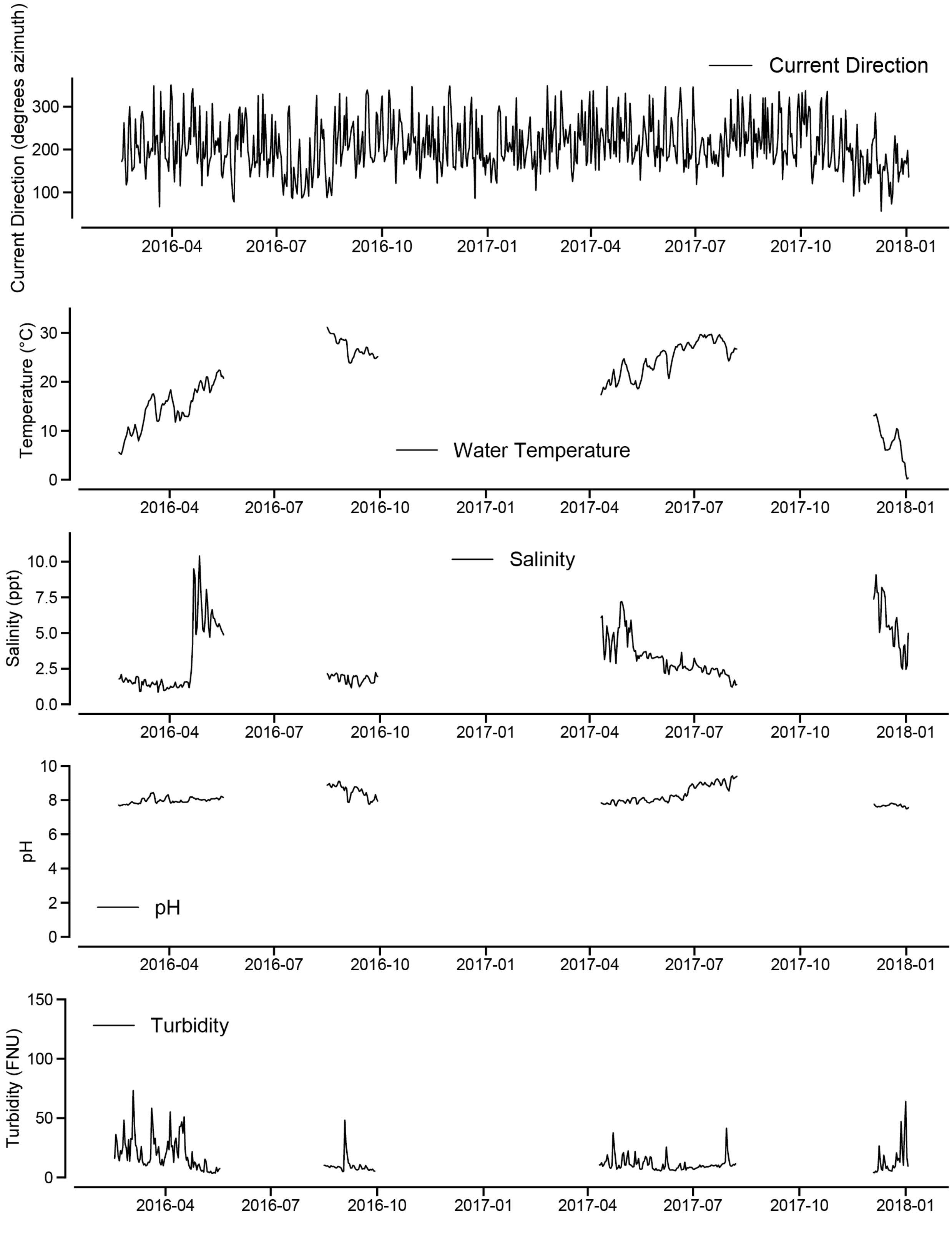

Current Direction
Current Direction (degrees azimuth)
300
200
100
2016-04
2016-07
2016-10
2017-01
2017-04
2017-07
2017-10
2018-01
Water Temperature
Temperature (°C)
30
20
10
0
Salinity
Salinity (ppt)
10.0
7.5
5.0
2.5
0.0
pH
pH
10
8
6
4
2
0
Turbidity
Turbidity (FNU)
150
100
50
0

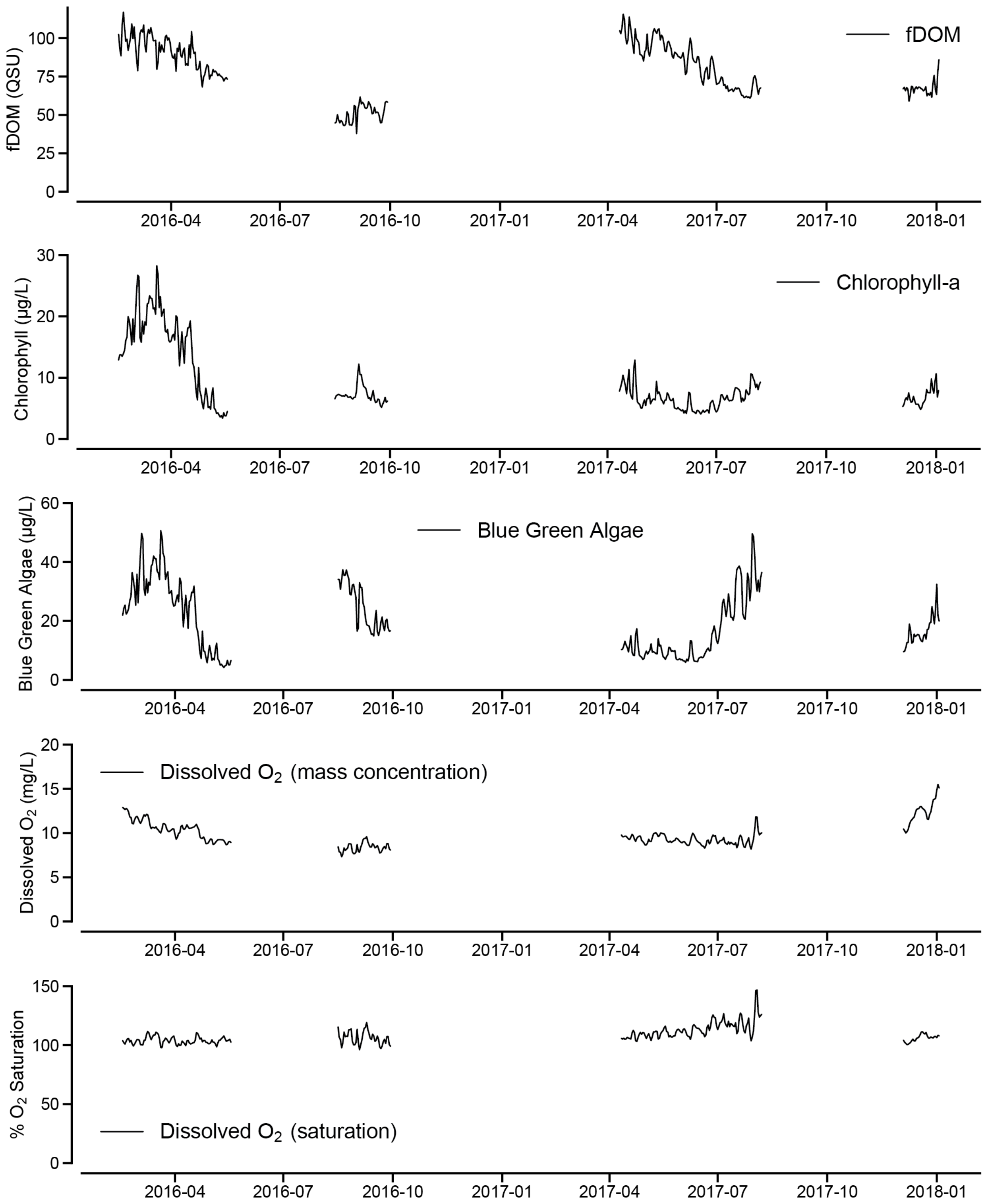
fDOM
fDOM (QSU)
Chlorophyll-a
Chlorophyll (µg/L)
Blue Green Algae
Blue Green Algae (µg/L)
Dissolved O2 (mass concentration)
Dissolved O2 (mg/L)
Dissolved O2 (saturation)
% O2 Saturation
2016-04
2016-07
2016-10
2017-01
2017-04
2017-07
2017-10
2018-01

## Platform CS02 Daily Averages

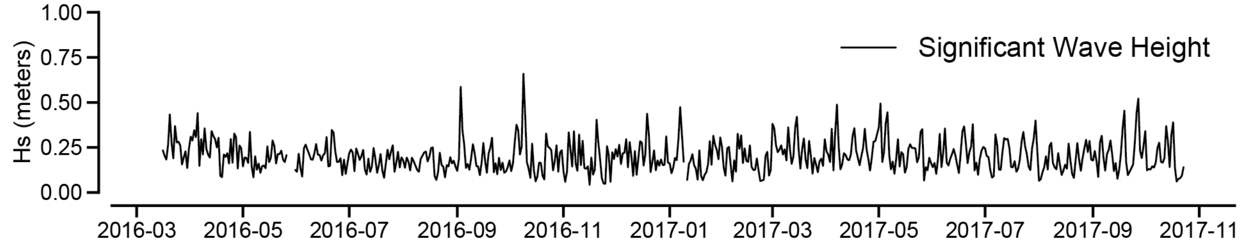


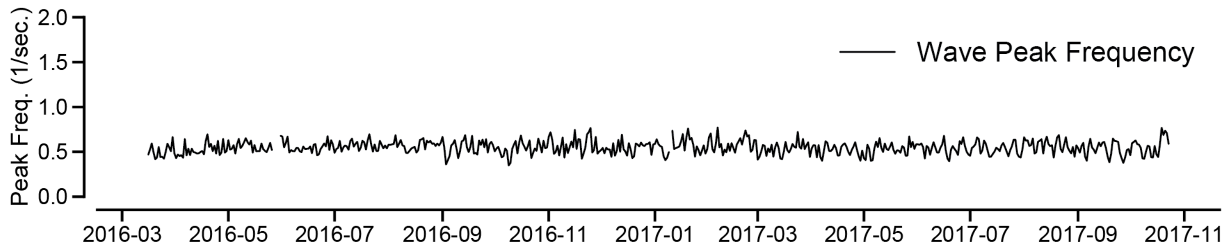


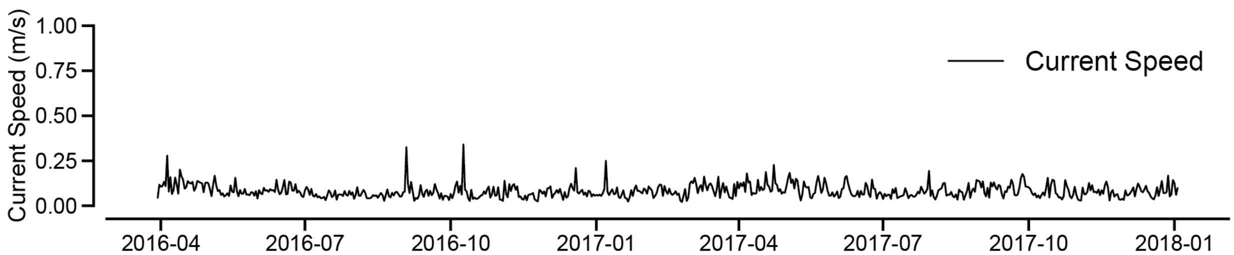


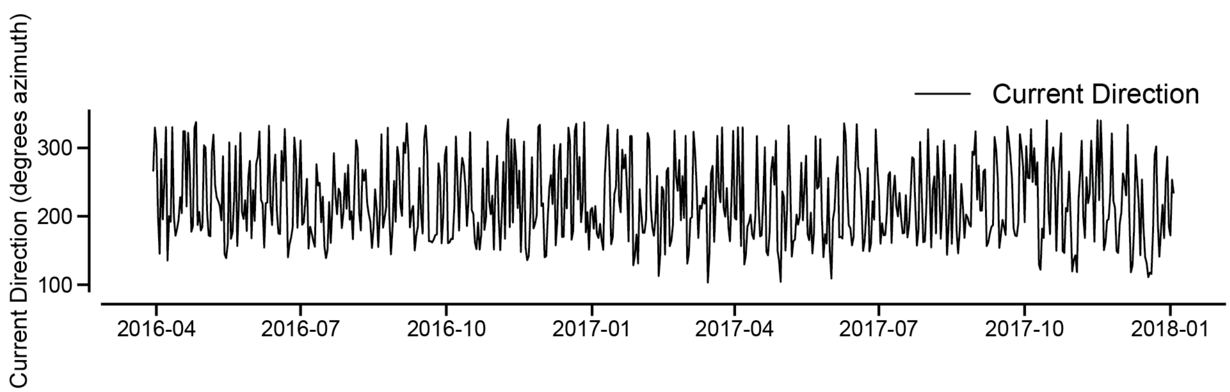


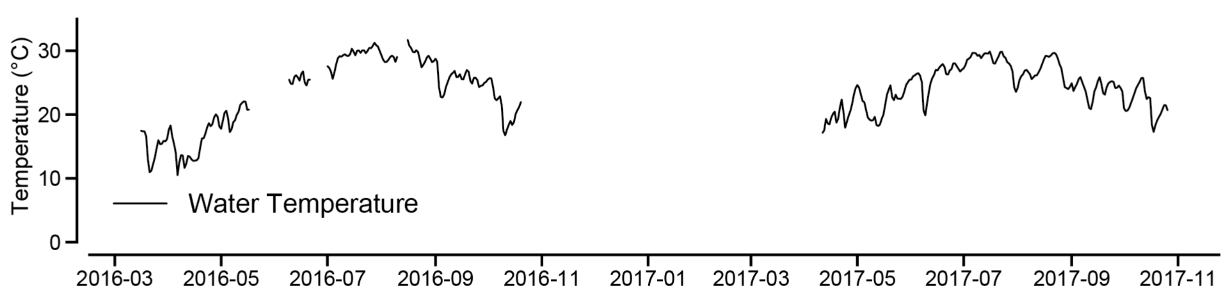

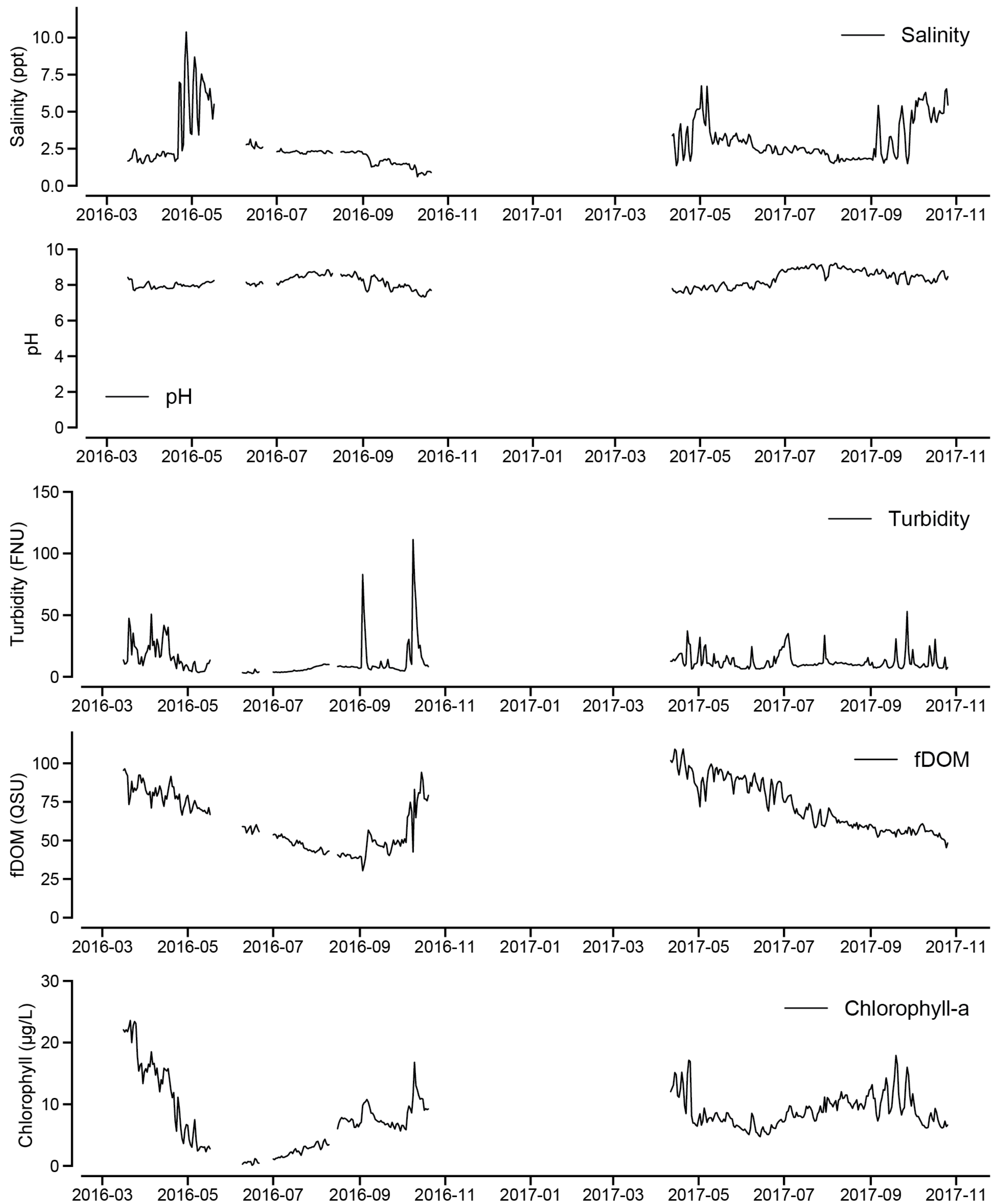
Salinity
Salinity (ppt)
0.0
2.5
5.0
7.5
10.0
pH
pH
0
2
4
6
8
10
Turbidity
Turbidity (FNU)
0
50
100
150
fDOM
fDOM (QSU)
0
25
50
75
100
Chlorophyll-a
Chlorophyll (µg/L)
0
10
20
30
2016-03
2016-05
2016-07
2016-09
2016-11
2017-01
2017-03
2017-05
2017-07
2017-09
2017-11

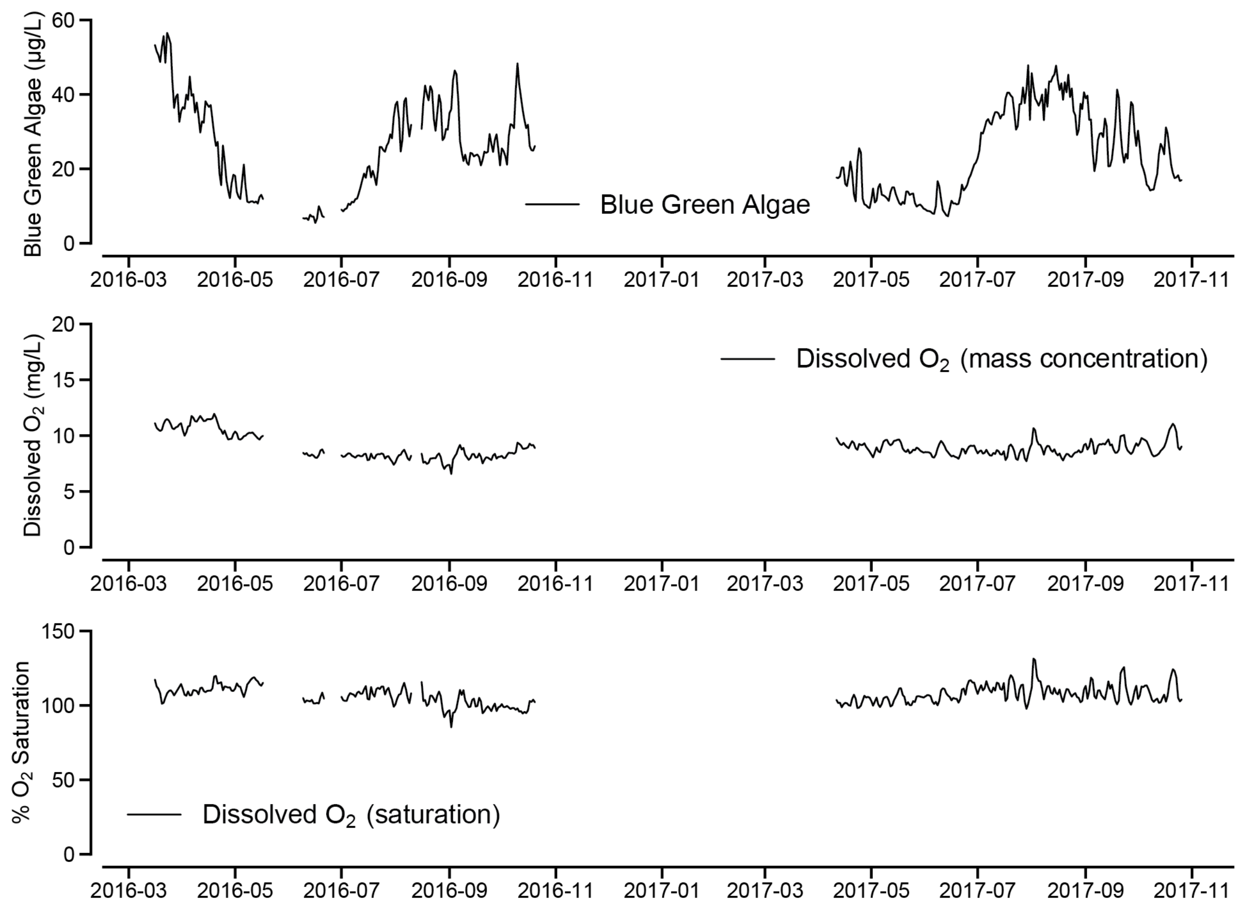

Blue Green Algae (µg/L)
60
40
20
0
Blue Green Algae
2016-03
2016-05
2016-07
2016-09
2016-11
2017-01
2017-03
2017-05
2017-07
2017-09
2017-11
Dissolved $O_2$ (mg/L)
20
15
10
5
0
Dissolved $O_2$ (mass concentration)
% $O_2$ Saturation
150
100
50
0
Dissolved $O_2$ (saturation)

**Platform CS03 Daily Averages**

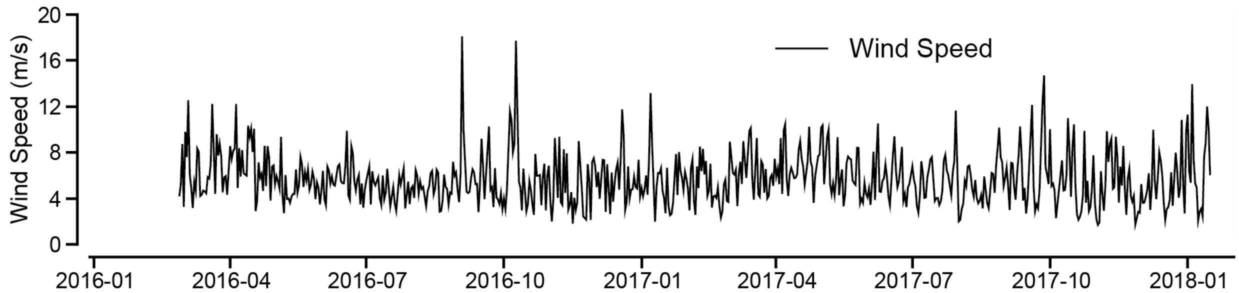


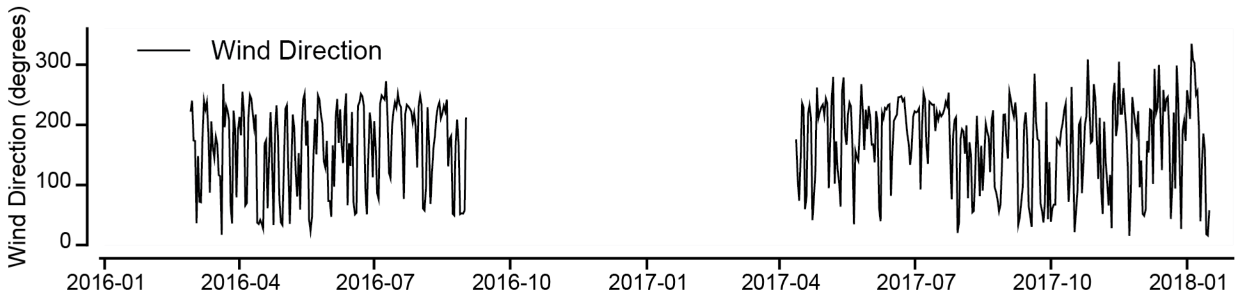


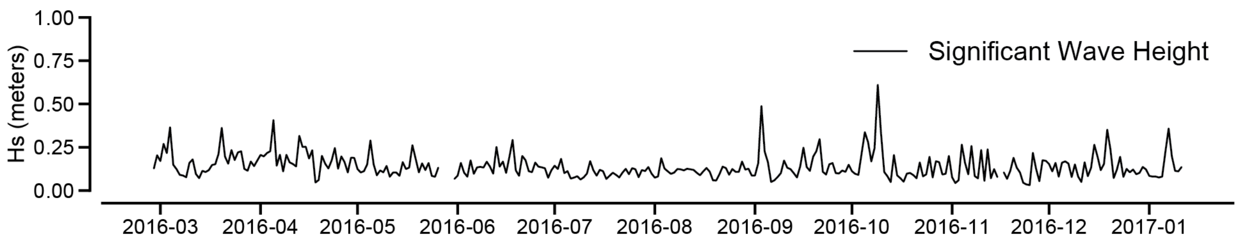


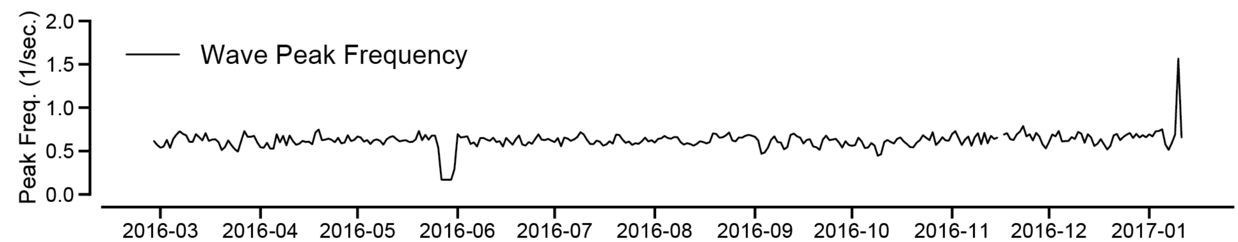


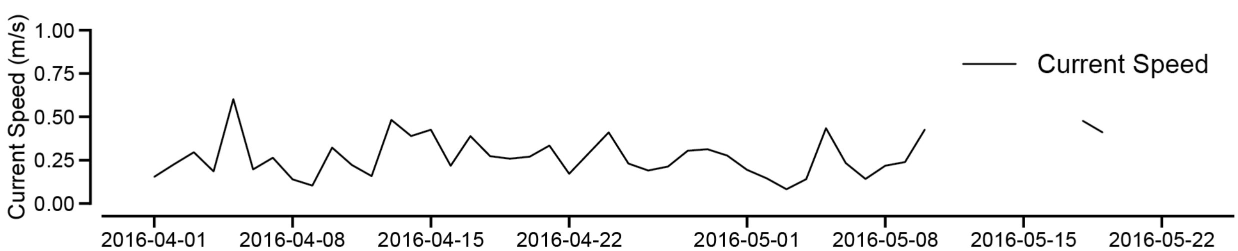

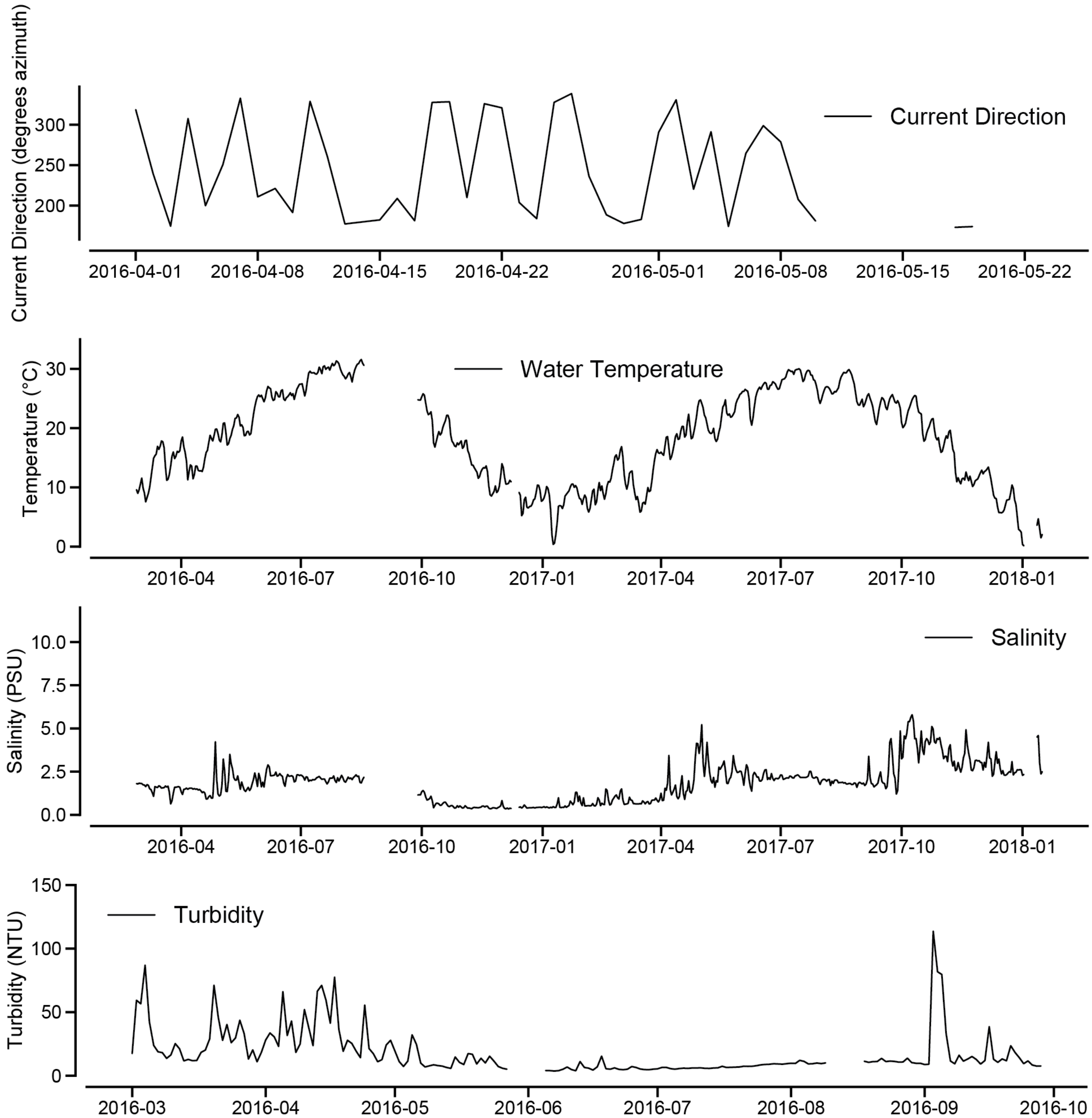
Current Direction (degrees azimuth)
300
250
200
2016-04-01
2016-04-08
2016-04-15
2016-04-22
2016-05-01
2016-05-08
2016-05-15
2016-05-22
Current Direction
Temperature (°C)
30
20
10
0
Water Temperature
2016-04
2016-07
2016-10
2017-01
2017-04
2017-07
2017-10
2018-01
Salinity (PSU)
10.0
7.5
5.0
2.5
0.0
Salinity
2016-04
2016-07
2016-10
2017-01
2017-04
2017-07
2017-10
2018-01
Turbidity (NTU)
150
100
50
0
Turbidity
2016-03
2016-04
2016-05
2016-06
2016-07
2016-08
2016-09
2016-10

**Platform CS04 Daily Averages**

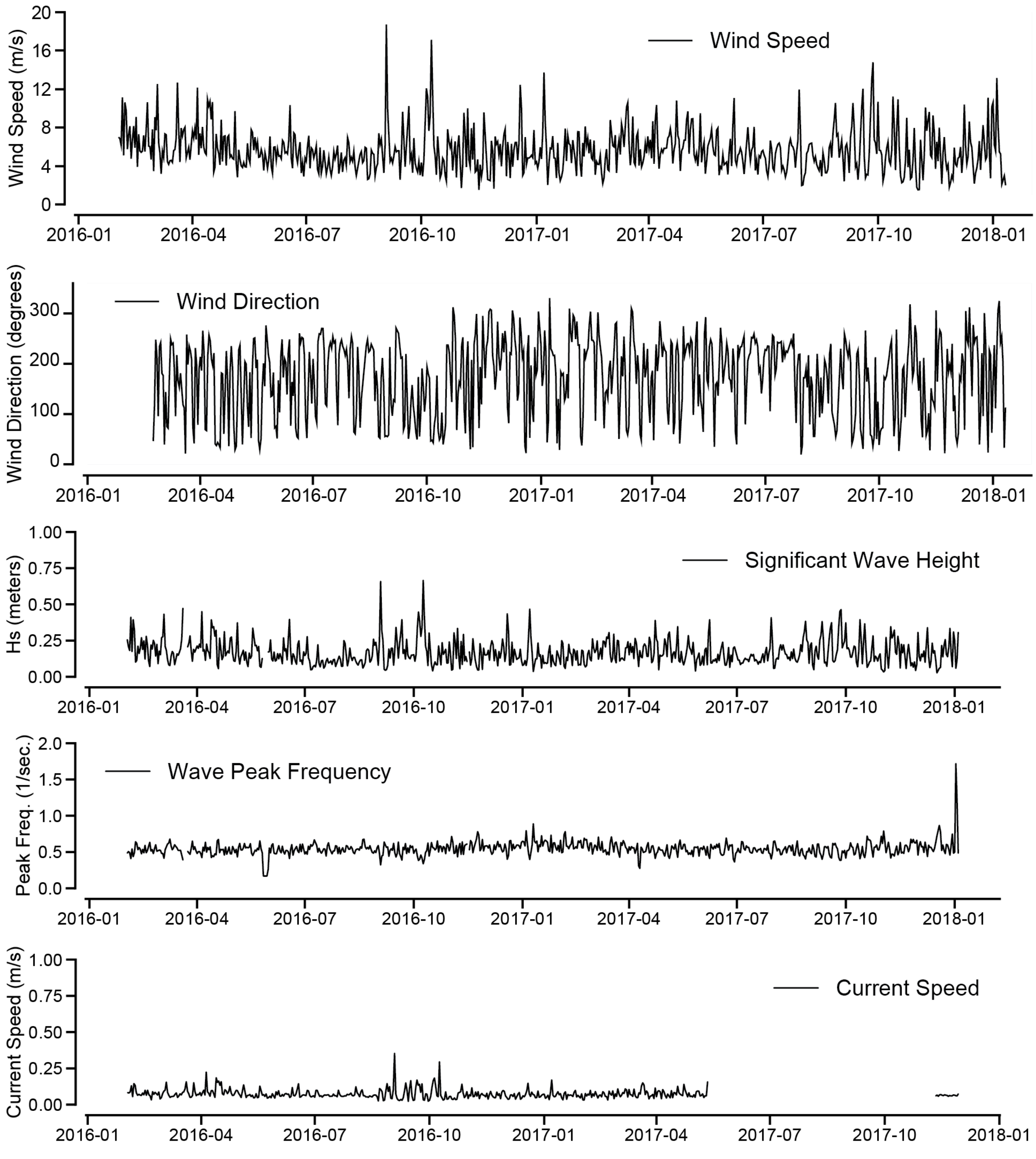

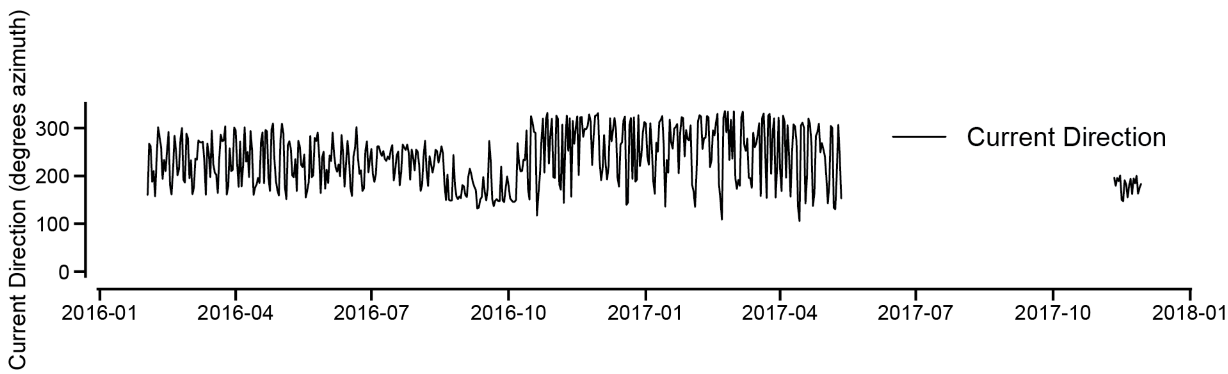
Current Direction (degrees azimuth)
300
200
100
0
2016-01
2016-04
2016-07
2016-10
2017-01
2017-04
2017-07
2017-10
2018-01
Current Direction

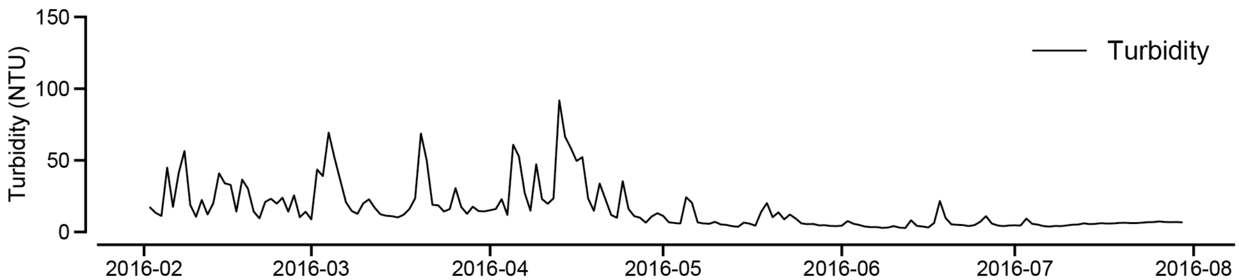
Turbidity (NTU)
150
100
50
0
2016-02
2016-03
2016-04
2016-05
2016-06
2016-07
2016-08
Turbidity

## Platform CS05 Daily Averages

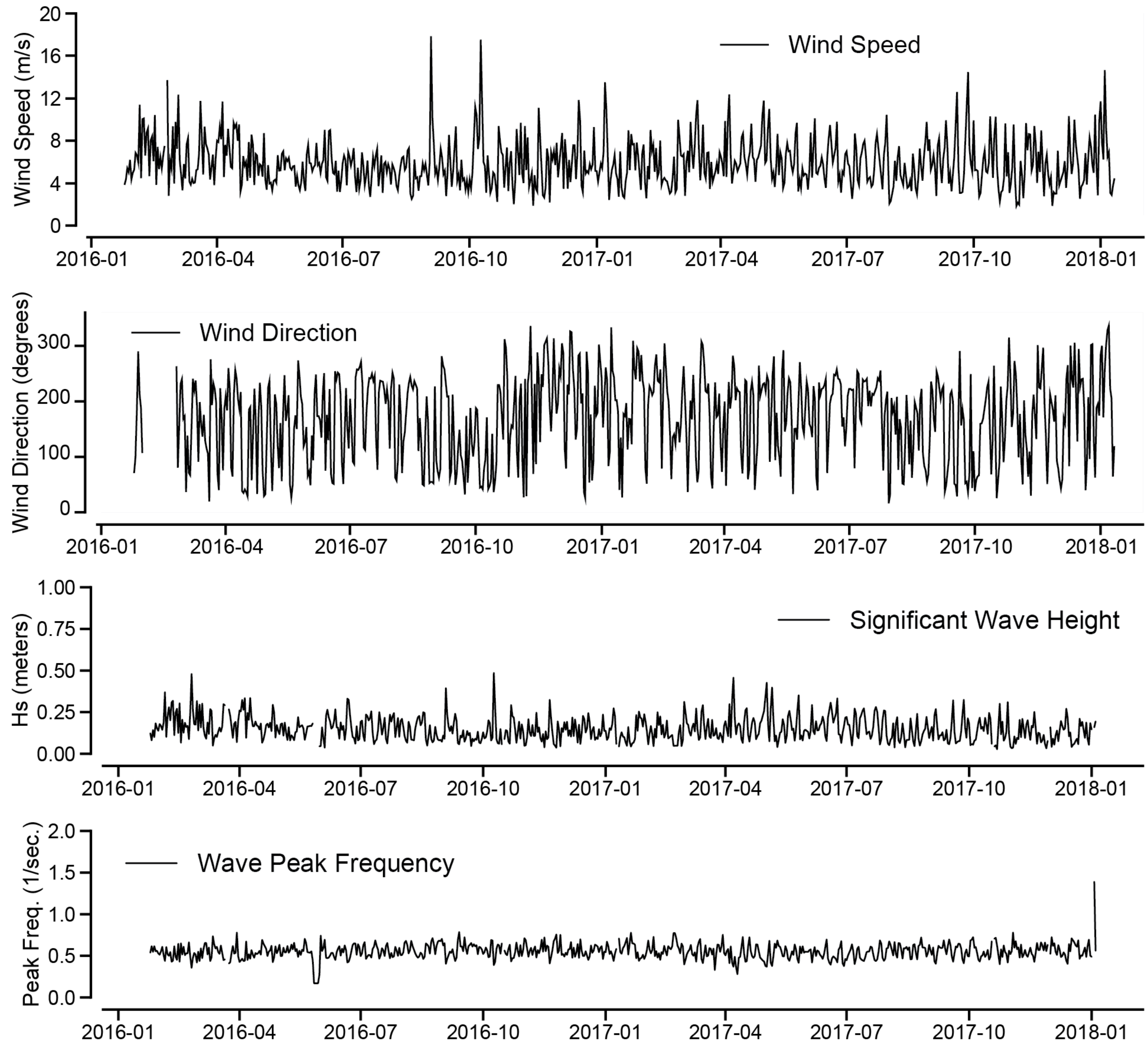

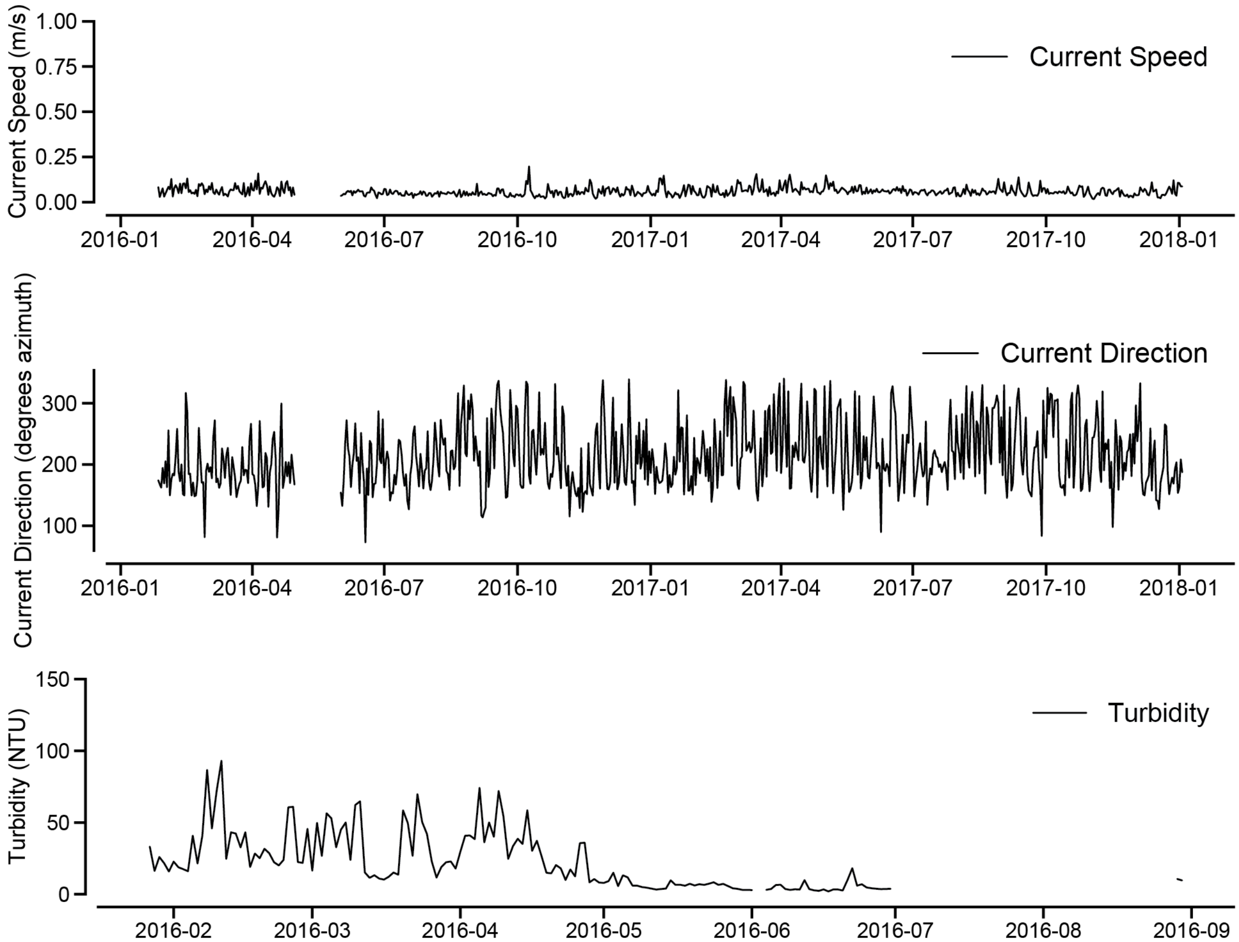

Current Speed (m/s)
1.00
0.75
0.50
0.25
0.00
Current Speed
2016-01
2016-04
2016-07
2016-10
2017-01
2017-04
2017-07
2017-10
2018-01
Current Direction (degrees azimuth)
300
200
100
Current Direction
2016-01
2016-04
2016-07
2016-10
2017-01
2017-04
2017-07
2017-10
2018-01
Turbidity (NTU)
150
100
50
0
Turbidity
2016-02
2016-03
2016-04
2016-05
2016-06
2016-07
2016-08
2016-09

## Lander Curri-N-Obs Daily Averages

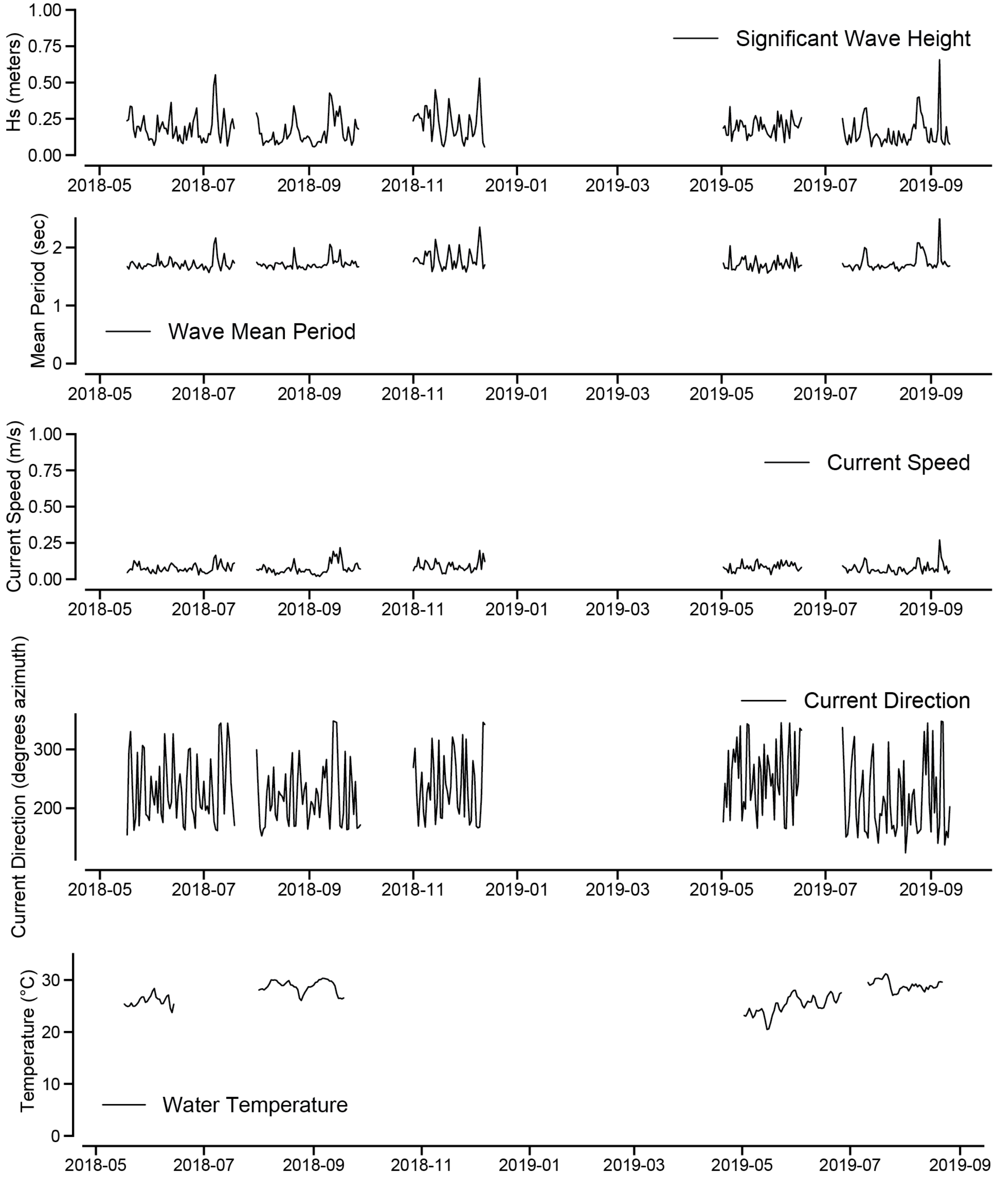

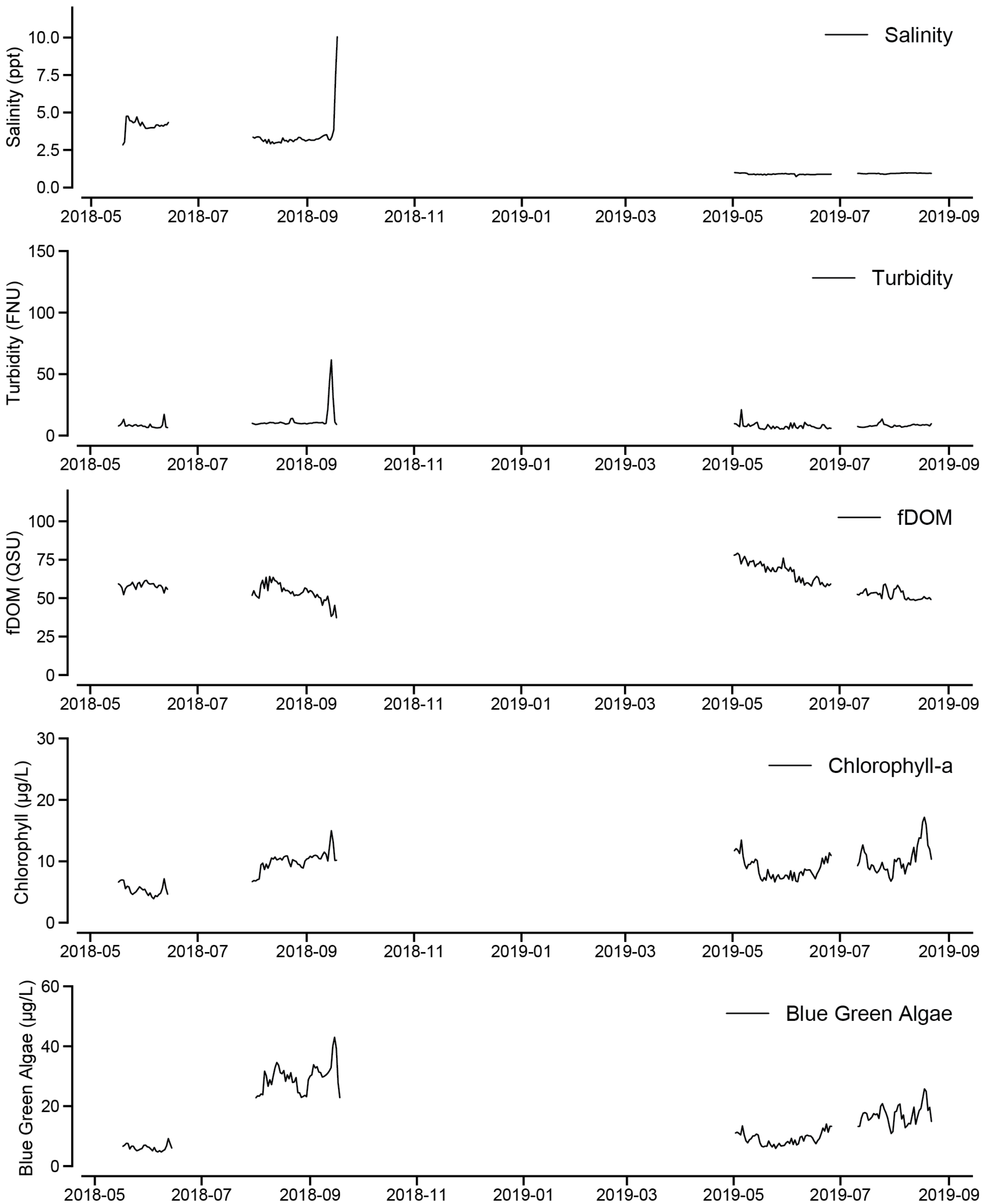
Salinity
Salinity (ppt)
10.0
7.5
5.0
2.5
0.0
Turbidity
Turbidity (FNU)
150
100
50
0
fDOM
fDOM (QSU)
100
75
50
25
0
Chlorophyll-a
Chlorophyll (µg/L)
30
20
10
0
Blue Green Algae
Blue Green Algae (µg/L)
60
40
20
0
2018-05
2018-07
2018-09
2018-11
2019-01
2019-03
2019-05
2019-07
2019-09

**Lander Curri-S-Obs Daily Averages**

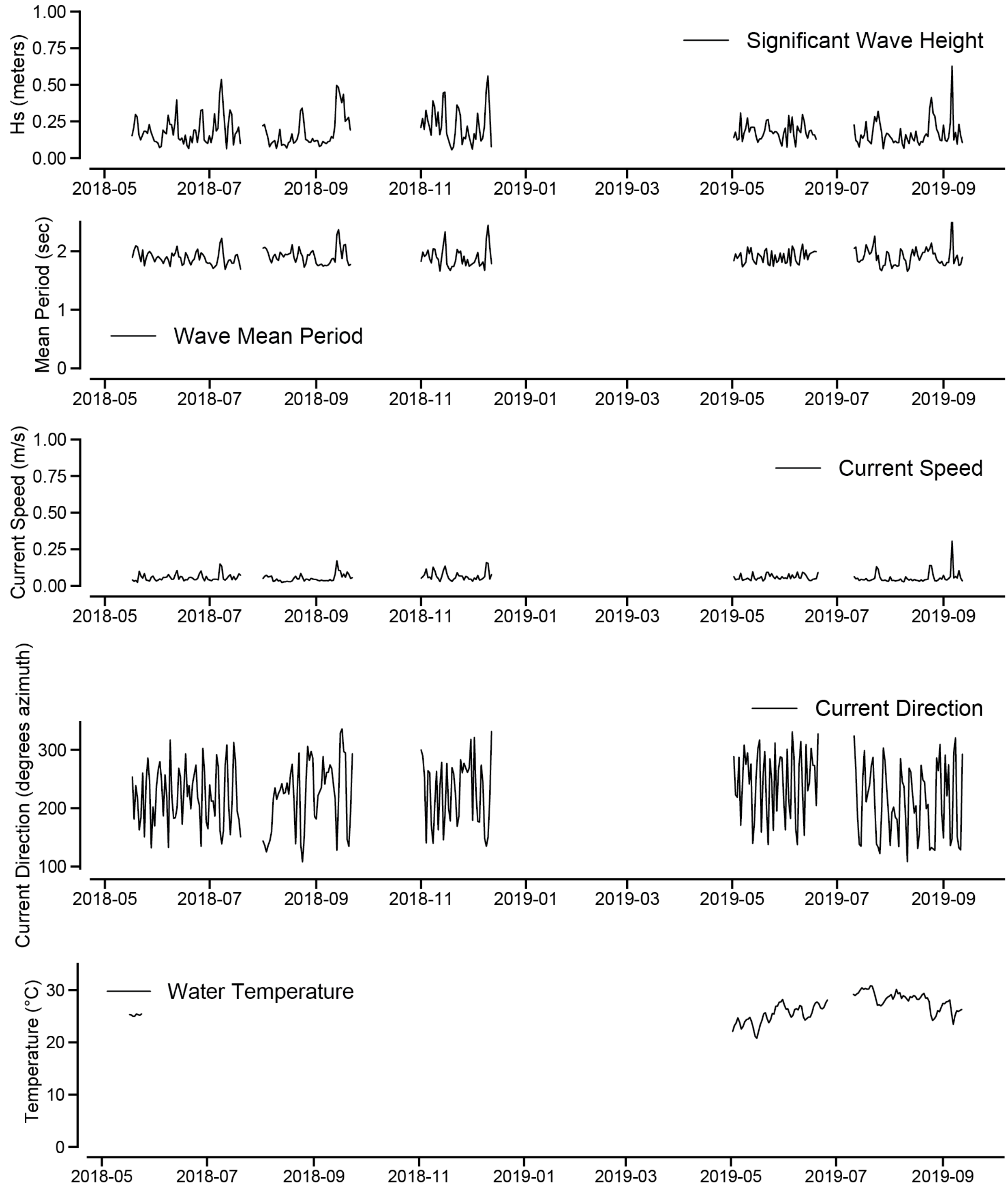

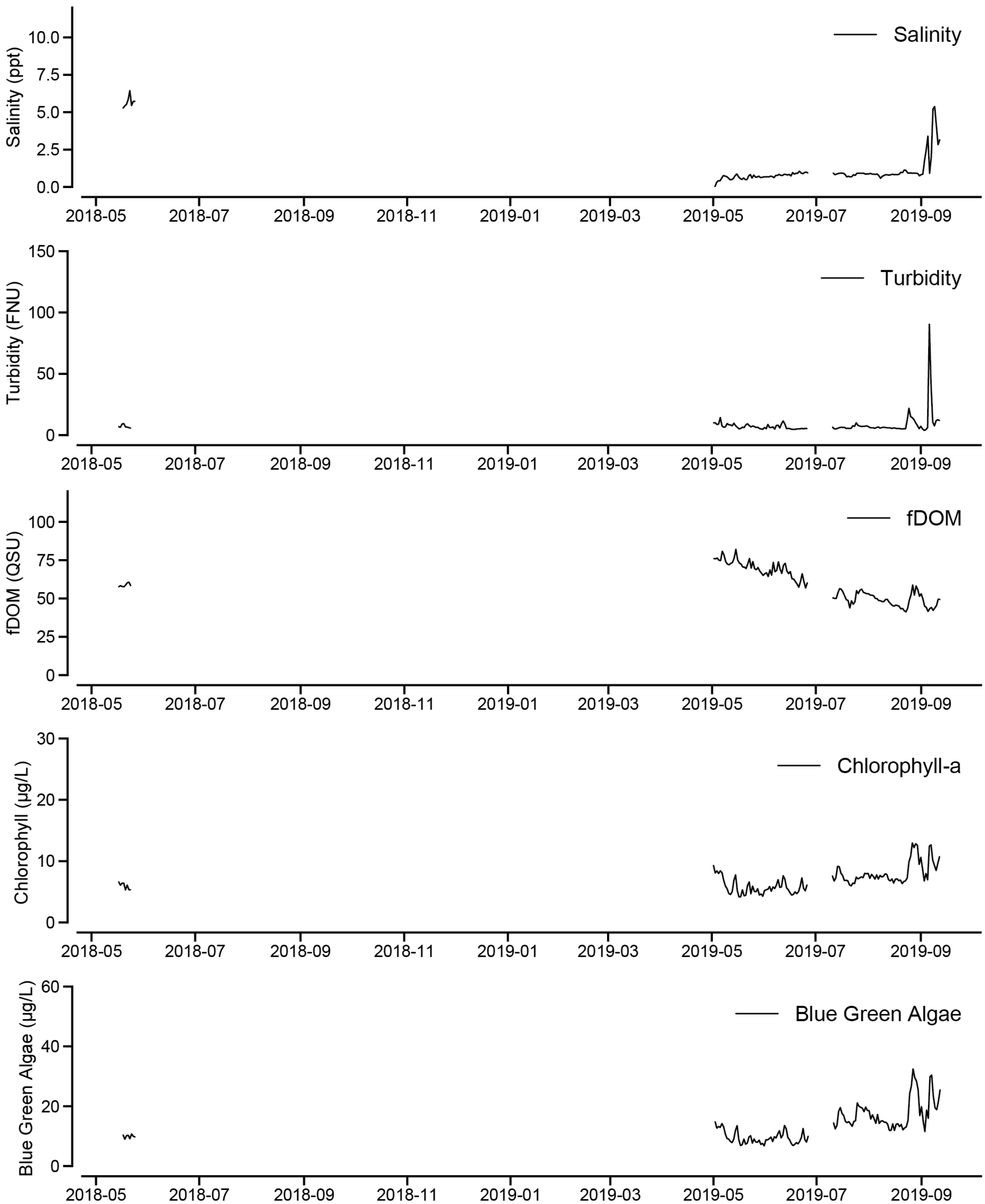
Salinity
Salinity (ppt)
0.0
2.5
5.0
7.5
10.0
Turbidity
Turbidity (FNU)
0
50
100
150
fDOM
fDOM (QSU)
0
25
50
75
100
Chlorophyll-a
Chlorophyll (µg/L)
0
10
20
30
Blue Green Algae
Blue Green Algae (µg/L)
0
20
40
60
2018-05
2018-07
2018-09
2018-11
2019-01
2019-03
2019-05
2019-07
2019-09

**Appendix E. Maps of Past SAV Surveys in Currituck Sound**

**Sincock et al., 1965:**

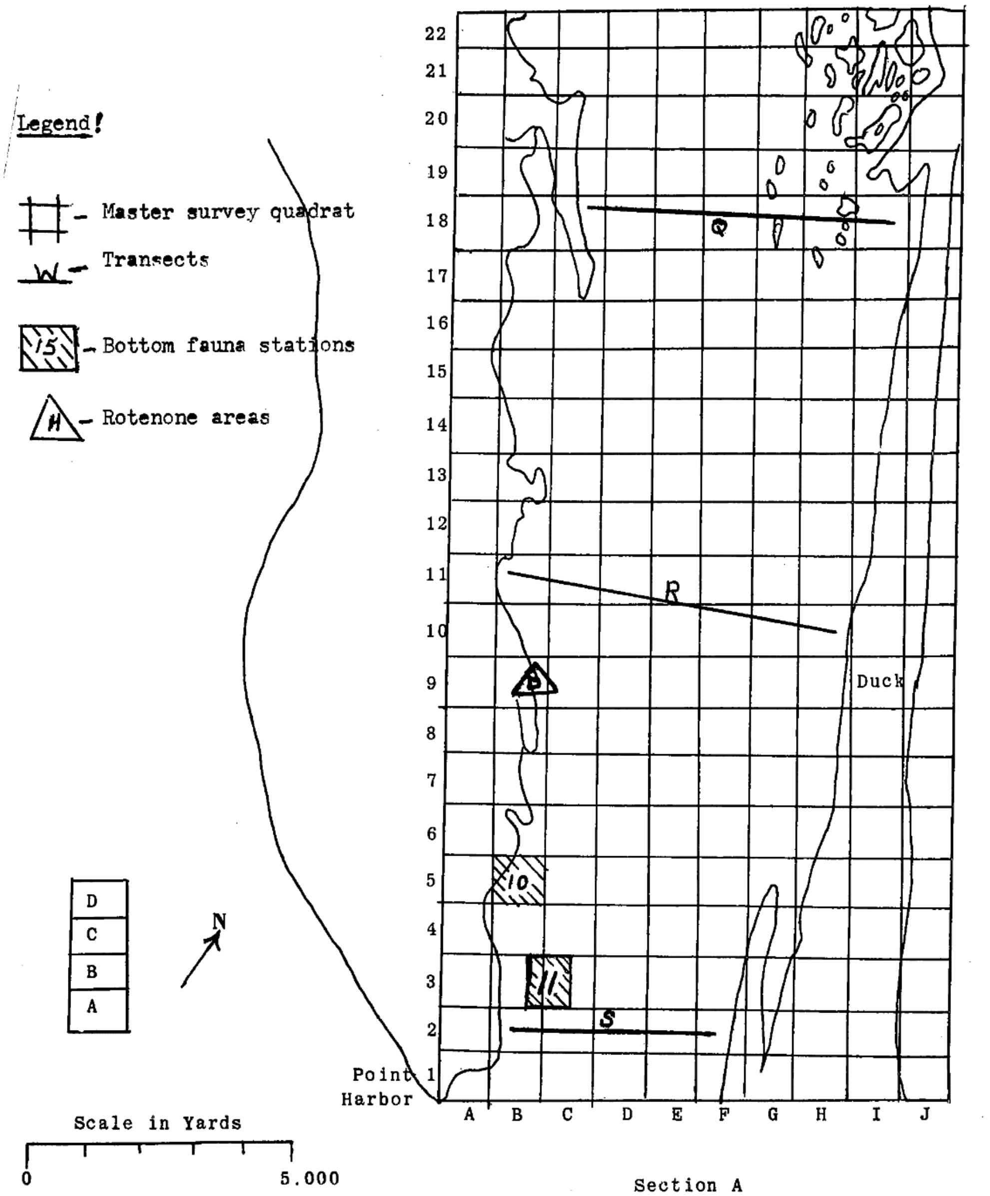


Figure ___. Location of Transects, Master Survey Quadrats, Bottom Fauna Stations and Rotenone Areas.

**Sincock et al., 1965 (continued):**

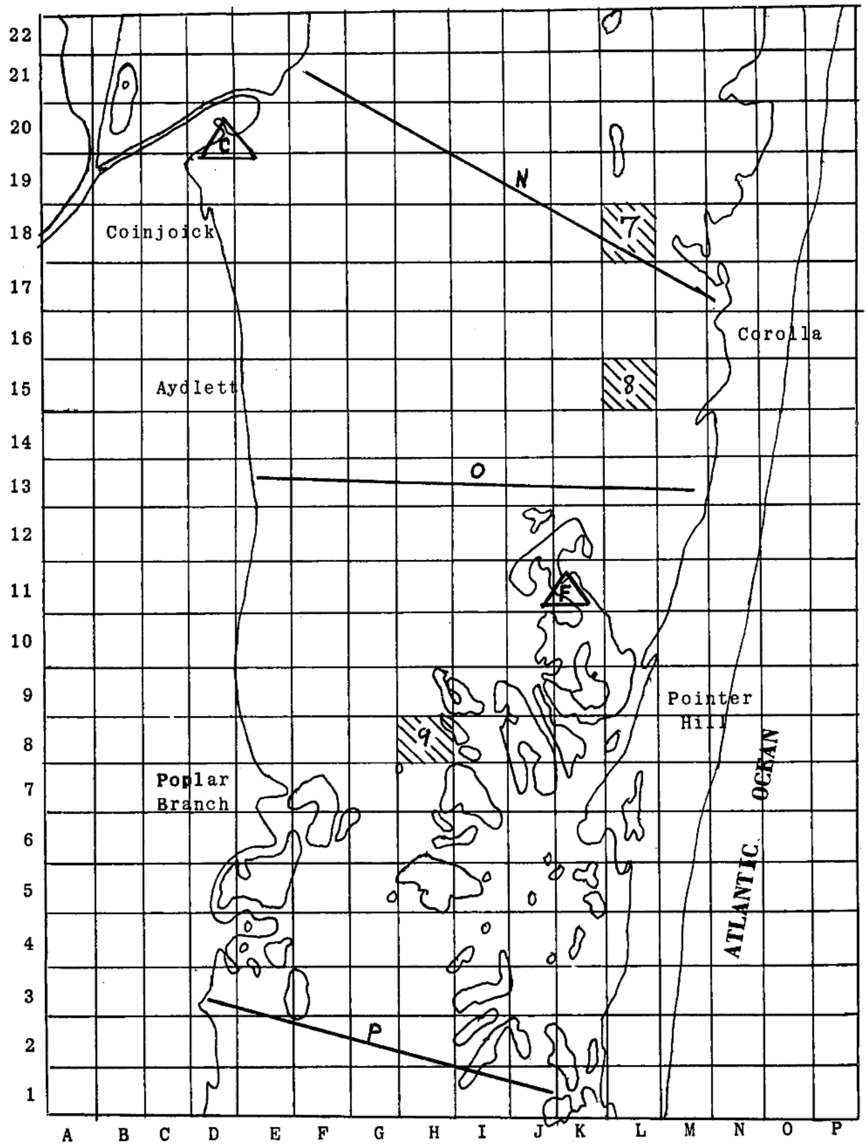


Section B

Figure ___. Location of Transects, Master Survey Quadrats, Bottom Fauna Stations and Rotenone Areas.

**Sincock et al., 1965 (continued):**

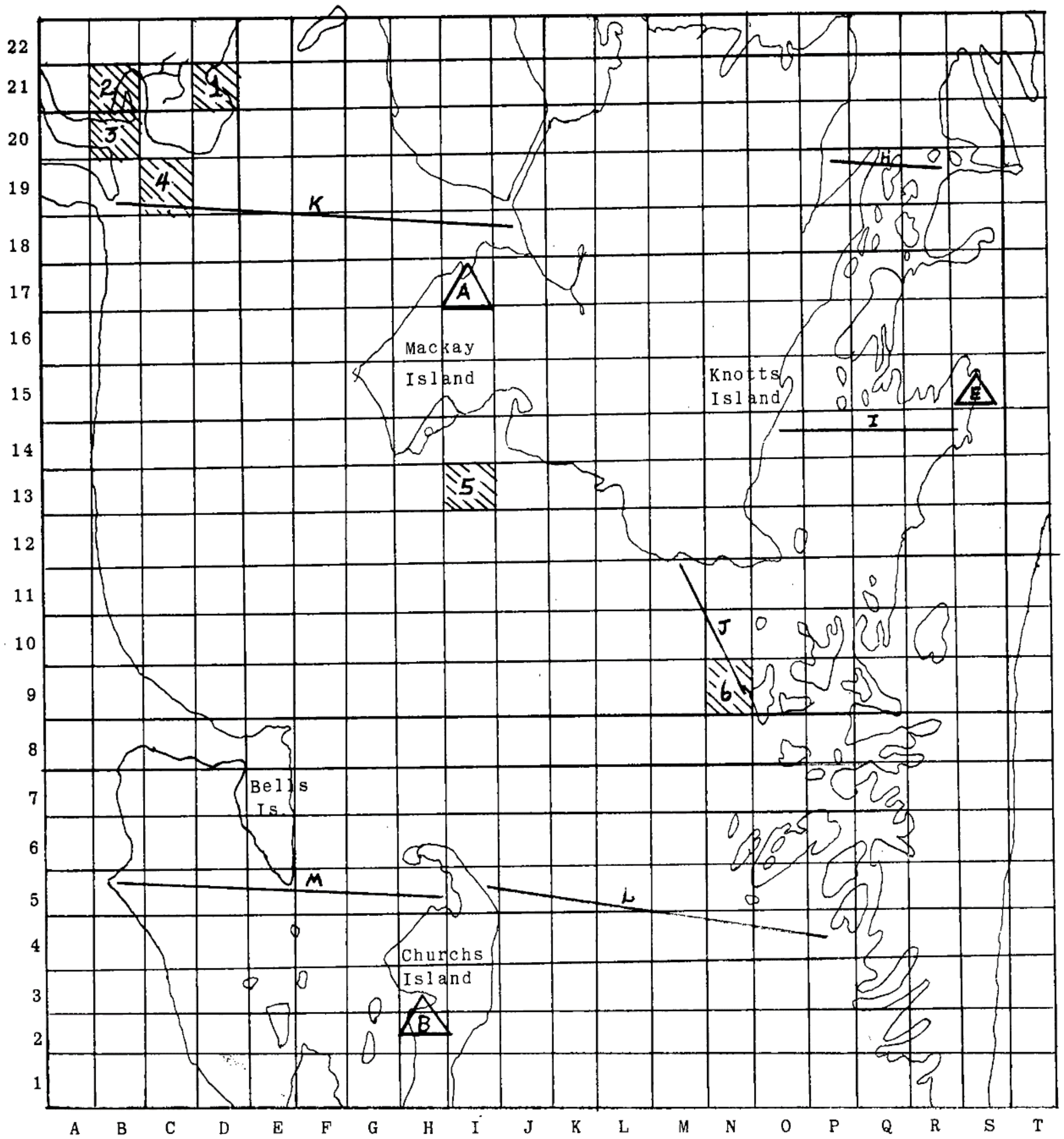


Section C

Figure ______ Location of Transects, Master Survey Quadrats, Bottom Fauna Stations and Rotenone Areas.

**Sincock et al., 1965 (continued):**

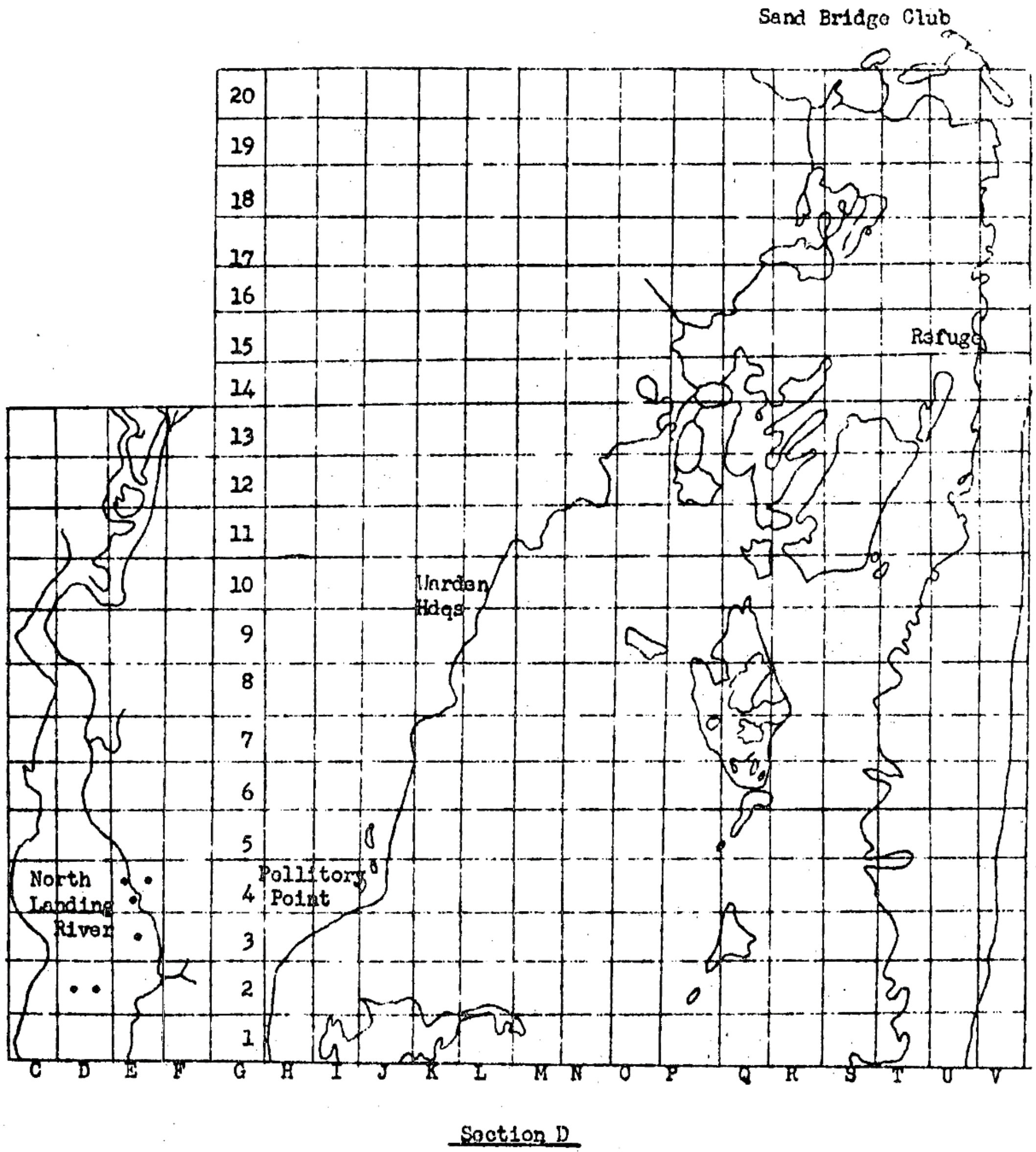


Figure____. Distribution of Shell Bottom, Master Survey, August 1962.

**Davis & Carey, 1981; Davis & Brinson, 1990:**

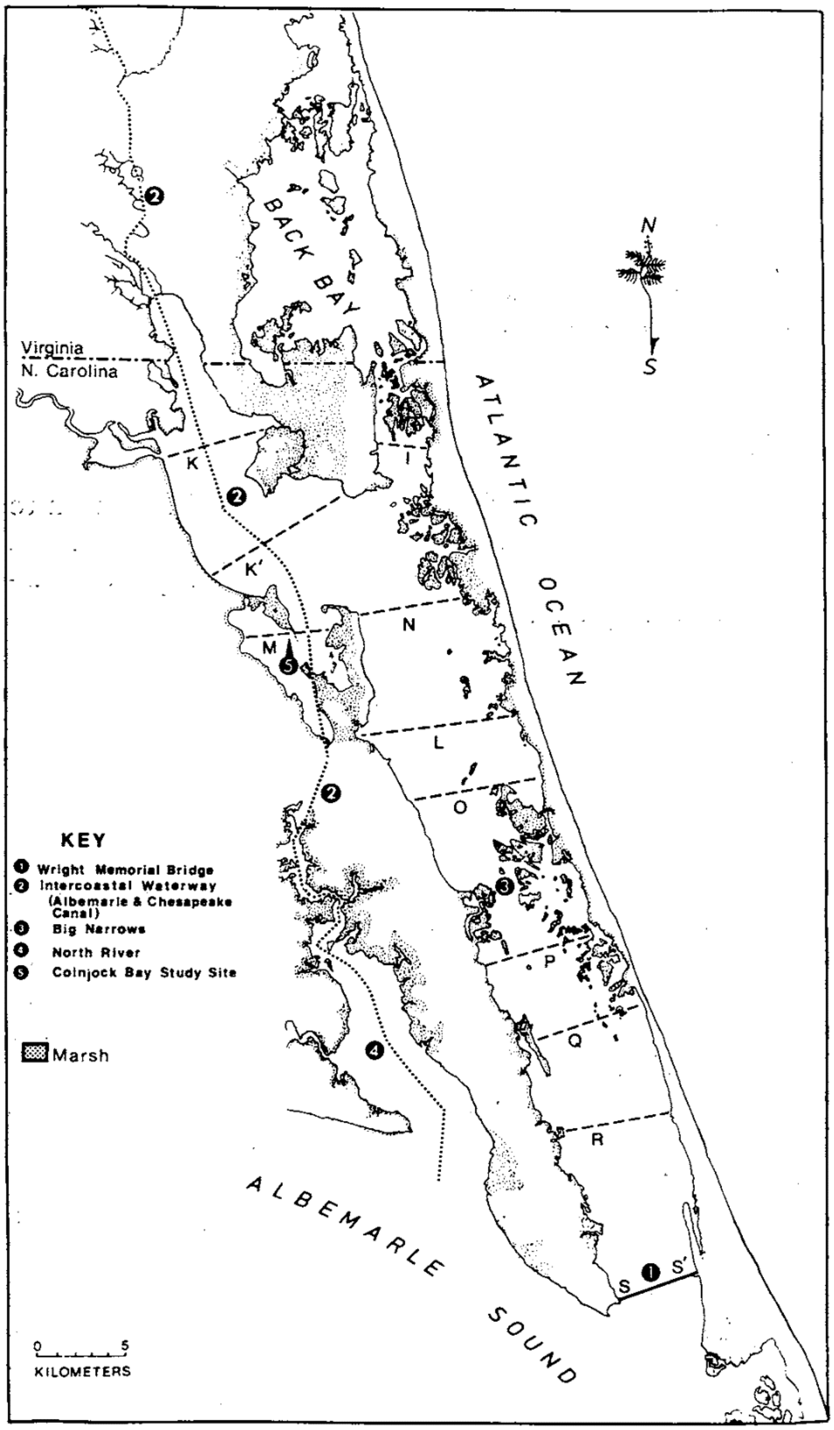


Figure 1. Currituck Sound and contiguous waters showing the Coinjock Bay study site, transects, and sampling stations.

**Hartis, 2013:**

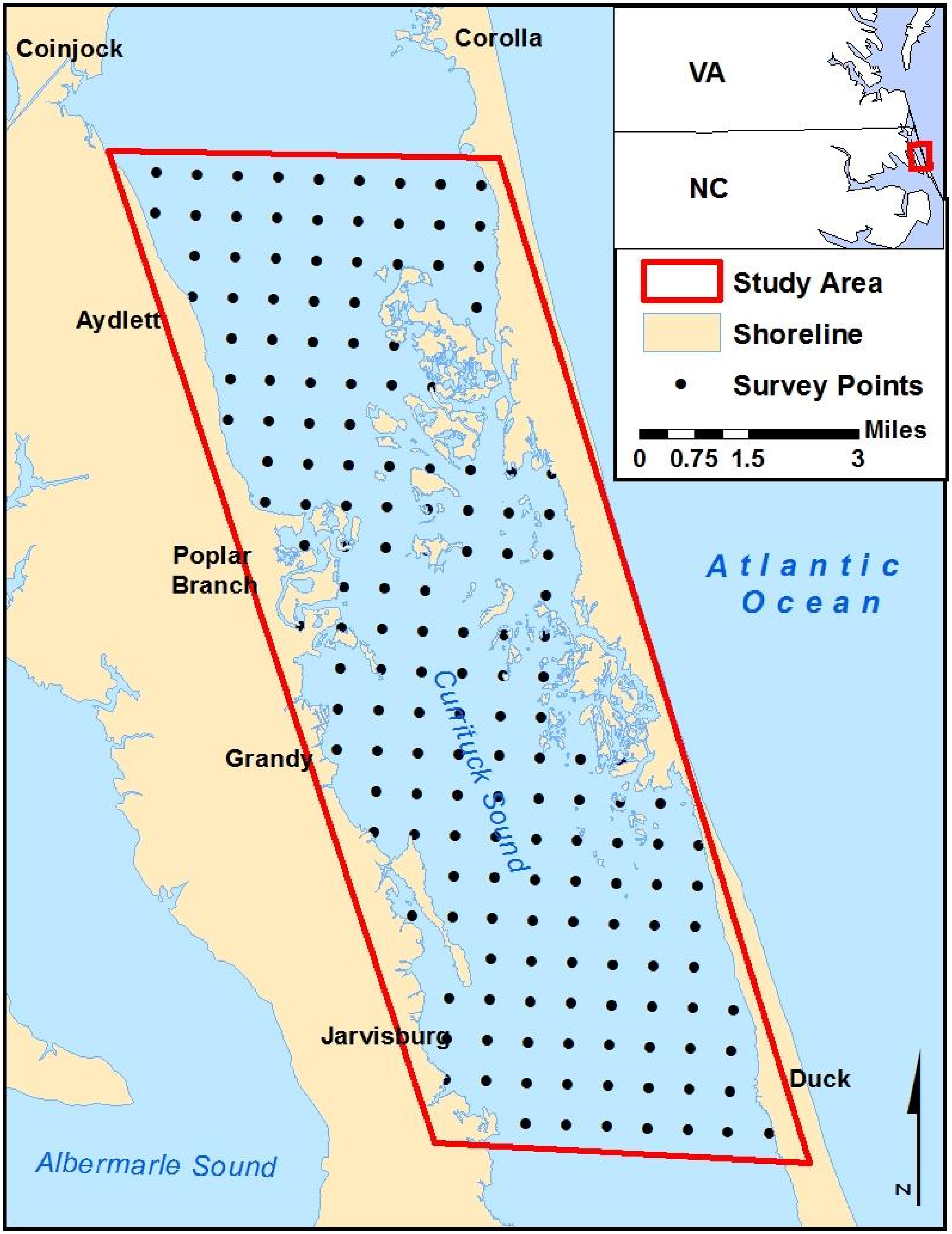

Coinjock
Corolla
VA
NC
Study Area
Shoreline
Survey Points
Miles
0 0.75 1.5 3
Aydlett
Poplar Branch
Atlantic Ocean
Currituck Sound
Grandy
Jarvisburg
Duck
Albermarle Sound
N